Development of bioremediation methods for soil and water contaminated with heavy metals in Kabwe mine

A dissertation submitted in partial fulfillment of the requirements for the degree of Doctorate in Engineering

By

WILSON MWANDIRA

Laboratory of Biotechnology for Resources Engineering,

Division of Sustainable Resources Engineering,

Graduate School of Engineering,

Hokkaido University, Japan

September 2019

Declaration

I declare that, except where specific reference is made in the text to the work conducted by other authors, this thesis is my own account of my research and contains as its main content work that has not previously been submitted for a degree at any university.

Name: W. Mwandira Signature: _____

Date: _____

Acknowledgment

Undertaking this Ph.D. has been a truly life-changing experience for me and it would not have been possible to do without the support and guidance that I received from my advisor Assoc. Prof. Kazunori NAKASHIMA. I appreciate his continuous support and for his patience, motivation, and immense knowledge. His guidance helped me in all the time of research and writing of this thesis. Besides my supervisor, I would like to express my sincere gratitude to my co-supervisors: Prof. Saturo KAWASAKI for his valuable discussions, comments, and encouragement throughout the study. In addition, I would like to express my sincere gratitude to Assistant Prof. Masaji KATO for his generous help.

I would like to thank the Japanese Government for the MONBUKAGAKUSHO (MEXT) scholarship which I highly appreciate. Additionally, the research was funded by the Japan International Cooperation Agency (JICA)/Japan Science and Technology Agency (JST), Science and Technology Research Partnership for Sustainable Development (SATREPS). This support is gratefully acknowledged.

Appreciate the logistical helped rendered throughout my study by Hitomi TADA and Yuka ISHIOKA. My sincere thank you goes to my fellow laboratory members past and present for the stimulating discussions and for all the fun we have had from 2016 to date. Finally, but by no means least, thanks go to Annie, Tionenji, Mpangela, Chifumu, Taonga, and Kodwani. They are the most important people in my world and I dedicate this thesis to them.

Table of contents

List of Figures

List of Tables

CHAPTER 1 INTRODUCTION

1.1 Background

The exploitation of mineral resources has been motivated by rapid urbanization and industrialization. This exploitation has significant effects on environmental receptors: people, water, air and soil (Rieuwerts, 2017). The most investigated heavy metals include chromium (Cr), cadmium (Cd), mercury (Hg), lead (Pb), nickel (Ni), and arsenic (As) due to the significant public health and the environmental risk they pose (Reible, 2017; Tchounwou et al., 2012). Of these, Pb has been studied extensively globally because of its effect on the human health (Papanikolaou et al., 2005) and the environment (Pallavi and Dubey, 2005) as it cannot be degraded to non-toxic forms and therefore have permanent effects on the ecosystem. Lead pollution can either be due to natural or anthropogenic processes. Natural sources of Pb include weathering of minerals, erosion and volcanic activities whereas anthropogenic source includes mining and smelting, electroplating industries, agriculture, sludge dumping, and atmospheric deposition affecting soil and water and consequently human health (Lippman, 1990).

Both water and soil resources require remediation to restore contaminated sites (Kříbek et al., 2019). Conventional methods for Pb removal from water include; chemical precipitation (Kurniawan et al., 2006), biochemical reactors (Rosca et al., 2016), electrolytic recovery (Shim et al., 2014), adsorption (Pinto et al., 2011), coagulation and flocculation (El Samrani et al., 2008), ion exchange (Dąbrowski et al., 2004), membrane filtration/reverse osmosis(Cui et al., 2014), constructed wetlands (Vymazal, 2014), and nanotechnology (Al-saad et al., 2012). On the other hand, the remediation of Pb from soil include soil washing (Liu et al., 2015), vitrification (Colombo et al., 2003), thermal treatment (Cocâr et al., 2011), chemical treatment (Burlakovs et al., 2012), electrokinetic (Karim, 2014), and phytostabilization (Leteinturier et al., 2001). However, the major drawbacks of these conventional technologies for water and soil treatment is their high operational costs, large chemicals used, high energy consumption and handling costs for sludge disposal (Ayangbenro and Babalola, 2017). In order to address these challenges, bioremediation is a promising alternative to conventional cleanup technology for both water and soil because it is faster, safer, and economical (Dixit et al., 2015).

The use of bioremediation plays a significant role in the restoration of a contaminated site as it is less disruptive to the contaminated environment compared to other cleanup methods. In this

context, the Ph.D. study was focused on developing novel bioremediation methods for both contaminated water and soil through a case study at the abandoned Kabwe Mine site, Zambia. Therefore, this thesis discusses sustainable bioremediation techniques for addressing the challenges of heavy metal with a bias to Pb and Zn contamination under three main topics: mine waste immobilization by microbial calcium carbonate precipitation (MICP), wastewater treatment by biosorption using novel indigenous bacteria and a cellulose-based biosorbent.

1.2 Literature review

This subsection deals with the literature review on microbial calcium carbonate precipitation (MICP) and wastewater treatment by bacteria and biosorbent.

1.2.1 Microbiologically induced calcium carbonate precipitation

Microbially induced calcium carbonate precipitation (MICP) is a bio-geochemical process that induces calcium carbonate ($CaCO_3$) to form biominerals. Biominerals surround every environment in the form of anthills, caves, shells of crabs or mollusks, teeth, bones, rocks, etc. (Addadi et al., 2003). MICP can either be biologically controlled or biologically induced (Dhami et al., 2013). Biologically controlled calcium carbonate-controlled formation is where the $CaCO_3$ biomineralization is achieved using a microorganism. On the other hand, biologically induced $CaCO_3$ biomineralization is dependent on the microenvironmental condition mediated by the organism. Different microorganisms can precipitate calcium carbonate, and these are:

(i) Photosynthesis microorganisms (cyanobacteria and algae)
(ii) Sulfate-reducing bacteria;
(iii) Organisms utilizing organic acids; and
(iv) Microorganisms involved in the nitrogen cycle.

Of these, the most desired groups of microorganisms are the ones can achieve $CaCO_3$ precipitation by urea hydrolysis because they can be easily controlled and produces biominerals in a short period: ureolytic bacteria. Ureolytic bacteria have been investigated more than the other microorganism because of precipitating biominerals in a short time (Amarakoon and Kawasaki, 2018; Bhattacharya et al., 2018; Duo et al., 2018; Xu et al., 2017). The mechanism involves the

hydrolysis of urea into ammonium and carbarmate by urease catalysis (Eq. (1.1)), resulting in $CaCO_3$ formation in the presence of Ca^{2+} ions (Eqs. (1.2) - (1.3)) (Whiffin et al., 2007).

$$CO(NH_2)_2 + H_2O \longrightarrow H_2NCOO^- + NH_4^+ \quad 1.1$$

$$H_2NCOO^- + H_2O \longrightarrow HCO_3^- + NH_3 \quad 1.2$$

$$Ca^{2+} + HCO_3^- + NH_3 \longrightarrow CaCO_3 + NH_4^+ \quad 1.3$$

The role of the bacteria, in this case, is to create an alkaline microenvironment that encourages calcium carbonate precipitation on the positively charged cell membrane of the bacteria as summarized by Eqs. (1.4) - (1.6)) in the presence of urea and calcium source.

$$Ca^{2+} + Cell \longrightarrow Cell\text{-}Ca^{2+} \quad 1.4$$

$$Cl^- + HCO_3^- + NH_3 \longrightarrow NH_4Cl + CO_3^- \quad 1.5$$

$$Cell\text{-}Ca^2 + CO_3^- \longrightarrow Cell\text{-}CaCO_3 \quad 1.6$$

The MICP technique mechanism is being proposed for the remediation of wastewater treatment (Umar et al., 2016), heavy metals immobilization (Zhu et al., 2016), consolidation (Abo-El-Enein et al., 2012), monument restoration (González et al., 2015), biocement (Whiffin et al., 2007), and CO_2 sequestration (Okyay and Rodrigues, 2015). Specifically, bioremediation of heavy metals using this technique is a promising technique for heavy metals (Pb^{2+}, Cd^{2+}, Zn^{2+} etc.) contaminated soils, sediment and water; and have been successful in recent studies (Kang et al., 2014; Zhu et al., 2016; Achal et al., 2012). In the presence of free toxic ions (e.g. Pb^{2+}), the calcium carbonate formed can either immobilize (Eq. (1.4)) or form undissolved substances, with the free ions onto the surfaces of calcium carbonate to a chemically stable and non-toxic form (Ivanov and Stabnikov, 2016). The use of this technique addresses two main geotechnical parameters: strength and permeability. Strength achieved with MICP assists in resisting the disruptive forces of wind and rain whereas reduced hydraulic conductivity reduces the ability of water to come in contact with the contaminant, and, therefore, reduces the leaching rate of the contaminant (Eryürük et al., 2015). This can be achieved via biostimulation or bioaugmentation (Chen and Achal, 2019).

1.2.2 Heavy metal removal by biosorption using bacteria

Biosorption is the removal of heavy metal from aqueous solution by biological materials such as bacteria (Khan et al., 2016), yeast (Rodríguez et al., 2018), algae (Anastopoulos and Kyzas, 2015), fungi (Prasad et al., 2013), or agricultural waste (Abdi and Kazemi, 2015). Even though many of these biomaterials have been isolated and identified, the isolation and identification of more and indigenously available biological materials are indispensable in sites heavily contaminated with heavy metals. Therefore, for these prokaryotes and eukaryotes to survive in heavy metal polluted environments they develop defense mechanisms which can be exploited for bioremediation purposes. These mechanisms include bioaccumulation (Ahemad and Malik, 2012), biomineralization (Achal et al., 2012a), biosorption (Irawati et al., 2017), and biotransformation (Mahbub et al., 2016). Figure 1.1 shows the various mechanisms by which bacteria can sequester heavy metals and these include active transport, precipitation, ion exchange, electrostatic attraction extracellular polymetric interaction, and complexation.

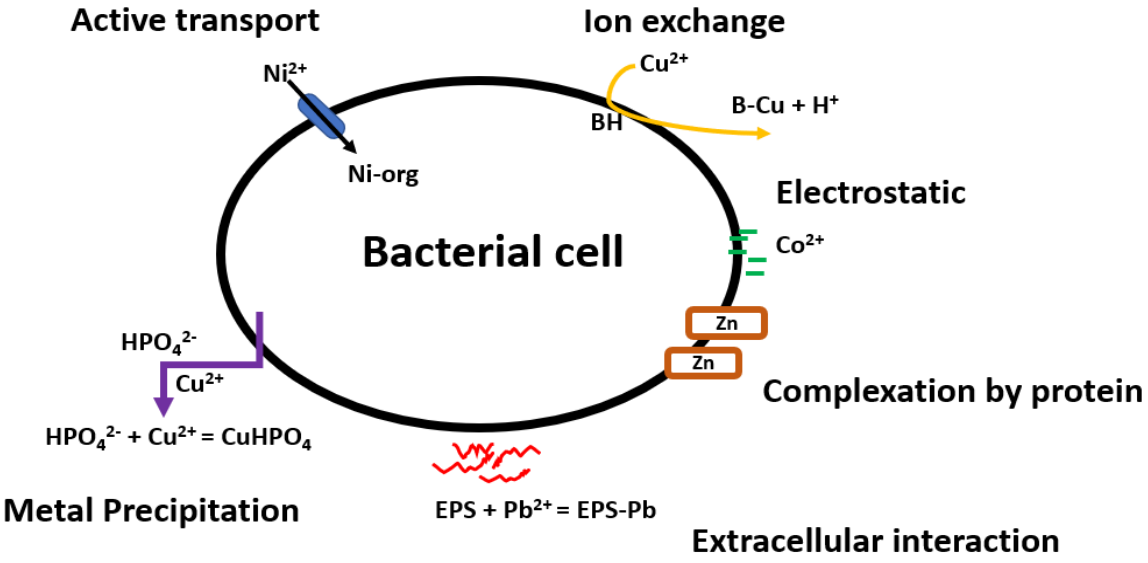

Fig. 1.1: Various mechanisms by which bacteria sequesters heavy metal from contaminated sites

Therefore, this study was motivated to isolate novel Pb-tolerant indigenous bacteria strains from Pb contaminated soil and evaluate their ability to remediate polluted wastewater from past mining activities. According to the authors' knowledge, this is the first study to isolate Pb resistant bacteria from Kabwe Mine Site for bioremediation purposes. Therefore, isolation of indigenous

bacteria strain is important because the isolated strain could possibly tolerate high heavy metal concentrations in different ways and may play a significant role in the restoration of a contaminated site as they are already adapted to the contaminated site and may potentially not change the local ecological integrity.

1.2.3 Heavy metal removal by biosorption using biosorbents

The removal of contaminants from mine water prior to discharge is receiving significant attention because of its effect on human health and the environment. Wastewater treatment is thus becoming a major focus of mine operations due to environmental concerns, stringent national regulations, integrated water resource management, and access to water by the local community near mining operations. Conventional methods for heavy metal removal from mine water include; chemical precipitation (Ayres et al., 1994; Kurniawan et al., 2006), biochemical reactors (Rosca et al., 2016), electrolytic recovery (Shim et al., 2014), adsorption (Pinto et al., 2011), coagulation and flocculation (El Samrani et al., 2008), ion exchange (Dąbrowski et al., 2004), reverse osmosis (Cui et al., 2014), constructed wetlands (Vymazal, 2014), and nanotechnology (Al-saad et al., 2012).

The major drawbacks of these conventional technologies are their high operational costs due to the chemicals used, high energy consumption and handling costs for sludge disposal. Since mine waters mainly contain one or more contaminants of concern, the biosorbent should be able to remove two or more toxic. An attractive alternative technology is to develop cheap and robust microorganism-based biosorbents that have high adsorption capacities for multielement, mechanically strong and rigid. In this study, developed a cheap and robust microorganism-based biosorbents constructed from a protein fusion of Metallothioneins (MTs) from *Synechococcus elongatus* PCC 7942 that bind N-terminally to cellulose-binding domains (CBD) from *C. thermocellum.* Cellulose is naturally the most abundant polymer on earth, inexpensive, chemically inert and a renewable source of organic compounds on the planet. Additionally, MTs are rich in cysteine residues and the presence of thiol groups (SH) in the cysteine chemical structure enables the capture and detoxification of toxic metal ions such as Pb^{2+}, Zn^{2+}, Hg and Ni^{2+}.

1.2.4 Study area

a) Location of the study area

The study area is the abandoned Pb-Zn mine site situated in Kabwe, Central province of Zambia (Fig. 1.2). Kabwe is located between Latitudes 15^{o} 27'-17^{o} 28'S and Longitudes 23^{o} 06' E-25^{o} 33'E. The mine commenced its operations in 1902 until its closure in 1994. Apart from Pb and Zn it also produced silver, manganese, cadmium, vanadium, and titanium in smaller quantities whose ore was being shipped overseas for smelting (Mufinda, 2015). The major stream draining the city is the Mine Canal into which water from both central business district and the closed mine are discharged into. Water from the canal discharges into large marshes east of the city and then water flows into the Muswishi River which consequently ends in the Lunsemfwa River. The Lunsemfwa River is a tributary of the Lukasashi and Luangwa Rivers in and part of the Zambezi River Basin.

b) The mine waste at the study area

The mineral ore at the mine included pyrite, sphalerite, chalcopyrite, bornite, covellite, chalcocite and tetrahedrite, and minor cerussite, willemite, and smithsonite (Nyambe et al., 2013). Thus, several methods of lead and zinc processes were tested early during the project implementation, hence the different types of mine waste due to the complex geology as shown in Fig. 1.2. In this study, only leach plant residue (LPR) and kiln slag (KS) were investigated due to its susceptible to wind and water erosion. These two wastes were selected for target material that should be remediated because they are deemed the most toxic and cover the largest area onsite. The LPR was deposited when the ZnS ore was produced by oxidation roasting using ZnO with sulfuric acid hence the pyritic waste. To recover Zinc, electrowinning was used, and then acid leaching was conducted which lead to the accumulation of the leaching residue: hence leach plant residues. The Wealz slag was produced from 1975 onwards when the Waelz kiln was used in the process. Zinc leach residue and coke were roasted in a rotary kiln whereas crude zinc oxide (volatilized recovered Zn) and thus the Wealz slag was produced.

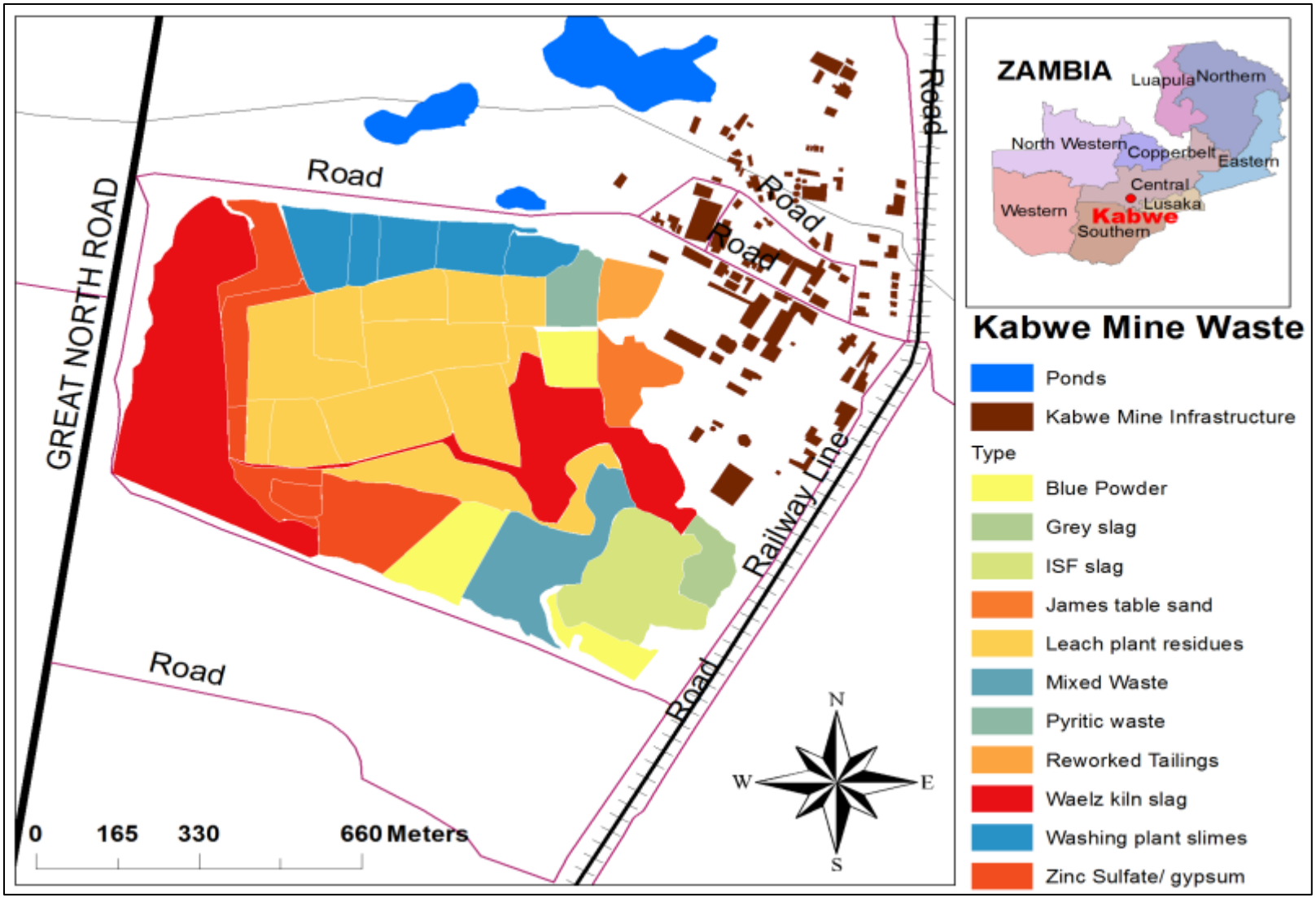

Fig. 1.2: Location of the study area showing the different mine waste at Kabwe Mine site, Zambia, Africa

1.3 Scope

The scope of this thesis is the development of novel bioremediation methods for alleviating heavy metal contamination in soil and water at abandoned Kabwe Mine Zambia as the study area. The thesis consists of two major sections with different subsections as shown in Fig 1.3. This thesis provides a summary of the four parts of the Ph.D. study, as well as an overview of the methods and the main findings of the laboratory investigations. It is structured as follow; Chapter 1 presents an introduction with case study area, motivation and literature review of previous work on the research topic. Soil bioremediation by MICP is presented in chapter 2 and 3 using *Pararhodobacter* sp and indigenous ureolytic bacteria, respectively, with the overall objective of immobilizing the mine waste hence preventing Pb metallic dust dispersion and reduce permeability. Water bioremediation by indigenous bacteria and cellulose-based biosorbent is presented in chapter 4 and 5. Finally, Chapter 6 provides concluding remarks based on the results obtained from Chapters 2, 3, 4 and 5 as a guide for future studies.

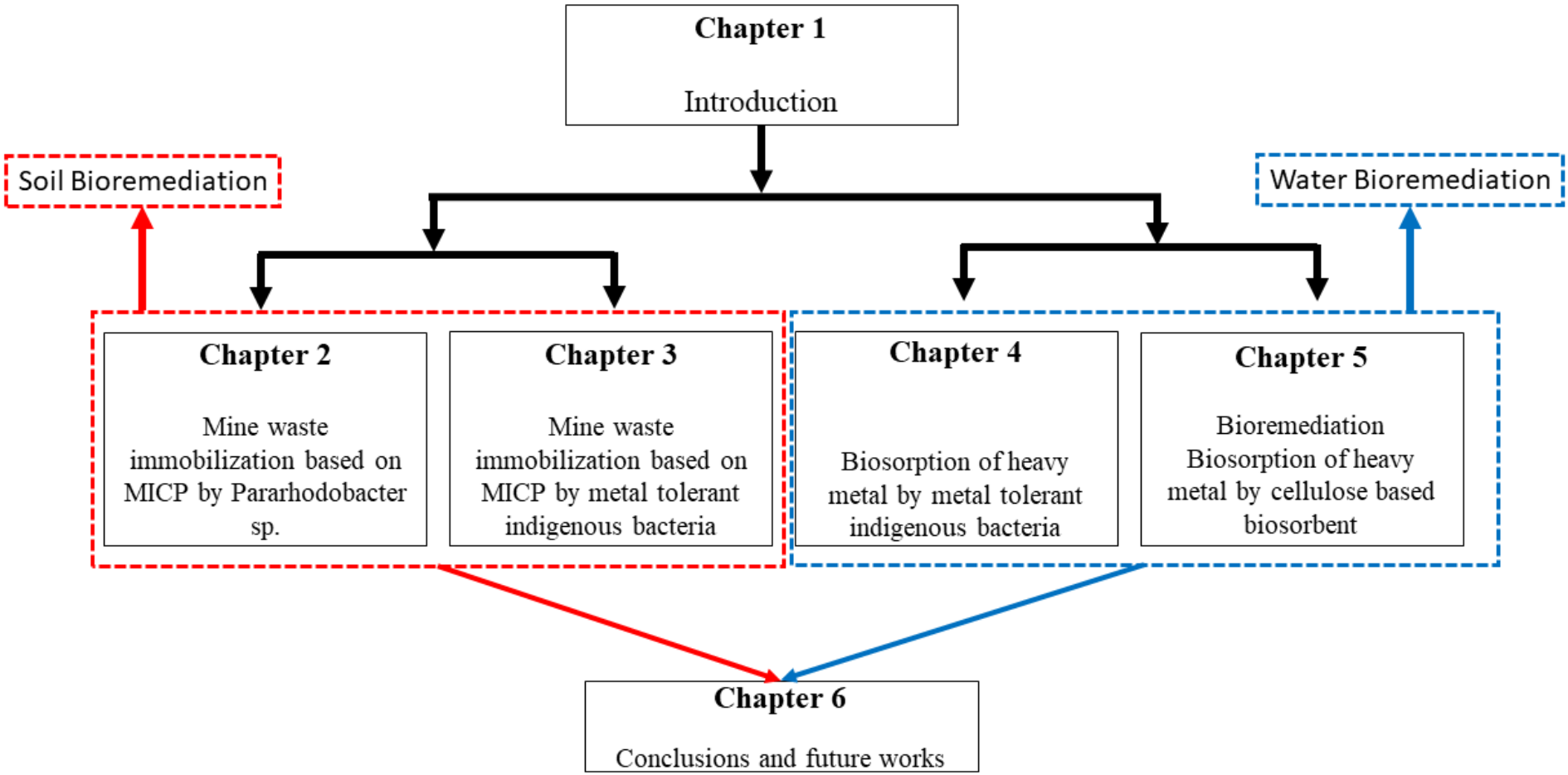

Figure 1.3: Scope of the thesis.

1.4 The originality of the study

Firstly, in chapter 2 adopted MICP for mine waste immobilization. In this Chapter, determine for the very first time the use of *Pararhodobacter* sp. for immobilization of Pb-contaminated mine waste and determined its effectiveness. Determination of the effectiveness of immobilization by MICP has never been investigated before. By using *Pararhodobacter* sp., it demonstrated the originality by testing an idea for application in the different field hence adding to knowledge in a way that has not previously been done before.

Secondly, in Chapter 3 undertook an original piece of work by isolating indigenous ureolytic bacteria from Kabwe, Zambia. From this research study, introduced two new ureolytic bacteria for the MICP process. The bacteria were *Oceanobacillus profundus* KBZ 1-3 and *Oceanobacillus profundus* KBZ 2-5. It was the originality of this research. Therefore, the research was original in terms of using techniques, procedures and applying these to an existing problem or to a context where they have not been tried before.

Thirdly, in chapter 4 undertook another original piece of work by using metal tolerant indigenous bacteria for biosorption of Zn and Pb from water. This application of existing ideas to treat wastewater is novel. Bacterium *Oceanobacillus Profundus* KBZ 3-2 was used, investigated and found to be useful for bioremediation purposes. The novelty was achieved by adding to knowledge in a way in that it has not previously been done by using this bacterium.

Finally, in chapter 5 undertook to develop a novel and robust microorganism-based adsorbent constructed from a protein fusion of Metallothioneins (MTs) from *Synechococcus elongatus PCC 7942* that bind N-terminally to cellulose-binding domains (CBD) from *C. thermocellum.* The use of a cellulose-based adsorbent is cost-effectiveness hence its significance

Moreover, have demonstrated that using different bioremediation approaches would holistically address the problem of heavy metal contamination from abandoned site world over.

References

Abdi, O., Kazemi, M., 2015. A review study of biosorption of heavy metals and comparison between different biosorbents. J. Mater. Environ. Sci. 6, 1386–1399.

Abo-El-Enein, S.A., Ali, A.H., Talkhan, F.N., Abdel-Gawwad, H.A., 2012. Utilization of microbial induced calcite precipitation for sand consolidation and mortar crack remediation. HBRC J. 8, 185–192. https://doi.org/10.1016/j.hbrcj.2013.02.001

Achal, V., Pan, X., Fu, Q., Zhang, D., 2012a. Biomineralization based remediation of As(III) contaminated soil by *Sporosarcina ginsengisoli*. J. Hazard. Mater. 201–202, 178–184. https://doi.org/10.1016/j.jhazmat.2011.11.067

Achal, V., Pan, X., Zhang, D., Fu, Q., 2012b. Bioremediation of Pb-contaminated soil based on microbially induced calcite precipitation. J. Microbiol. Biotechnol. 22, 244–247. https://doi.org/10.4014/jmb.1108.08033

Addadi, L., Raz, S., Weiner, S., 2003. Taking advantage of disorder: Amorphous calcium carbonate and its roles in biomineralization. Adv. Mater. 15, 959–970. https://doi.org/10.1002/adma.200300381

Ahemad, M., Malik, A., 2012. Bioaccumulation of heavy metals by zinc resistant bacteria isolated from agricultural soils irrigated with wastewater. Bacteriol. J. https://doi.org/10.3923/bj.2012.12.21

Al-saad, K. a, Amr, M. a, Hadi, D.T., Arar, R.S., Al-sulaiti, M.M., Abdulmalik, T. a, Alssahamary, N.M., Kwak, J.C., 2012. Iron oxide nanoparticles : applicability for heavy metal removal from contaminated water. Arab J. Nucl. Sci. Appl. 45, 335–346.

Amarakoon, G.G.N.N., Kawasaki, S., 2018. Factors affecting sand solidification using MICP with *Pararhodobacter sp*. Mater. Trans. 59, 72–81. https://doi.org/10.2320/matertrans.M-M2017849

Anastopoulos, I., Kyzas, G.Z., 2015. Progress in batch biosorption of heavy metals onto algae. J. Mol. Liq. 209, 77–86. https://doi.org/10.1016/j.molliq.2015.05.023

Ayangbenro, A.S., Babalola, O.O., 2017. A new strategy for heavy metal polluted environments: A review of microbial biosorbents. Int. J. Environ. Res. Public Health 14. https://doi.org/10.3390/ijerph14010094

Ayres, D.M., Davis, A.P., Gietka, P.M., 1994. Removing heavy metals from waste water. Environ. Sci. 6, 1–21. https://doi.org/10.1021/es60065a006

Bhattacharya, A., Naik, S.N., Khare, S.K., 2018. Harnessing the bio-mineralization ability of urease producing *Serratia marcescens* and *Enterobacter cloacae* EMB19 for remediation of heavy metal cadmium (II). J. Environ. Manage. 215, 143–152. https://doi.org/10.1016/j.jenvman.2018.03.055

Burlakovs, J., Klavins, M., Karklina, A., 2012. Remediation of soil contamination with heavy metals by using zeolite and humic acid additives. Latv. J. Chem. 51. https://doi.org/10.2478/v10161-012-0019-6

Chen, X., Achal, V., 2019. Biostimulation of carbonate precipitation process in soil for copper immobilization. J. Hazard. Mater. https://doi.org/10.1016/j.jhazmat.2019.01.108

Cocâr, D.M., Dinu, R.N., Dumitrescu, C., Re, A.M., Tanasiev, V., 2011. Risk-based approach for thermal treatment of soils contaminated with heavy metals 2009, 5–8. https://doi.org/10.1051/e3sconf/20130101005

Colombo, P., Brusatin, G., Bernardo, E., Scarinci, G., 2003. Inertization and reuse of waste materials by vitrification and fabrication of glass-based products. Curr. Opin. Solid State Mater. Sci. 7, 225–239. https://doi.org/10.1016/j.cossms.2003.08.002

Cui, Y., Ge, Q., Liu, X.Y., Chung, T.S., 2014. Novel forward osmosis process to effectively remove heavy metal ions. J. Memb. Sci. 467, 188–194. https://doi.org/10.1016/j.memsci.2014.05.034

Dąbrowski, A., Hubicki, Z., Podkościelny, P., Robens, E., 2004. Selective removal of the heavy metal ions from waters and industrial wastewaters by ion-exchange method. Chemosphere 56, 91–106. https://doi.org/10.1016/j.chemosphere.2004.03.006

Dhami, N.K., Reddy, M.S., Mukherjee, M.S., 2013. Biomineralization of calcium carbonates and their engineered applications: A review. Front. Microbiol. 4, 1–13. https://doi.org/10.3389/fmicb.2013.00314

Dixit, R., Wasiullah, Malaviya, D., Pandiyan, K., Singh, U.B., Sahu, A., Shukla, R., Singh, B.P., Rai, J.P., Sharma, P.K., Lade, H., Paul, D., 2015. Bioremediation of heavy metals from soil and aquatic environment: An overview of principles and criteria of fundamental processes. Sustain. 7, 2189–2212. https://doi.org/10.3390/su7022189

Duo, L., Kan-liang, T., Hui-li, Z., Yu-yao, W., Kang-yi, N., Shi-can, Z., 2018. Experimental investigation of solidifying desert aeolian sand using microbially induced calcite precipitation. Constr. Build. Mater. 172, 251–262.

https://doi.org/10.1016/j.conbuildmat.2018.03.255

El Samrani, A.G., Lartiges, B.S., Villiéras, F., 2008. Chemical coagulation of combined sewer overflow: Heavy metal removal and treatment optimization. Water Res. 42, 951–960. https://doi.org/10.1016/j.watres.2007.09.009

Eryürük, K., Yang, S., Suzuki, D., Sakaguchi, I., Akatsuka, T., Tsuchiya, T., Katayama, A., 2015. Reducing hydraulic conductivity of porous media using $CaCO_3$ precipitation induced by *Sporosarcina pasteurii*. J. Biosci. Bioeng. 119, 331–336. https://doi.org/10.1016/j.jbiosc.2014.08.009

González, I., Mayoral, E., Ortiz, P., Segura, D., Vazquez, A., Barba, C., Ortiz, R., Romero, A., 2015. Use of microorganisms to improve the cementation of granular structures. Applications in the restoration of monuments. Geophys. Res. Abstr. EGU Gen. Assem. 17, 2015–14339.

Irawati, W., Riak, S., Sopiah, N., Sulistia, S., 2017. Heavy metal tolerance in indigenous bacteria isolated from the industrial sewage in Kemisan River, Tangerang, Banten, Indonesia. BIODIVERSITAS 18, 1481–1486. https://doi.org/10.13057/biodiv/d180426

Ivanov, V., Stabnikov, V., 2016. Construction biotechnology: biogeochemistry, microbiology and biotechnology of construction materials and processes. Springer. https://doi.org/10.1007/978-981-10-1445-1

Kang, C.H., Han, S.H., Shin, Y., Oh, S.J., So, J.S., 2014. Bioremediation of Cd by microbially induced calcite precipitation. Appl. Biochem. Biotechnol. 172, 2907–2915. https://doi.org/10.1007/s12010-014-0737-1

Karim, M.A., 2014. Electrokinetics and soil decontamination: concepts and overview (Review). J. Electrochem. Sci. Eng. 4. https://doi.org/10.5599/jese.2014.0054

Khan, Z., Rehman, A., Hussain, S.Z., Nisar, M.A., Zulfiqar, S., Shakoori, A.R., 2016. Cadmium resistance and uptake by bacterium, *Salmonella enterica* 43C, isolated from industrial effluent. AMB Express 6. https://doi.org/10.1186/s13568-016-0225-9

Kříbek, B., Nyambe, I., Majer, V., Knésl, I., Mihaljevič, M., Ettler, V., Vaněk, A., Penížek, V., Sracek, O., 2019. Soil contamination near the Kabwe Pb-Zn smelter in Zambia: Environmental impacts and remediation measures proposal. J. Geochemical Explor. 197, 159–173. https://doi.org/10.1016/j.gexplo.2018.11.018

Kurniawan, T.A., Chan, G.Y.S., Lo, W.H., Babel, S., 2006. Physico-chemical treatment techniques for wastewater laden with heavy metals. Chem. Eng. J. 118, 83–98.

https://doi.org/10.1016/j.cej.2006.01.015

Leteinturier, B., Laroche, J., Matera, J., Malaisse., F., 2001. Reclamation of lead/zinc processing wastes at Kabwe, Zambia: a phytogeochemical approach. South Africa J. Sci. 97, 624–627.

Lippman, M., 1990. Lead and human health : Background and recent findings. Environ. Res. 51, 1–24.

Liu, H., Yan, Y., Shao, D., Li, D., Zhang, Y., 2015. Remediation of the contaminated soils by washing with an aqueous Cysteamine Lixiviant 1–4.

Mahbub, K.R., Krishnan, K., Megharaj, M., Naidu, R., 2016. Bioremediation potential of a highly mercury resistant bacterial strain *Sphingobium* SA2 isolated from contaminated soil. Chemosphere 144, 330–337. https://doi.org/10.1016/j.chemosphere.2015.08.061

Mufinda, B., 2015. A History of Mining in Broken Hill (Kabwe): 1902-1929. University of the Free State. *Thesis*

Nyambe, I.A., Chirwa, M., Chaziya, B., 2013. Impacts of past mining activities on the ecosystem and on human health in Kabwe Town, Zambia, in: Workshop on Environmental and Health Impacts of Mining Activities in the Sub-Saharan African Countries. p. 33.

Okyay, T.O., Rodrigues, D.F., 2015. Biotic and abiotic effects on CO_2 sequestration during microbially-induced calcium carbonate precipitation. FEMS Microbiol. Ecol. 91, 1–13. https://doi.org/10.1093/femsec/fiv017

Pallavi, S., Dubey, R.S., 2005. Lead toxicity in plants. Brazil J. plant Physiol. 17, 35–52. https://doi.org/http://dx.doi.org/10.1590/S1677-0420200500010000.

Papanikolaou, N.C., Hatzidaki, E.G., Belivanis, S., 2005. Lead toxicity update . A brief review Lead toxicity update . A brief review. Med. Sci. Monit. 11, 329–336.

Pinto, P.X., Al-Abed, S.R., Reisman, D.J., 2011. Biosorption of heavy metals from mining influenced water onto chitin products. Chem. Eng. J. 166, 1002–1009. https://doi.org/10.1016/j.cej.2010.11.091

Prasad, a S.A., Varatharaju, G., Anushri, C., Dhivyasree, S., 2013. Biosorption of Lead by *Pleurotus florida* and *Trichoderma viride* 3, 66–78.

Reible, D.D., 2017. Fundamentals of environmental engineering. CRC Press. https://doi.org/10.1201/9780203755303

Rieuwerts, J., 2017. The elements of environmental pollution. Routledge. https://doi.org/10.4324/9780203798690

Rodríguez, I.A., Cárdenas-González, J.F., Juárez, V.M.M., Pérez, A.R., Zarate, M. de G.M., Castillo, N.C.P., 2018. Biosorption of heavy metals by *Candida albicans*. Adv. Bioremediation Phytoremediation. https://doi.org/10.5772/intechopen.72454

Rosca, M., Hlihor, R.M., Cozma, P., ComĂniţĂ, E.D., Simion, I.M., Gavrilescu, M., 2016. Potential of biosorption and bioaccumulation processes for heavy metals removal in bioreactors. 2015 E-Health Bioeng. Conf. EHB 2015 31–34. https://doi.org/10.1109/EHB.2015.7391487

Shim, Ho Y, Lee, K.S., Lee, D.S., Jeon, D.S., Park, M.S., Shin, J.S., Lee, Y.K., Goo, J.W., Kim, S.B., Chung, D.Y., Shim, H Y, 2014. Application of electrocoagulation and electrolysis on the precipitation of heavy metals and particulate solids in washwater from the soil washing. J. Agric. Chem. Environ. J. Agric. Chem. Environ. 3, 130–138. https://doi.org/10.4236/jacen.2014.34015

Tchounwou, P.B., Yedjou, C.G., Patlolla, A.K., Sutton, D.J., 2012. Heavy metal toxicity and the environment. EXS 101, 133–64. https://doi.org/10.1007/978-3-7643-8340-4_6

Umar, M., Kassim, K.A., Ping Chiet, K.T., 2016. Biological process of soil improvement in civil engineering: A review. J. Rock Mech. Geotech. Eng. 8, 767–774. https://doi.org/10.1016/j.jrmge.2016.02.004

Vymazal, J., 2014. Constructed wetlands for treatment of industrial wastewaters: A review. Ecol. Eng. 73, 724–751. https://doi.org/10.1016/j.ecoleng.2014.09.034

Whiffin, V.S., van Paassen, L.A., Harkes, M.P., 2007. Microbial carbonate precipitation as a soil improvement technique. Geomicrobiol. J. 24, 417–423. https://doi.org/10.1080/01490450701436505

Xu, G., Li, Dongwei, Jiao, B., Li, Dou, Yin, Y., Lun, L., Zhao, Z., Li, S., 2017. Biomineralization of a calcifying ureolytic bacterium *Microbacterium* sp. GM-1. Electron. J. Biotechnol. 25, 21–27. https://doi.org/10.1016/j.ejbt.2016.10.008

Zhu, X., Li, W., Zhan, L., Huang, M., Zhang, Q., Achal, V., 2016. The large-scale process of microbial carbonate precipitation for nickel remediation from an industrial soil. Environ. Pollut. 219, 149–155. https://doi.org/10.1016/j.envpol.2016.10.047

CHAPTER 2 IMMOBILIZATION OF SAND AND MINE WASTE USING *PARARHODOBACTER* SP.

2.1 Introduction

In this study, MICP was investigated as a method for the biocementation of Pb-contaminated kiln slag (KS) and leach plant residue (LPR) in Kabwe, Zambia. These wastes have been investigated by many researchers as a source of Pb contamination in surface and groundwater (Kribek et al., 2009) and soil (Tembo et al., 2006) in and around mine sites, and as a source of Pb exposure in children (Yabe et al., 2018), and cattle (Yabe et al., 2011). These Pb-contaminated mining wastes in Kabwe, Zambia, led the city to be labeled as one of the 10 most polluted places on Earth in 2013 (Blacksmith, 2013).

The objective of this chapter was to stabilize the mine waste and evaluate the effectiveness of this treatment method in eliminating the risk of these wastes to human health. Samples of untreated and biocemented wastes were characterized based on strength, slaking behavior, water absorption and hydraulic conductivity. Long-term chemical stability was determined by conducting mass leaching tests on the waste samples using U.S. EPA Method 1315 and analyzing the pH, conductivity, and Pb concentration of the leachate. The authors found no previous studies that evaluated the efficacy of MICP based biocementation of mine waste by investigating both strength and leachability of a pollutant of concern. Such investigations would be valuable in facilitating the long-term design of bioremediation systems using MICP based biocementation for mine waste contaminated with heavy metals. An improved understanding of this process and mechanism will provide a scientific basis for the development of sound strategies for the provision and sustainable use of ureolytic bacteria for bioremediation of Pb-contaminated sites such as the Kabwe area in Zambia.

2.2 Objectives

The objectives of Chapter 2 were to:

i. Investigate the effects of Pb on microbial growth and urease activity;
ii. Determine the effectiveness of Pb removal by *Pararhodobacter* sp. by bioprecipitation;
iii. Determine the solidification conditions for *Pararhodobacter* sp. for coarse and fine sand; and

iv. Evaluate the effectiveness of biocementation of mine waste by *Pararhodobacter* sp.

2.3 Materials and methods

2.3.1 Sand and mine waste

Fig. 2.1 shows the Toyoura sand, Misunami sand, KS and LPR used for the experiment. Their physical and chemical properties are shown in Table 2.1. The mine wastes used in this study were collected from the abandoned Kabwe Mine.

Table 2.1: Selected physical and chemical properties of KS and LPR

Parameter	Toyoura Sand	Mizunami sand	Kiln slag (KS)	Leach plant residue (LPR)
Mean diameter (D_{50}) (μm)	0.17	1.6	1000	9
Density (ρ_s) (g/cm^3)	2.64	2.67	2.88	2.39
Bioavailable Pb (mg/L)	0.00	0.00	5.40	7.87

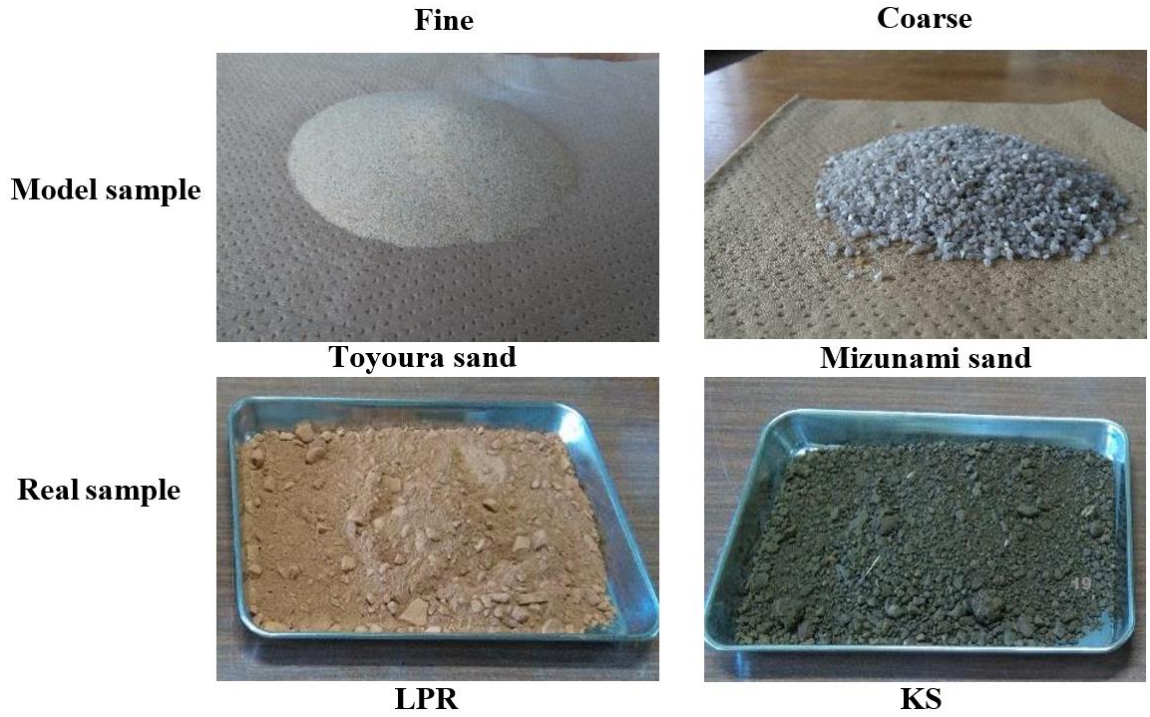

Fig. 2.1: Toyoura sand, Mizunami sand, LPR and KS used in this chapter

2.3.2 Bacteria and growth media

The ureolytic bacterium, *Pararhodobacter* sp. used in this chapter was isolated from the soil near beach rock in Okinawa, Japan (Danjo and Kawasaki, 2016).

The ZoBell2216 medium was used: 5.0 g/L Hipolypeptone, 1.0 g/L yeast extract, and 0.1 g/L $FePO_4$ prepared with artificial seawater and the final solution adjusted to pH 7.6–7.8 using 1M NaOH.

2.3.3 Cementation solution

The cementation solution was composed of 0.5 M urea; 0.5 M calcium chloride; 0.02 M sodium hydrogen carbonate; and 0.2 M ammonium chloride and nutrient broth 3 g/L.

2.3.4 Other materials and equipment

(a) Calcium Ion Meter (Horiba LAQUAtwin, CA-11, Maine, USA) was used to measure calcium ion concentration (Fig. 2.2).

Fig. 2.2: Calcium ion meter with standard solutions for calibration

(b) Low vacuum scanning electron microscope (SEM) machine (TM 3000 Miniscope, HITACHI) was used to observe the microscopic images of cemented sand test pieces (Fig. 2.3).

Fig. 2.3: Low vacuum SEM instrument

(c) X-ray diffraction (XRD) (MiniFlex™, Rigaku Co., Ltd., Tokyo, Japan) was used to identify mineral phases (Fig. 2.4).

Fig. 2.4: MiniFlex XRD equipment

(d) Calcimetric meter was used to determine the amount of $CaCO_3$ deposited within sand grains (Fig. 2.5).

Fig. 2.5: Calcimetric meter setup

(e) Metal ion concentration was determined by inductively coupled plasma atomic emission spectroscopy (ICP-AES-9820, Shimadzu Corporation, Tokyo, Japan) (Fig. 2.6).

Fig. 2.6: Inductively coupled plasma atomic emission spectroscopy

(f) Hydraulic conductivity was measured by the falling head method using a DIK 4000 system (Daiki Rika Kogyo Co., Ltd., Saitama, Japan) (Fig. 2.7).

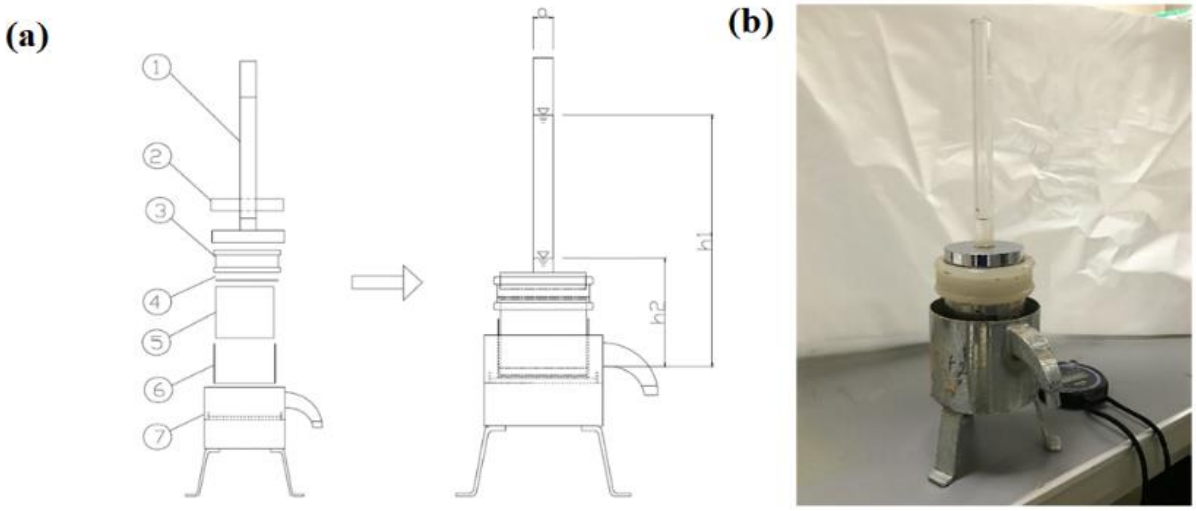

Fig. 2.7. (a) DIK 4000 system for measuring hydraulic conductivity where 1 = scale tube; 2 = weight for supporting scale tube; 3 = silicon rubber ring; 4 =O ring; 5 = cylindrical sample holder; 6 = casing for sample holder; 7 = water tank. (b) DIK 4000 system used in this study with a stopwatch

(g) Needle Penetrometer (SH-70, Maruto Testing Machine Company, Tokyo, Japan) was used to estimate Unconfined compressive strength (UCS).

(h) Other reagents included phenol, hydrochloric acid, nitric acid, sodium nitroprusside, and hypochlorite reagent.

(i) MATCH 3.4 software was used in conjunction with the International Centre for Diffraction Data (ICDD) database for identification of crystalline phases of XRD data.

2.4 Experimental methods

2.4.1 Effect of Pb on microbial growth

The effect of Pb on *Pararhodobacter* sp. was evaluated to elucidate its usefulness in bioremediation. Different concentrations of Pb^{2+} (0.00, 0.01, and 0.5 mM) were prepared in 100 mL Erlenmeyer flasks containing *Pararhodobacter* sp. and ZoBell2216 culture medium and the time course of cell growth was determined based on the optical density (OD_{600}) values at 600 nm by UV-visible for 14 days in the presence of Pb^{2+} following the schematic diagram in Fig. 2.8.

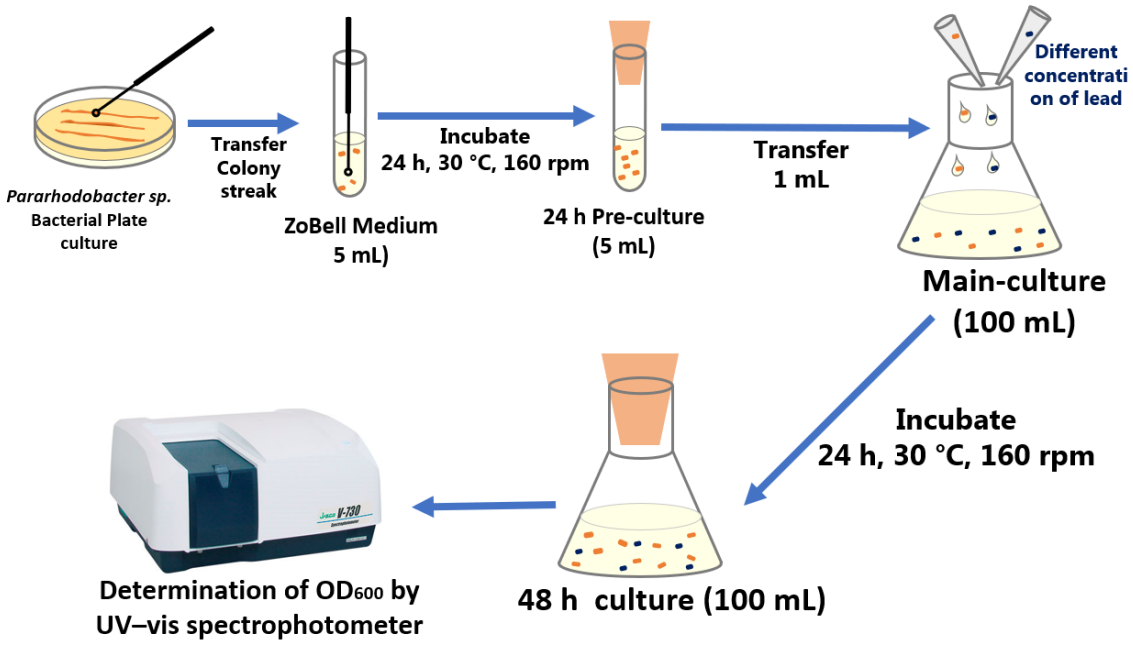

Fig. 2.8: Flow chart on how the effect of Pb on *Pararhodobacter* sp was determined

2.4.2 Effect of Pb on urease activity

The urease activity of bacterial cells was determined by monitoring ammonium ions generated in urea hydrolysis using the indophenol blue method based on Berthelot's reaction in a water bath maintained at 30 °C (Weatherburn, 1967; Natarajan, 1995). To determine the effects of Pb on urease activity, different concentrations of lead (0 - 0.5 mM) were added. Samples were then collected at intervals of 5 min (0, 5, 10 and 15 min) and passed through a 0.22 µm filter to remove cells. Next, a 2 mL aliquot of the filtered sample was mixed with phenol nitroprusside reagent (4 mL) (0.25 M phenol in 100 mL of deionized water containing 23 µM of sodium nitroprusside) and hypochlorite reagent (4 mL) (0.05 M sodium hydroxide in 100 mL of deionized water containing 7.5 mL bleach (5 % NaOCl)). Each reaction mixture was vortexed and then incubated at 50 °C - 60 °C for 10 minutes.

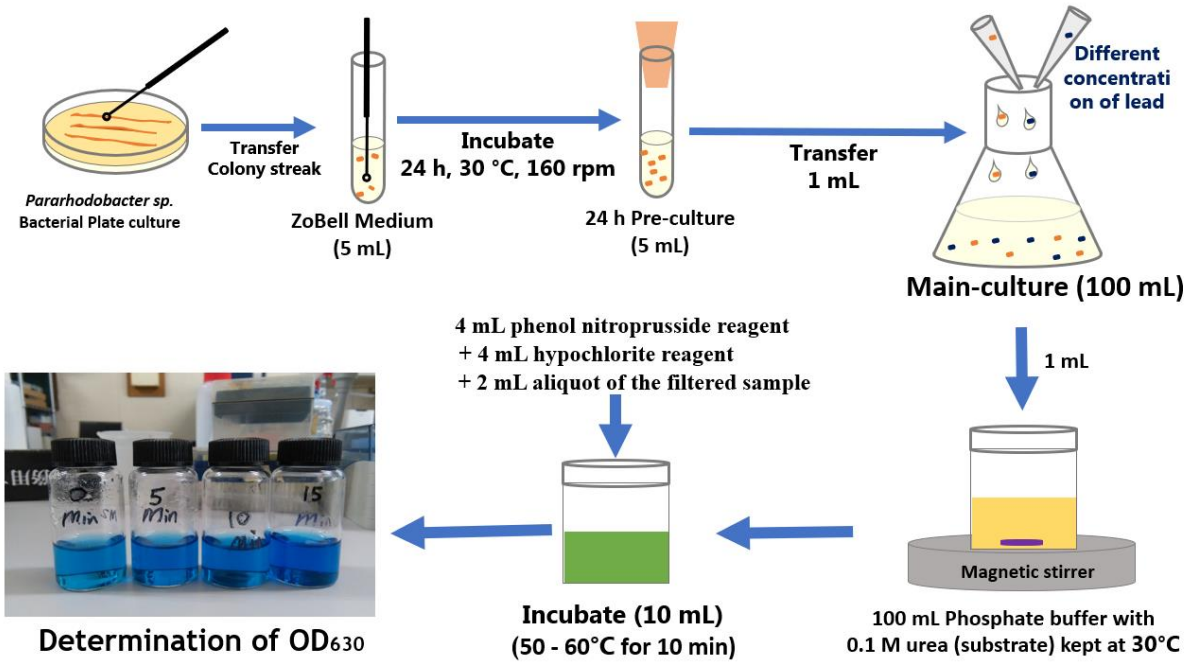

Fig. 2.9: Flow chart for determination of urease activity using the indophenol blue method

The amount of ammonium ion released because of urea hydrolysis was determined by referring to a previously prepared standard curve relating the absorbance at 630 nm to ammonium ion concentration (0–10 mg/L) (Fig. 2.9). Using this curve, one unit of urease activity (U) was defined as the amount of enzyme that would hydrolyze 1 µmol of urea per minute. The release of 2 µmol of ammonia is equivalent to the hydrolysis of 1 µmol of urea. Fig. 2.9 summarizes the process followed to determine the effect of Pb urease activity.

2.4.3 Bioprecipitation of calcium carbonate and Pb

Pararhodobacter sp. was precultured for 24 h in 5 mL ZoBell2216 medium, after which 1 mL of preculture was inoculated into 100 mL of the main culture at 30 °C for 48 h with continuous aeration at 160 rpm. The bacterial suspension (5 mL) was then added to 2 mL calcium chloride (0.5 M) and 2 mL urea (0.5 M), after which different lead final concentrations were added (0 mM, 0.01 mM and 5 mM). The mixture was subsequently incubated for 6 h at 30 °C with shaking (160 rpm) and then further centrifuged (15,000 rpm for 5 minutes) to collect the precipitate. The concentration of Pb in the supernatant was determined by inductively coupled plasma atomic emission spectroscopy whereas the precipitate was analyzed by XRD/SEM as shown in Fig. 2.10.

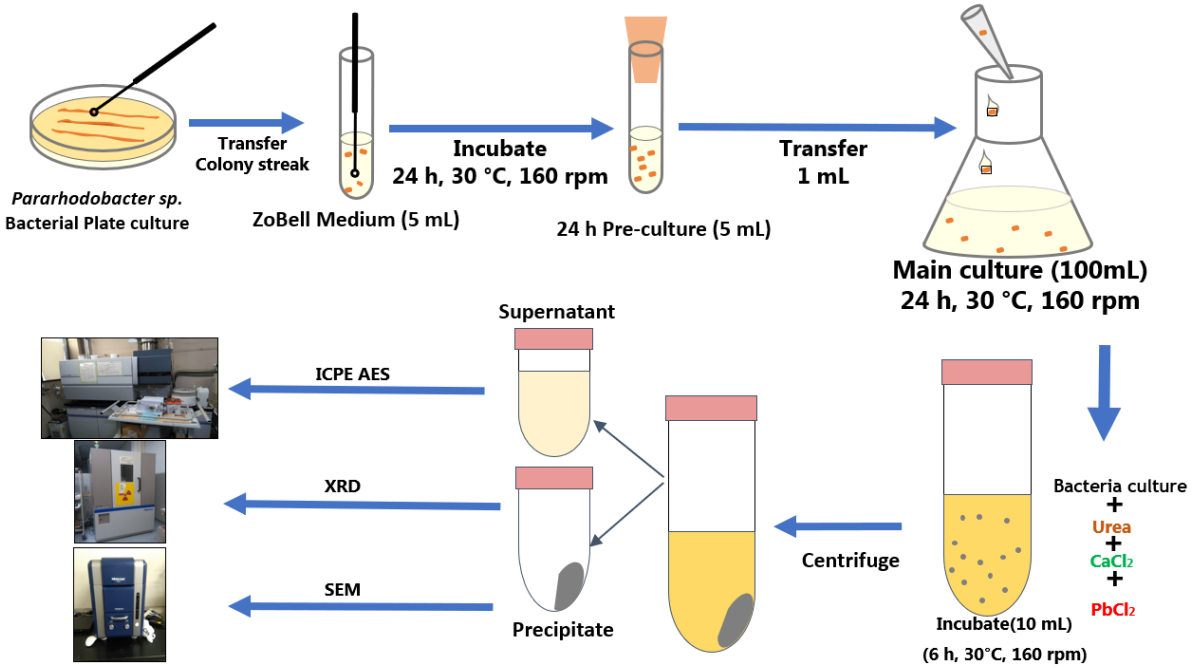

Fig. 2.10: Flow chart for bioprecipitation experiments

2.4.4 Biocementation of sand

All syringe biocementation experiments were conducted in an incubator at 30 °C. 40 g of fine, coarse sand and mine waste were oven-dried at 105 °C for 48 h and then placed in a 35 mL syringe (mean diameter, D_{50} = 2.5 cm and height, h = 7 cm). The laboratory experiment was designed to mimic the field conditions in Kabwe mine as closely as possible based on grain size, with the very fine and coarse sand representing the plant residue and kiln slag, respectively. The mixed system was selected to mimic slag used to cover leached plant residue to prevent water and wind erosion on site. Bacterial culture (16 mL) (OD_{600} = 1.0 = 10^9 CFU/mL) and 20 mL of cementation solution were sequentially added to the syringe and drained, leaving about 2 mL of the solution above the surface of the sand to maintain wet conditions. The outlet solution from the syringe was measured for pH and Ca^{2+}. After 14 days of curing, the UCS was estimated using a needle penetration device. Fig. 2.11 shows the conceptual model for the biocementation experiment.

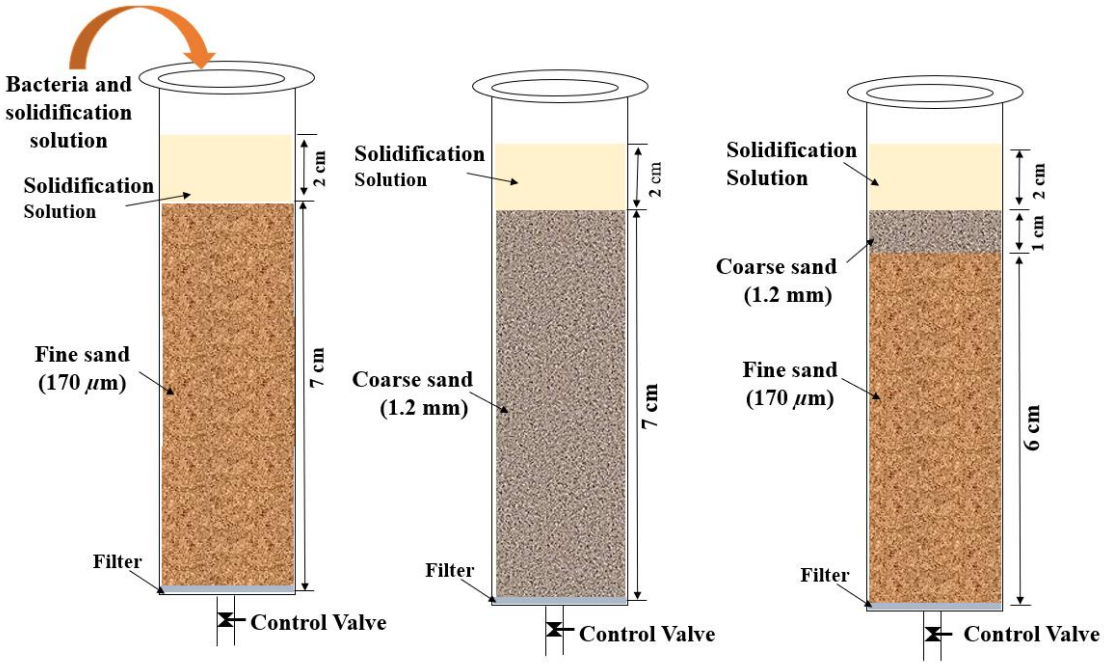

Fig. 2.11: Conceptual setup and of the syringe biocementation of coarse- and fine-grained sand

2.4.5 Evaluation of the effectiveness of biocementation of mine waste by *Pararhodobacter* sp.

Physical testing procedures

a) Biocementation procedure of mine waste and strength determination

Immersed and flow through methods were used to biocement the waste. In the first set of experiments, 2 mL of cementation solution was left above the surface of the waste to mimic saturated conditions, so this procedure was called the immersed method (Fig. 2.12(a)). The second set of experiments was conducted such that solution was added sequentially with all solution drained, so this procedure was called the flow through method (Fig. 2.12(b)). Additionally, KS/LPR was an amendment formulated to mimic the mixing of 50% KS and 50% LPR by weight to represent the mix of materials in waste piles at the mine site with cases in Table 2.2.

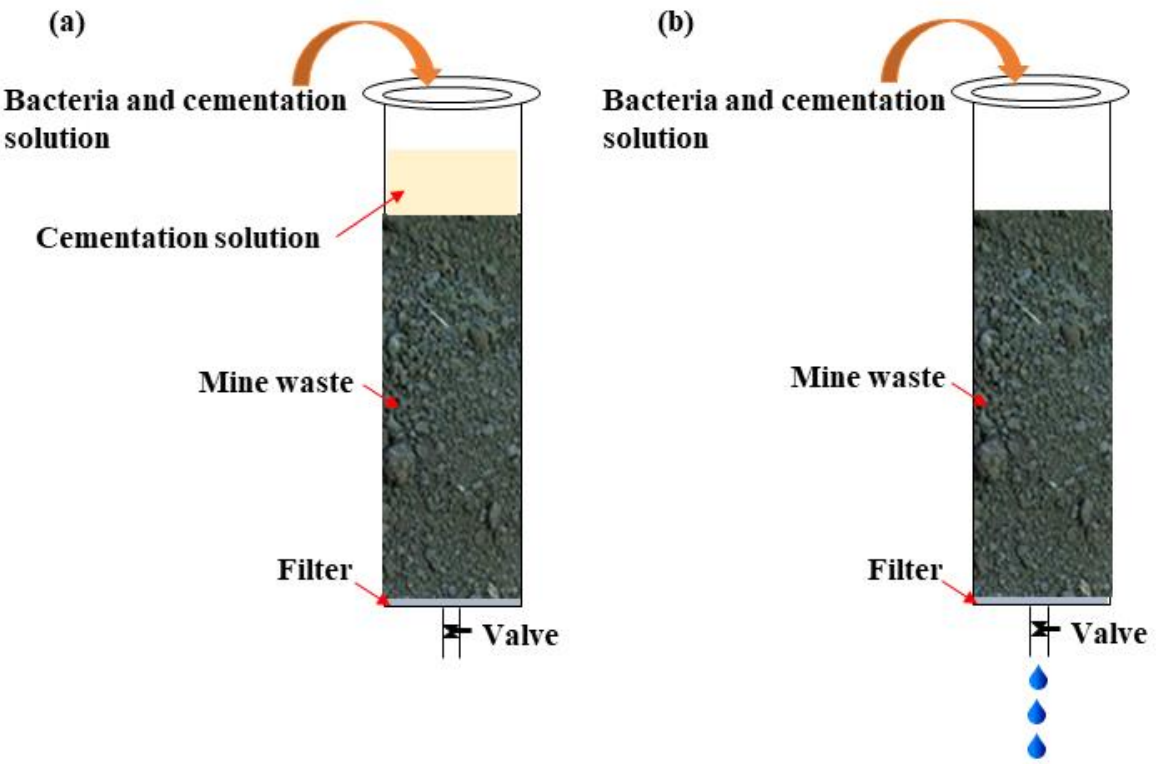

Fig. 2.12: Experimental setups for (a) immersed and (b) flow through methods for biocementation mine wastes

Unconfined compressive strength (UCS) was measured using a needle penetration device (SH-70, Maruto Testing Machine Company, Tokyo, Japan) according to ISRM (International Society for Rock Mechanics 2015). To determine the strength of a sample, the needle penetration inclination (Np) value of each sample were measured using the needle penetration device and the UCS was estimated from Np value. The strength of the sample (Np value) was calculated using Equation 2.1

$$Np = F / D \qquad 2.1$$

Where F is the penetration load (N) and D is the depth of penetration (mm). The unit of Np is N/mm. From the chart of UCS-Np correlation, estimated UCS value was determined.

Table 2.2: Biocementation conditions of the mine waste

	Material type	Treatment type	Bacteria	Cementation addition
Case 1	KS and LPR	Flow through	No	Distilled water
Case 2	KS and LPR	Immersed	No	Distilled water
Case 3	KS	Flow through	Yes	Yes
Case 4	KS	Immersed	Yes	Yes
Case 5	KS and LPR	Flow through	Yes	Yes
Case 6	KS and LPR	Immersed	Yes	Yes

b) Capillary water absorption tests

The water absorption tests were conducted in accordance with ASTM C1585-13 (ASTM International 2013). The surface subjected to water absorption was immersed in water (2±1 mm depth) in a shallow tray and covered to prevent air circulation and contact with atmospheric water vapor. The water absorption coefficient [S, kg/(m^2·$h^{0.5}$)] was determined by the slope of the curve of the water absorbed per unit area (kg/m^2) and the square root of the sinking time ($sec^{0.5}$). The tests were conducted on untreated KS and KS/LPR as well as biocemented KS and KS/LPR that was prepared by both immersed and flow through methods.

c) Jar slake test

The jar slake tests were conducted according to ASTM D4644-16 (ASTM International 2016). In brief, samples of biocemented KS and KS/LPR were oven-dried at 105 °C, cooled and placed into empty plastic antistatic weighing dishes. Distilled water was poured into the dishes to submerge each sample for 24 h, and the samples were observed and described after 30 min and after 24 h. The samples were classified as 1-6 with corresponding descriptions as follows: (1) degrades to a pile of flakes or mud; (2) breaks rapidly and/or forms many chips; (3) breaks slowly and/or forms few chips; (4) breaks rapidly and/or develops several fractures; (5) breaks slowly and/or develops few fractures; and (6) no change. The tests were conducted on untreated KS and KS/LPR as well as biocemented KS and KS/LPR that was prepared by both immersed and flow through methods.

d) Hydraulic conductivity

Hydraulic conductivity was conducted by the falling head method using a DIK 4000 system (Daiki Rika Kogyo Co., Ltd., Saitama, Japan) according to ASTM D5084-03 (ASTM International 2003). The molds for DIK 4000 were used for solidification of samples which has an outside dimension of width 530 mm x diameter 260 mm x height of 380 mm. To calculate the hydraulic conductivity, Equation 2.2 was used.

$$K = \frac{2.3a.L}{A.t} \log_{10} \frac{h_1}{h_2} \qquad 2.2$$

Where K (m/sec) is the hydraulic conductivity; a = 0.503 cm^2 cross-sectional area of the scale tube, L = 5.1 cm which is thickness of the sample; A = 19.6 cm^2 which is the sectional area of sample; h_1 = 17 cm; h_2 = 7 cm; and t is the time (sec) taken for water level to drop from top to bottom of the scale tube.

Chemical characterization methods

a) $CaCO_3$ content

The $CaCO_3$ content was determined using calcimetric method using 3M HCl acid according to literature (Hukue et al., 2001). The untreated and top center part of a biocemented KS and KS/LPR treated by immersed and flow through methods. A standard curve was developed to relate gas pressure and the amount of $CaCO_3$ present as shown in Fig. 2.13 The $CaCO_3$ content was calculated using Equation 2.3

$$CaCO_3 \text{ Content } (\%) = \frac{W_c}{W_s - W_c} \qquad 2.3$$

Where Wc = weight of corresponding $CaCO_3$ (g) content; and Ws = Initial dry mass (g) of the specimen.

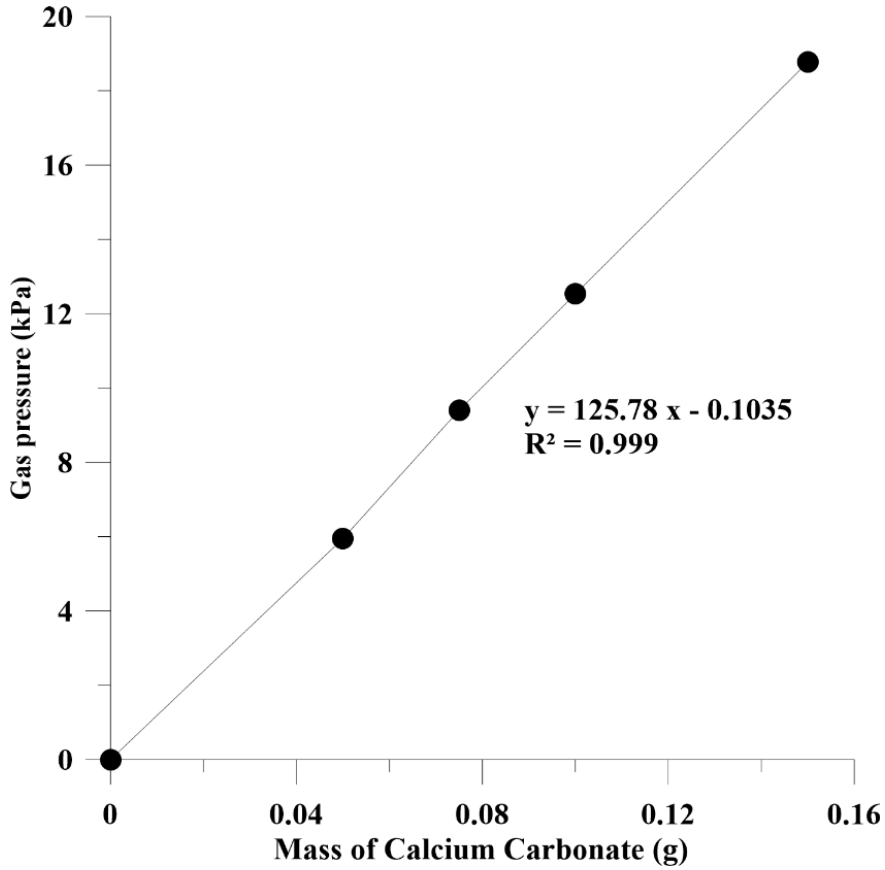

Fig. 2.13: Relationship between gas pressure and mass of calcium carbonate.

b) Leaching test of biocemented KS and KS/LPR

US EPA Method 1315 for mass transfer rates of constituents in monolithic materials using a semi-dynamic tank leaching procedure was used to determine the cumulative release of Pb from the biocemented KS and KS/LPR, as shown in Fig. 2.14 (U.S. EPA 2017). The mass transfer leaching method was used to determine the cumulative release of Pb from the biocemented KS and KS/LPR, as shown in Fig. 2.14. To determine the rate of release, biocemented KS and KS/LPR samples, biocemented by the flow-through method, were immersed in deionized water with the liquid–surface area ratio (L/A) maintained at 9 ± 1 mL/cm^2. Leaching was allowed to continue for 231 days with leachate collected in a sealed high-density polyethylene (HDPE) bucket at defined intervals. Leachate was collected after 8 h, 1 day, 2 days, every 7 days from day 7 through day 49, after 63 days, and every 14 days from day 63 through day 231. Pb^{2+} concentration, pH, and conductivity were measured for the collected leachate at the end of each interval. The leachate was filtered through a 0.45 µm nylon

filter into a polypropylene centrifuge tube, acidified, and stored in a refrigerator at 4 °C for analysis by ICP-AES.

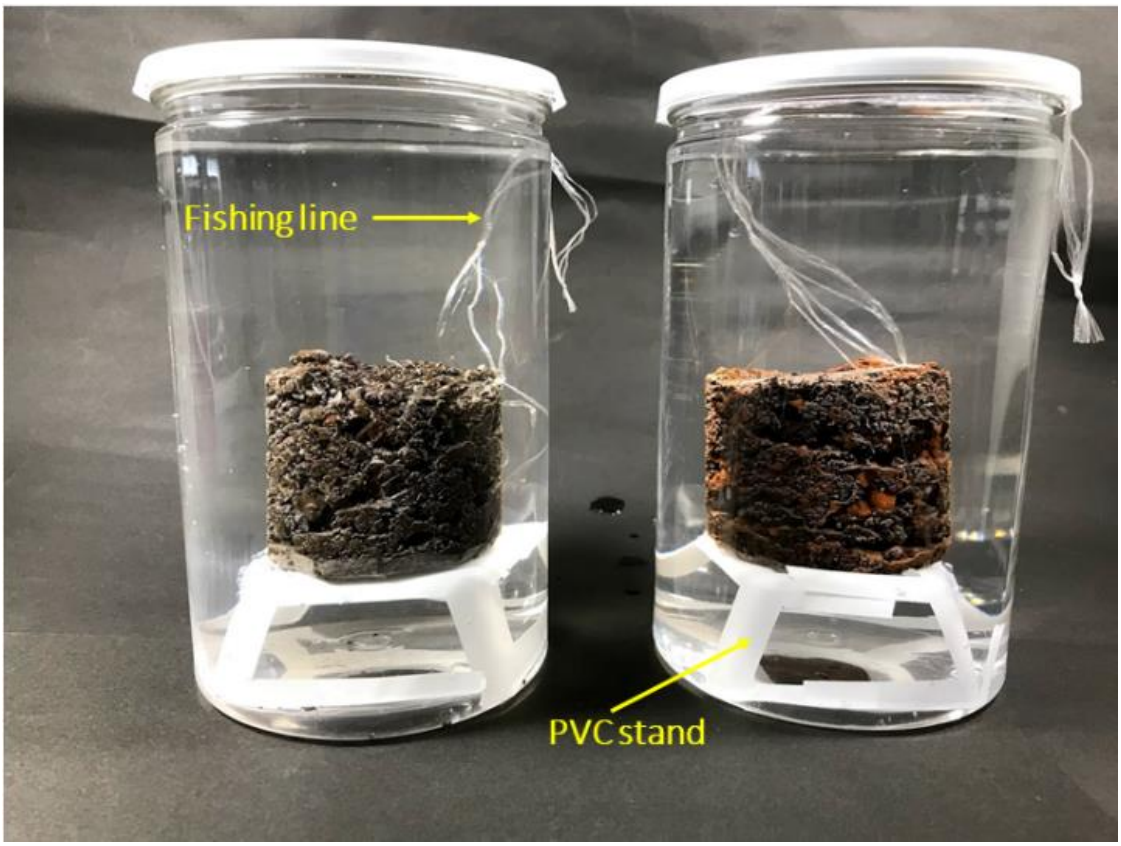

Fig. 2.14 USA EPA Method 1315 setup of the 3D leaching configuration of (a) biocemented KS and (b) biocemented KS/LPR

2.5 Results and discussion

2.5.1 Effect of Pb on microbial growth

The effect of Pb on microbial growth is shown in Fig. 2.15. *Pararhodobacter* sp. clearly exhibited increased growth following the lag, logarithmic, stationary, and retardation phases in Pb-free media (Fig. 2.15a). In the presence of Pb, the logarithmic phase was slightly retarded and an overall decrease in growth was observed. The effects of Pb on microbial growth were negligible, whereas no growth was observed for concentrations greater than 1 mM (data not shown). These results indicate that *Pararhodobacter* sp. can be used for bioremediation of Pb, even though it was not isolated from a Pb contaminated site (Kang et al., 2015). The measured pH of the solution decreased during the logarithmic phase, then increased consistently (Fig. 2.15b). It is unclear why a high pH was maintained during incubation; however, this could have occurred because of the release of metabolites in the solution, such as ammonia, by the live

cells. The ammonia generation could have originated from amino acids contained in the yeast extract. In many studies, increased pH was only recorded when urea was added to the growth media. These findings are in tandem with those of previous studies, although the effects of Pb ions differ for different microorganisms because of different inhibitory concentrations among organisms (Govarthanan et al., 2013; Naik and Dubey, 2013).

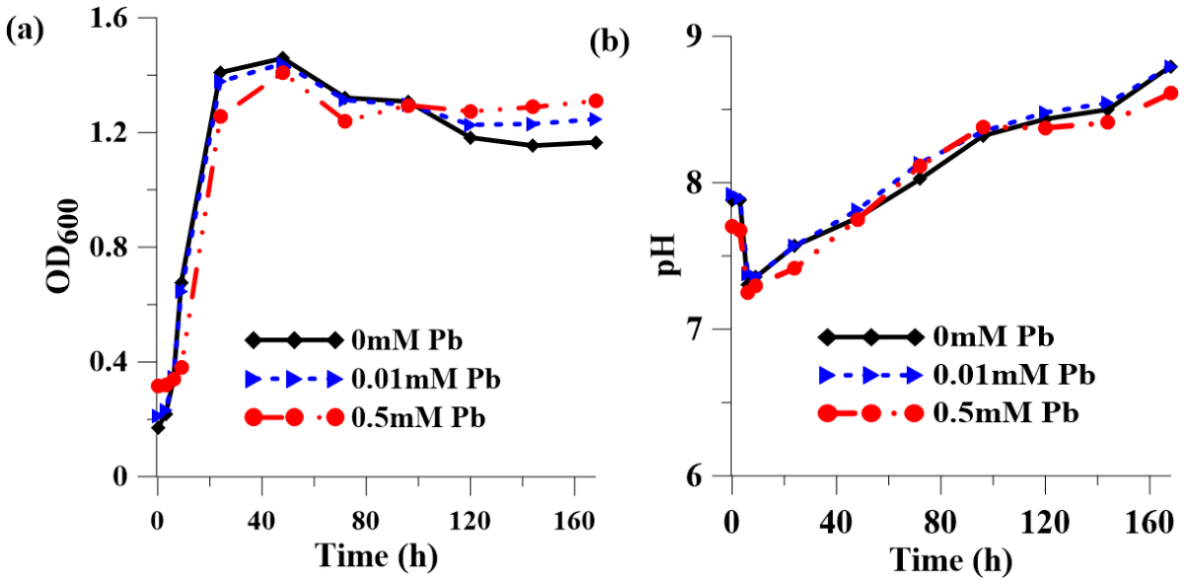

Fig. 2.15: Effect of Pb on *Pararhodobacter* sp. growth curve based on OD_{600} method

2.5.2 Effect of Pb on urease activity

Urease activity of bacterial cells was studied because it serves as a good bioindicator of enzyme activity in the MICP bioremediation technique and is used to assess environmental health changes occurring in the soil environment. As shown in Fig. 2.16, the urease activity was not significantly affected by Pb. This pattern, which was probably because of the effects of Pb on enzyme activity, reinforces the findings reported by Fujita et al. (2017), who found that urease accumulated in/on cells of *Pararhodobacter* sp. However, it has been reported that a significant decrease in enzyme activity and microbial activity because of heavy metals pollution of aquatic and soil ecosystems (Begum et al., 2009). The present study revealed a negligible decreased in urease and microbial activity. These results were probably because of other factors such as synergy of heavy metals as reported by Nwuche and Ugoji (2008), who observed inhibition of soil microbial activities in response to a combination of Cu and Zn.

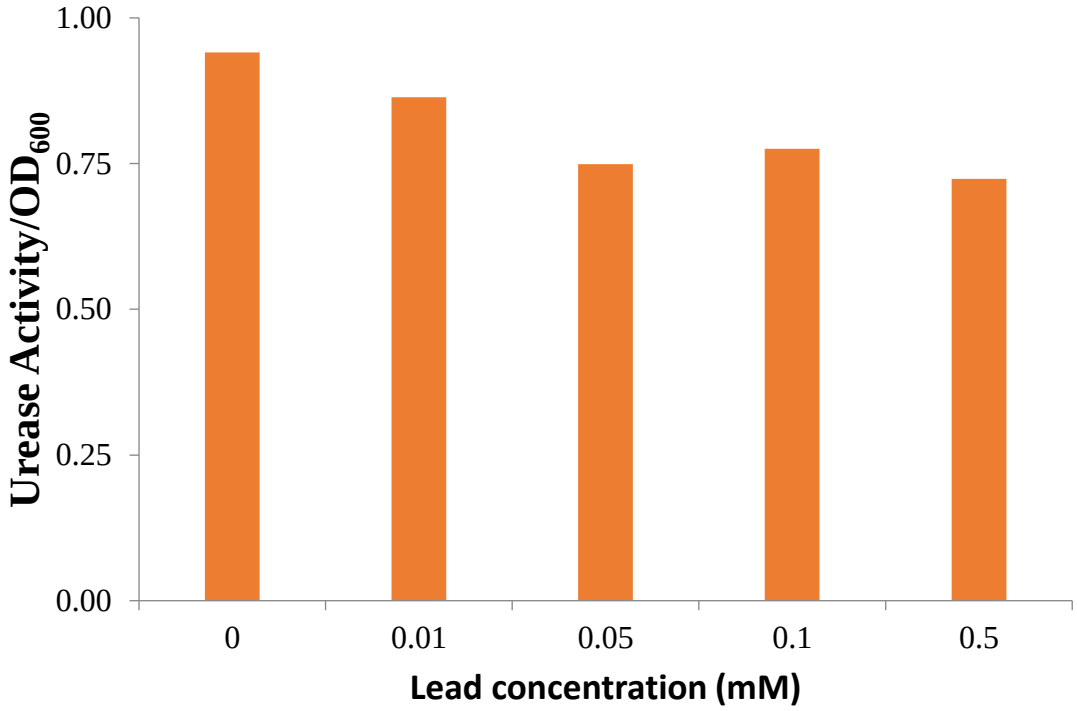

Fig. 2.16: Effect of Pb on urease activity based on the OD_{600} of *Pararhodobacter* sp. Values are averages from two independent experiments.

2.5.3 Pb bioprecipitation by *Pararhodobacter* sp

Pararhodobacter sp. was effective at complete removal of Pb^{2+}. Comparison of the removal percentage of Pb during bioprecipitation between this study and previous studies shows comparable figures to other ureolytic bacteria isolated from various sites such as *Rhodobacter spharoides* isolated from an oil field achieved 90.31% (Li et al., 2016); *Enterobacter cloacae* isolated from an abandoned mine achieved 68.1% (Kang et al., 2015); *Sporosarcina pasteurii* achieved 100% (Mugwar and Harbottle, 2016)**;** and *Terrabacter tumescens* achieved 100% (Li et al., 2015). The capability of *Pararhodobacter* to completely remove Pb lies in its ability to efficiently hydrolyze urea to generate carbonate ions and elevate the pH to alkaline conditions (8.0–9.1), which promotes precipitation of Pb and $CaCO_3$.

Fig. 2.17 shows SEM images and XRD patterns of the control (a, c) and bioremediated (b, d) precipitates. Fig. 2.17(a) shows the spherical particles of $CaCO_3$ precipitated in the absence of Pb and confirmed by XRD analysis in Fig. 2.17(b). This finding has been observed from previous studies that reported different polymorphs of $CaCO_3$ in the form of vaterite and calcite being formed when biomineralization occurs via mediation by bacteria (Park et al.,

2010; González-Muñoz et al., 2010). Vaterite does not occur in abundance in the natural environment but is an important precursor in the calcite formation of a more stable form of $CaCO_3$ (Nehrke and Van Cappellen, 2006). Furthermore, Fig. 2.17(b) shows the SEM image of precipitate in the presence of Pb. In the figure, framboidal aggregates were identified as vaterite, whereas spherical and rhombohedral shaped precipitates were identified as calcite. In the MICP process, $CaCO_3$ can adsorb or incorporate free toxic ions Pb^{2+} through substitution of the divalent calcium ion in the $CaCO_3$ lattice (Fig. 2.17(d)). Detoxification of the Pb into insoluble form occurs when the toxic free ion is transformed into a chemically stable and non-toxic form of lead as elucidated in another study by Li et al., (2013). These characteristics affect dissolution and solubility Pb in mine waste.

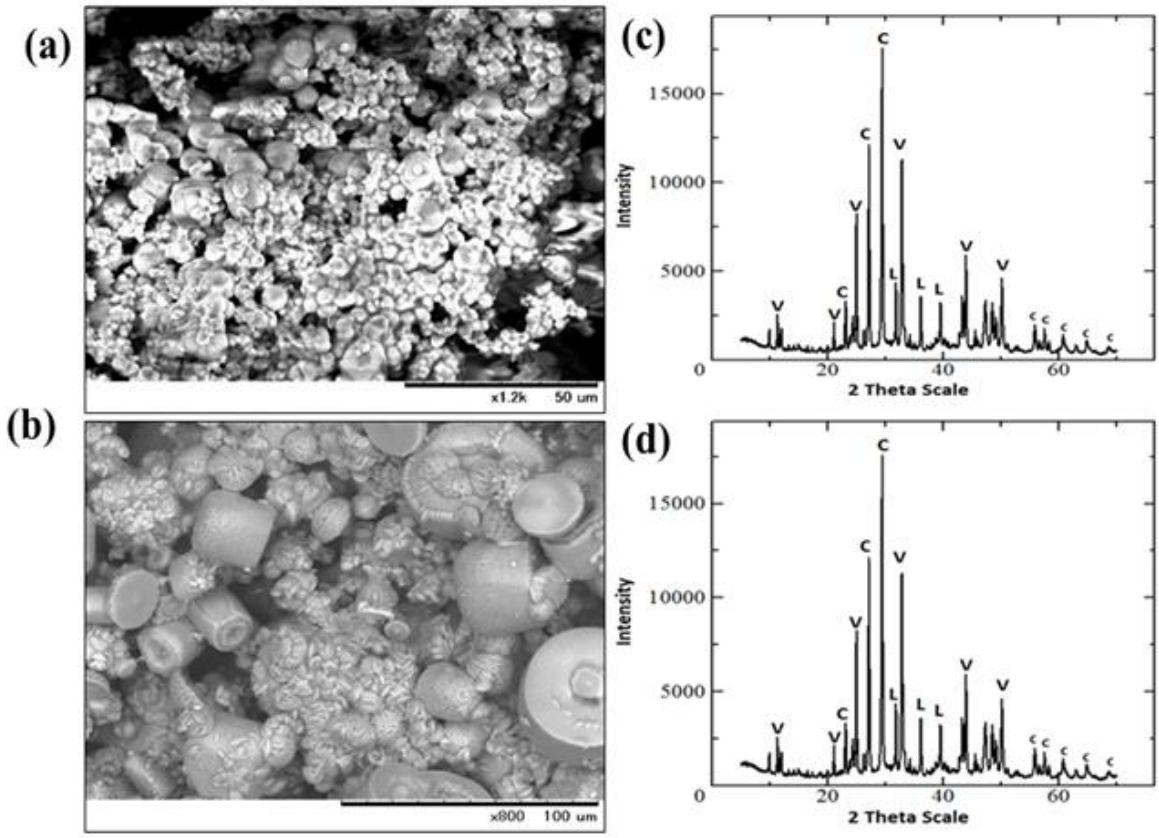

Fig. 2.17: SEM images (a, b) and XRD data (c, d) of precipitates formed by *Pararhodobacter* sp. in the absence (a, c) and presence of 5 mM Pb (b, d). (C = Calcite ($CaCO_3$); V = Vaterite ($CaCO_3$); L = Lead Oxide (PbO)).

2.5.4 Syringe biocementation experiment

Pictorial images of sand samples from all syringe biocementation experiments after 14 days are shown in Fig. 2.18. The UCS comparison of the results obtained after varying the injection interval (once, twice, four and seven times) is summarized in Table 2.3 and graphically shown in Fig. 2.18. The classification scheme adopted in this paper was based on that developed by Shafii-Rad and Clough (1982), in which weakly cemented sand was defined as having a UCS of less than 0.3 MPa, moderately cemented sand was defined as having a UCS between 0.4 Mpa and 1 MPa and solidified sand was that with greater than 1 MPa (Shafii and Clough, 1982). As shown in Fig. 2.19, generally the UCS increased with increasing injection interval as well as the top part of the sample was solidified more than the bottom. This increase in UCS at the top can be attributed to calcite crystals forming cohesive bonds between sand grains mediated by *Pararhodobacter* sp, which accumulated at the top of the sample.

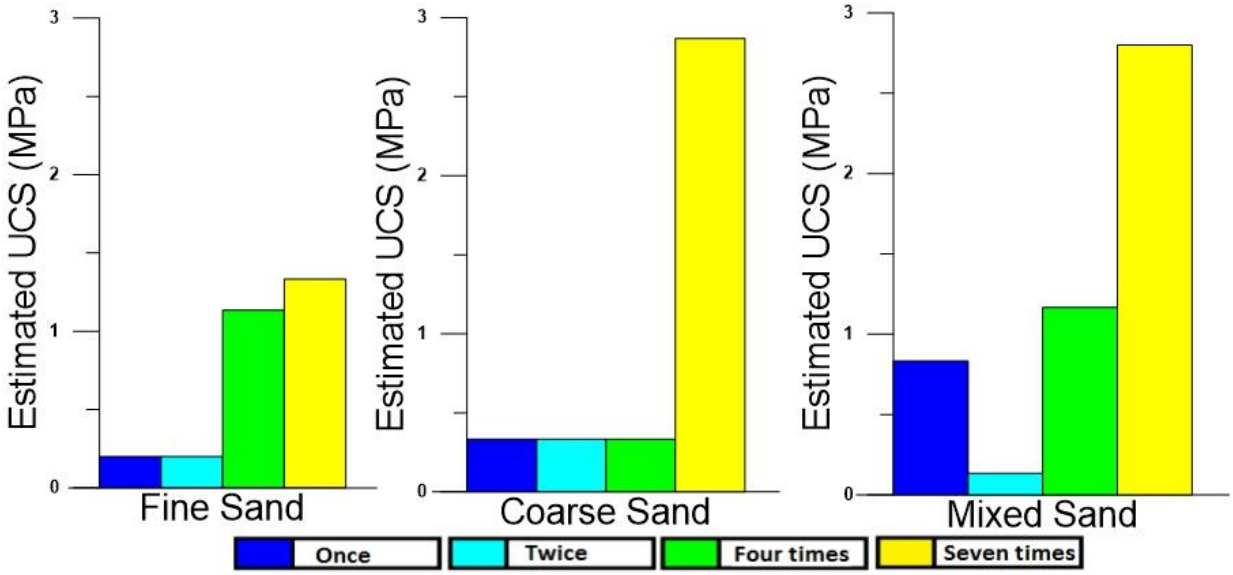

Fig. 2.18: UCS comparison of the results obtained when varying the bacteria injection for fine, coarse and mixed sand.

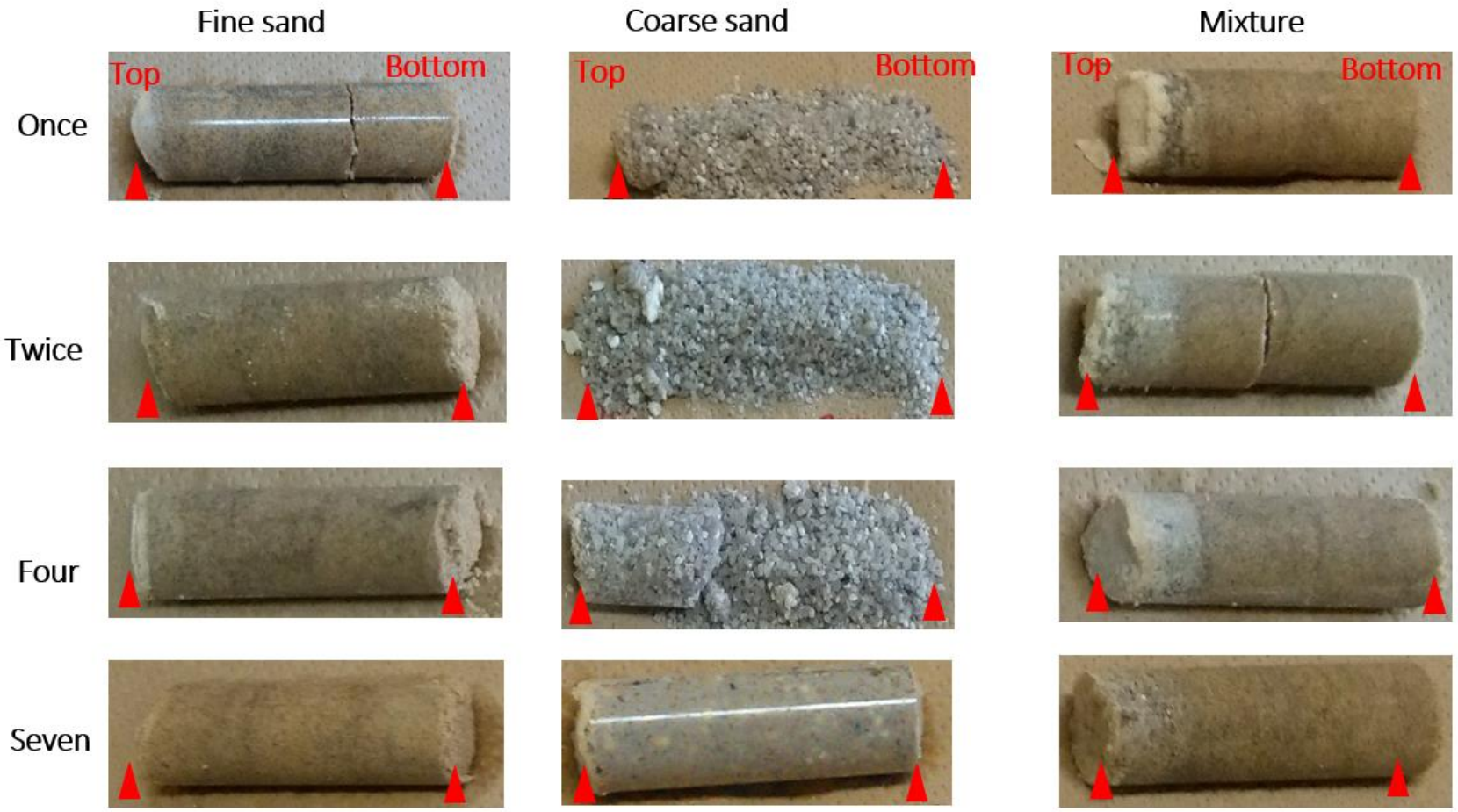

Fig. 2.19: Pictorial images of the results of all syringe tests after 14 days while varying the bacterial injection interval to once, twice, four and seven times. Left, fine sand; center, coarse sand; right, mixture of course and fine sand

Table 2.3: Results of coarse and fine sand at different injection intervals and the biocementation conditions

	Sand particle size	Bacterial injection times	Biocementation solution injection	Bacterial OD_{600}	Temp. (°C)	Timing (Day)	Condition of biocementation		
							Top	Middle	Bottom
Case 1	170 µm	Once	Daily	1.0	30	14	Moderately solidified	Not solidified	Not solidified
Case 2	1.2 mm	Once	Daily	1.00	30	14	Solidified	Not solidified	Not solidified
Case 3	170 µm/1.2 mm	Once	Daily	1.00	30	14	Solidified	Not solidified	Not solidified
Case 4	170 µm	Twice	Daily	1.00	30	14	Moderately solidified	Not solidified	Not solidified
Case 5	1.2 mm	Twice	Daily	1.00	30	14	Not solidified	Not solidified	Not solidified
Case 6	170 µm/1.2 mm	Twice	Daily	1.00	30	14	Weakly solidified	Not solidified	Not solidified
Case 1	170 µm	Four times	Daily	1.00	30	14	Solidified	Solidified	Solidified
Case 2	1.2 mm	Four times	Daily	1.00	30	14	Solidified	Not solidified	Not solidified
Case 3	170 µm/1.2 mm	Four times	Daily	1.00	30	14	Moderately Solidified	Solidified	Solidified
Case 4	170 µm	Seven times	Daily	1.00	30	14	Solidified	Solidified	Solidified
Case 5	1.2 mm	Seven times	Daily	1.00	30	14	Solidified	Solidified	Solidified
Case 6	170 µm/1.2 mm	Seven times	Daily	1.00	30	14	Solidified	Solidified	Solidified

Increasing cohesive bonds result in cementation leading to decreased permeability, as was observed during the investigation. Therefore, MICP can both immobilize the Pb and induce high resistance of the contaminated materials to erosion. This phenomenon was also observed when conducting a steep slope experiment using *Sporosarcina pasteurii* (Salifu et al., 2016a). Overall, the data obtained using the syringe test demonstrated that MICP is a viable option for use in coarse- and fine-grained sand. In syringe experiments, the pH value ranged from 8.0 to 9.5, which is similar to what has been observed in other studies (Stocks-Fischer et al., 1999). The calcium ion concentration was lower in the first 7 days of the experiment, indicating deposition of calcite in the column and a decrease in the deposition in the latter half. Clogging of the porous media was greater in coarse sand than in finely graded sand. This clogging was because of the cell growth and calcium carbonate formation that accompany the MICP process.

2.5.5 Evaluation of the effectiveness of biocementation of mine waste by *Pararhodobacter*

After having determined the biocementation conditions using the model samples from subsection 2.5.1 to 2.5.4 these conditions are summarized in Table 2.4.

Table 2.4: Solidification conditions for the fine and coarse sand

Parameter	Solidification condition
Temperature	30 ^{o}C
Bacterial concentration (OD_{600})	4.0
Bacterial injection interval	4.0
Calcium source concentration	0.5 M
Urea concentration	0.5 M

These conditions were applied to KS and LPR in this subsection. Both physical and chemical characterization of the control and biocemented were investigated in order to determine the effectiveness of MICP on mine waste biocementation as an immobilization technique as illustrated in Fig. 2.20

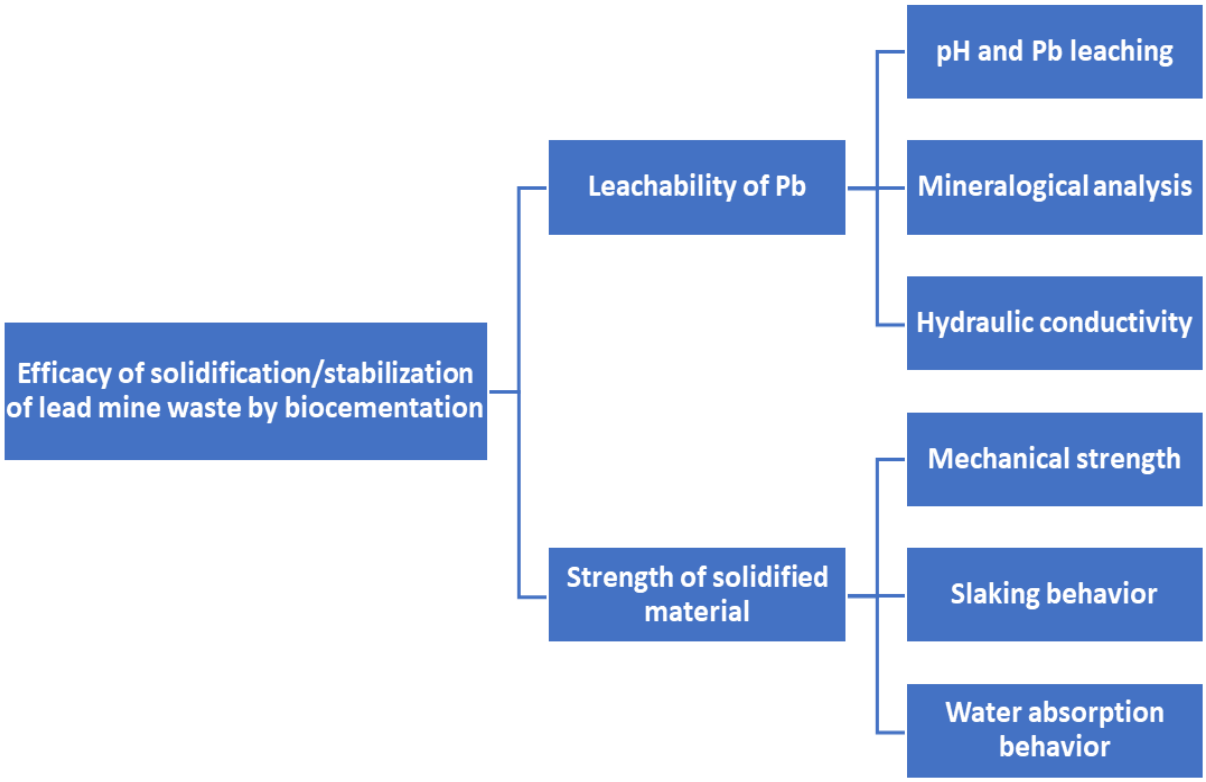

Fig. 2.20: Flowchart showing the research methodology adopted in this study to evaluate both the leachability and the strength of immobilized mine waste

Physical characterization of the biocemented waste

a. UCS of biocemented mine wastes

UCS was used to determine the effectiveness of the MICP cementation process on the mine wastes. Fig. 2.21 shows untreated and biocemented KS and KS/LPR prepared by the immersed and flow through methods and Table 2.5 shows the corresponding estimated UCS results. Preparation by the immersed method resulted in biocemented waste with greater strength for both KS and KS/LPR. Biocemented KS, prepared by the immersed method, had a maximum estimated UCS of 8.0 MPa, compared to 5.0 MPa when prepared by the flow through the method. Biocemented KS/LPR, prepared by the immersed method, had a maximum UCS of 4.0 MPa, compared to only 2.8 MPa when prepared by the flow-through method. This result is comparable to increases in compressive strength reported by previous researchers for MICP of mine tailing and Cr slag using *Bacillus* sp. CS8 and *Sporosarcina pasteurii*, respectively (Chen et al., 2017; Achal et al., 2013).

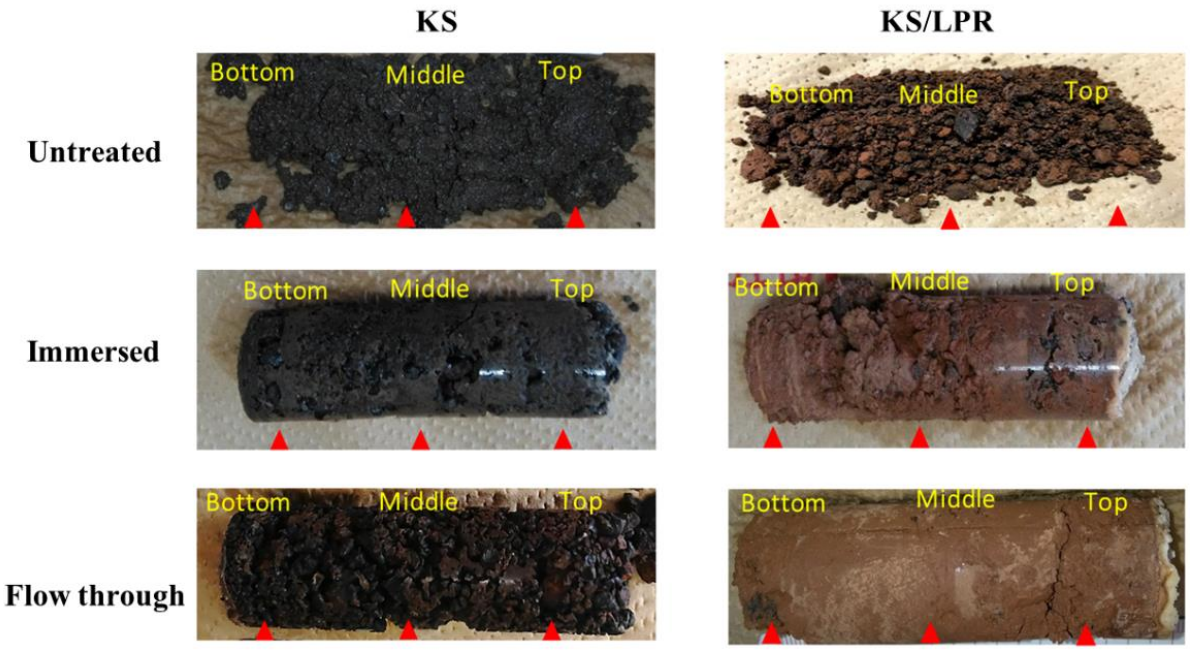

Fig. 2.21: Comparative view of untreated and treated KS and KS/LPR prepared by the immersed and flow through methods

Table 2.5: Estimated UCS of untreated and biocemented KS and KS/LPR by the immersed and flow through method.

	Estimated UCS of KS (MPa)			Estimated UCS of KS/LPR (MPa)		
	Top	Middle	Bottom	Top	Middle	Bottom
Untreated	0.0	0.0	0.0	0.0	0.0	0.0
Immersed	8.0	1.8	1.7	4.0	0.0	0.0
Flow through	5.0	4.6	2.5	2.8	2.1	0.5

Statistical analysis revealed that there was a non-significant difference found between the control and KS treated by immersed method ($p = 0.10$). This result could be due to the accumulation of reactants and bacteria at the injection point hence the top only of the specimen was solidified whereas comparison between the means of the control and flow through method yielded a significant difference ($p = 0.02$). This further agrees with the results of a previous study that found that the flow through method models environmental conditions and is more conducive for effective formation of $CaCO_3$ crystals at various degrees of saturation (Cheng et al. 2013). For KS/LPR, statistical analysis revealed that there was no significant difference

between the control and both immersed ($p = 0.933$) and flow through ($p = 0.06$) treatment methods. The fine nature of the LPR that retards the flow of bacteria down.

Therefore, flow through was the most preferred of the two methods. The top of the column closest to the injection point is probably exposed to significantly more reactants than the bottom as described by previous studies that observed clogging due to the accumulation of bacteria and reactants near the injection point (Cheng and Cord-Ruwisch 2014; Eryürük et al. 2015; Dhami et al. 2016). Additionally, it was observed the stabilized products of in-situ MICP were not blown by the wind. A handheld blower was used to blow on unstabilized and stabilized mine waste at different angles. No dust was observed for biocemented KS and KS/LPR prepared by either the immersed or the flow through methods, while the unstabilized waste was completely dispersed.

b. Capillary water absorption

Table 2.6 shows the water absorption results of untreated KS and KS/LPR, as well as biocemented KS and KS/LPR prepared by the immersed and flow through methods. The untreated KS and KS/LPR had a water absorption coefficient of 3.56 kg m^{-2} $h^{-0.5}$ and 6.56 kg m^{-2} $h^{-0.5}$ respectively. The water absorption coefficient for biocemented KS was 1.31 kg m^{-2} $h^{-0.5}$ for the immersed method and 1.96 kg m^{-2} $h^{-0.5}$ for the flow-through method, whereas the water absorption coefficient for KS/LPR was 2.42 kg m^{-2} $h^{-0.5}$ for the immersed method and 5.92 kg m^{-2} $h^{-0.5}$ for the flow-through method.

The general trend observed was that KS had a lower absorption coefficient than KS/LPR. Biocemented KS prepared by the immersed method had the lowest water absorption coefficient, meaning that it would absorb the least water and result in the most overland runoff into local streams. Table 2.6 shows that the absorption coefficients observed in this study are similar to those observed in previous studies for materials such as brick, damp-proof courses (Lopez-Arce et al., 2009), and concrete (Demirci and Sahin, 2014). The decreased water absorption of the biocemented waste can be attributed to pore filling by $CaCO_3$. This deposition increased the compressive strength and led to a decreased capillary absorption rate. Possible sources of capillary water include rain, runoff from slopes of the mine waste, and capillary rise of groundwater. These results suggest that MICP can bind loose waste material to reduce water absorption, thereby reducing infiltration and increasing runoff, which could prevent water transport of Pb-laden mine wastes into the surrounding water bodies.

Table 2.6: Water absorption results of untreated and biocemented KS and KS/LPR prepared by immersed and flow through methods

Type of material	Untreated	Immersed method ($kgm^{-2}h^{-0.5}$)	Flow through method ($kgm^{-2}h^{-0.5}$)
Control	0.00	0.00	0.00
KS	3.56	1.31	1.96
KS/LPR	6.56	2.42	5.92

c. Slaking behavior

Slaking tests were conducted to determine the stability of the biocemented mine wastes and to qualitatively predict their resistance to erosion. These tests are important to evaluate the influence of wetting and drying cycles on the biocemented wastes. Fig. 2.22 shows the slaking behavior of untreated and biocemented KS, and KS/LPR at 0 min, 30 min, and 24 h, respectively.

As shown in Fig. 2.22, the untreated KS and KS/LPR easily degraded into a pile of mud after the addition of water and were given a classification of 1. These results indicate that untreated KS and KS/LPR would not resist disruptive forces such as rain or wind and would continue to leach Pb^{2+} freely and to disperse easily to the surrounding flora and fauna. However, the biocemented KS and KS/LPR, prepared by both immersed and flow through methods, resisted slaking. They were given a classification of 6 since no reaction occurred after immersion in water for 24 h. This was confirmed even after five cycles of wetting and drying of the same sample. These results suggest that the biocemented KS and KS/LPR would be stable and resist the disruptive forces of wind and rain.

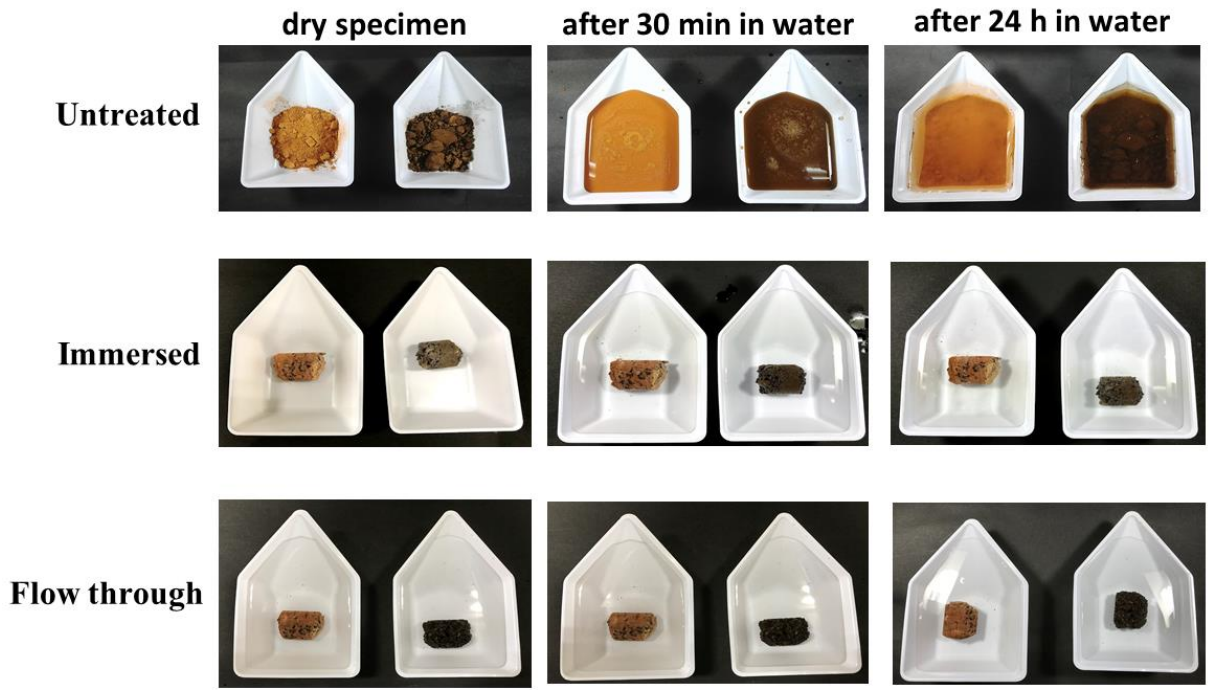

Fig. 2.22: Slaking test images of untreated KS and KS/LPR and biocemented KS and KS/LPR for dry specimen, 30 minutes after immersion in water, and 24 h after immersion: Left: KS/LPR Right: KS

d. Hydraulic conductivity

Hydraulic conductivity provides a measure of how easily water can pass through a material. For biocemented hazardous materials, reduced hydraulic conductivity is desired because it reduces the ability of water to contact contaminants, and, therefore, reduces contaminant leaching rates. The hydraulic conductivity results for untreated and biocemented waste samples are shown in Table 2.7. Untreated KS and KS/LPR had hydraulic conductivity values of 1.2×10^{-3} m/s and 8.8×10^{-4} m/s, respectively. However, after biocementation using the immersed method, KS and KS/LPR had hydraulic conductivity values that were reduced by two orders of magnitude and one order of magnitude, respectively. Using the flow-through method, KS and KS/LPR had hydraulic conductivity reduced by one order of magnitude and two orders of magnitude, respectively.

Table 2.7: Hydraulic conductivity of untreated and biocemented KS and KS/LPR prepared by immersed and flow through methods

	Untreated (m/s)	**Biocemented by immersed method (m/s)**	**Biocemented by flow through method (m/s)**
Control	0	0	0
KS	1.2×10^{-3}	3.9×10^{-5}	3.2×10^{-4}
KS/LPR	8.8×10^{-4}	5.8×10^{-5}	2.1×10^{-6}

The reduction in hydraulic conductivity of biocemented waste can be attributed to pore filling by $CaCO_3$ crystal growth, which results in increased grain diameter and, consequently, decreased pore size (Eryürük et al., 2015). When the hydraulic conductivity of KS was compared to that of KS/LPR, it was observed that KS had a lower hydraulic conductivity. This can be explained by the fact that KS had larger pore sizes, so the reduction in hydraulic conductivity was insignificant in both the flow through and immersed methods compared to the result for KS/LPR. The lower hydraulic conductivity achieved with MICP in this study reduces the ability of water to come in contact with the contaminant, and, therefore, reduces the leaching rate of the contaminant.

Chemical testing procedures

a. $CaCO_3$ content

The untreated KS and KS/LPR had 0.3±0.16 % and 0.7±0.15 % $CaCO_3$ content whereas biocemented KS had 16.5±0.2 % and 9±0.20 % and KS/LPR had 35±0.10 % and 41.1±0.12% treated by immersed and flow through methods respectively. The relationship between UCS and $CaCO_3$ content was done because it is one of the most important engineering factors in MICP mediated processes. As seen in Fig. 2.23, the untreated KS and KS/LPR has low $CaCO_3$ content and hence no strength. The UCS of biocemented KS increases with $CaCO_3$ content which suggested that the $CaCO_3$ play a significant role in the strength of sand and had been suggested by previous studies (Amarakoon and Kawasaki, 2018; Mwandira et al., 2017). However, the opposite is true for the KS/LPR as strength reduced with increased $CaCO_3$ content probably due to the geometric compatibility of bacteria transportation in fined grained materials (Ng et al., 2012a). Even though the small pore sized of the LPR is solved by mixing the KS and LPR, the free passage of bacteria could be limited as evidenced by high strength at

the top only in the immersed condition compared to the flow-through method where the bacteria gravitates to the middle and bottom. Therefore, the KS had lower $CaCO_3$ content than KS/LPR because of particle size. The LPR provided a large surface area for precipitation of $CaCO_3$ hence the increased content compared to the KS.

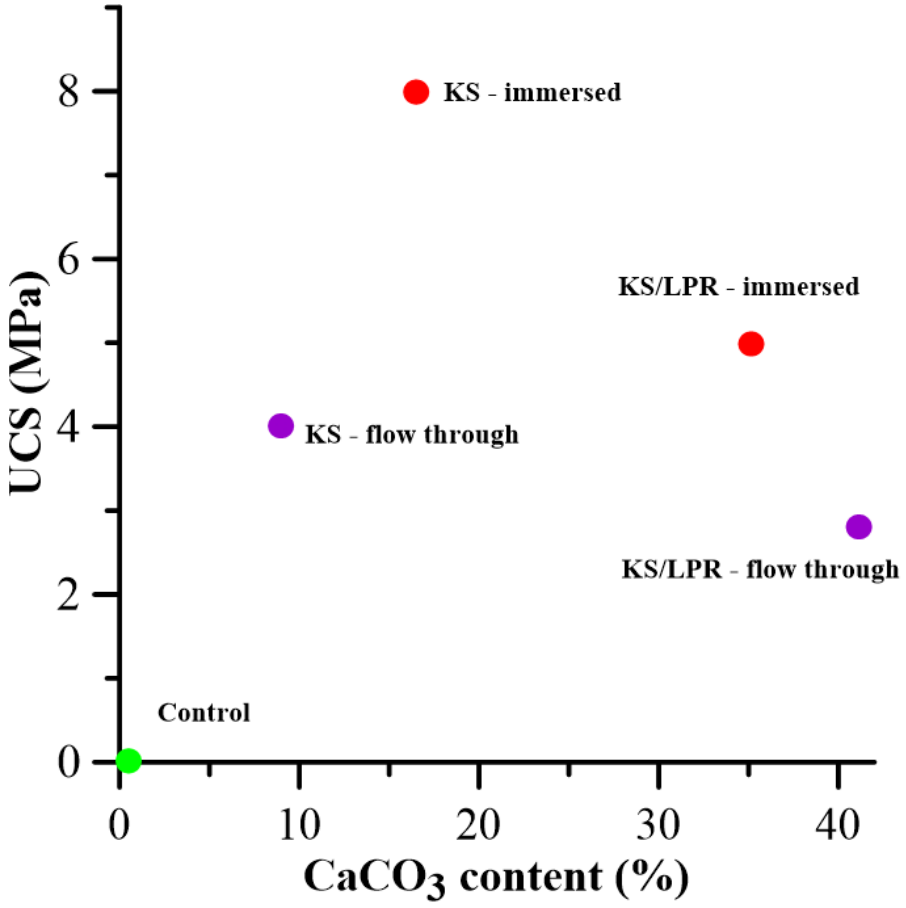

Fig. 2.23. Effect of $CaCO_3$ content on the UCS of on untreated, biocemented KS and KS/LPR treated by immersed and flow through methods.

b. XRD

XRD analysis of the untreated waste revealed that the mineral composition includes quartz, hematite, goethite, magnetite, cerussite, and anglesite, as illustrated in Fig. 2.24. This composition is typical of waste from sites that have undergone mining activities (Bhuiyan et al., 2010; Hammarstrom et al., 2005). The quartz, hematite, goethite and magnetite mineral components were due to the ore host rock which is characteristic of the geology in the mine area. The Pb-based minerals identified - cerussite, and anglesite - are associated with sulfide-bearing mine wastes, which are the main source of contamination in and around the Kabwe mine site.

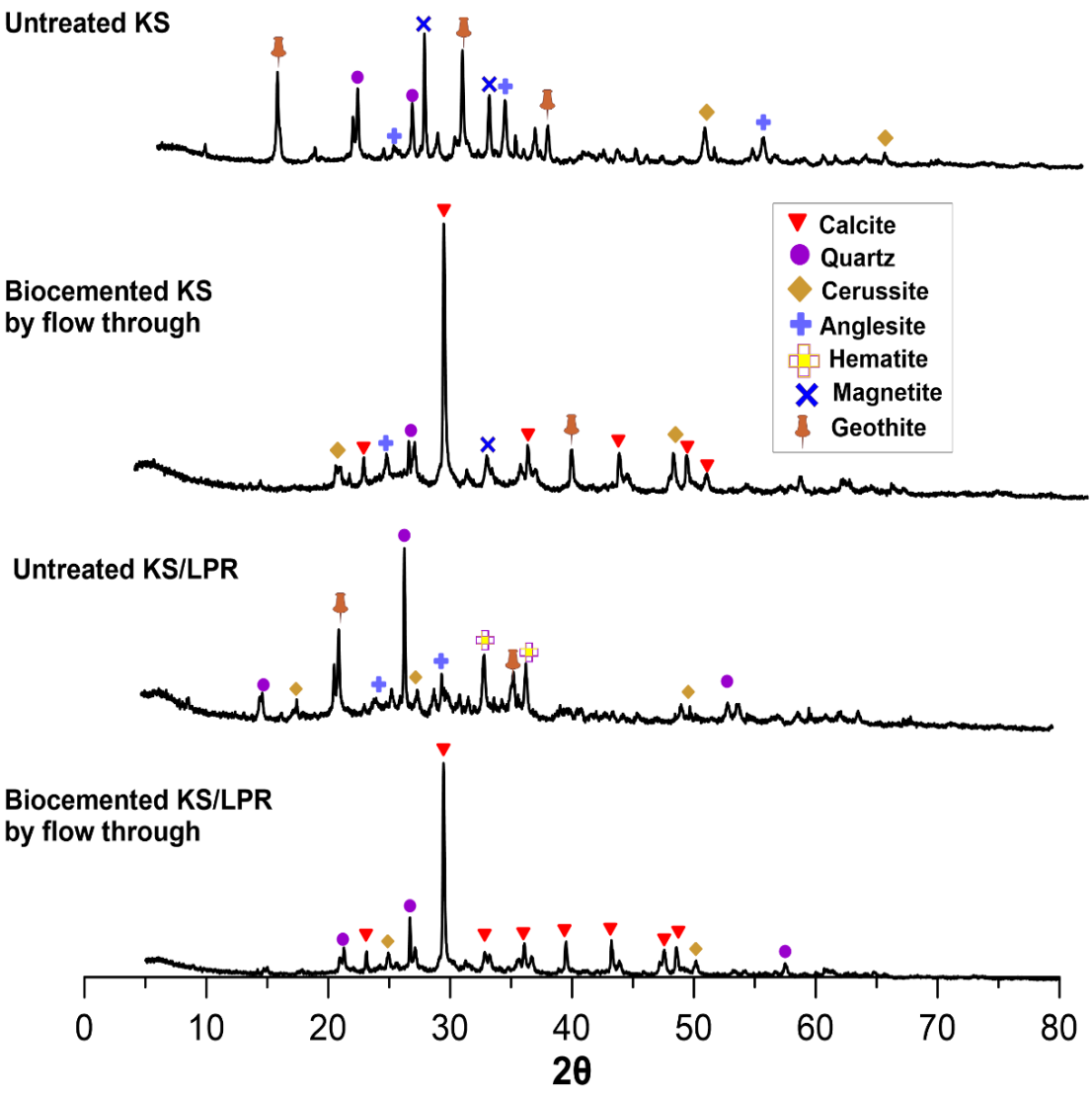

Fig. 2.24: Typical XRD patterns of untreated and biocemented KS and KS/LPR

XRD patterns of the biocemented waste were similar to those of the original waste, with calcite as the most abundant mineral component as expected due to the ureolysis process. According to the XRD results, the Pb minerals in the untreated KS and KS/LPR were immobilized without changing their identity. The $CaCO_3$ precipitated in the voids of the wastes, acting as a binder to the hazardous contaminants and rendering them less soluble and/or less toxic and less likely to cause toxicity to humans, animals, and the environment in and around the mine site.

c. SEM and EDS

The results of SEM analysis of untreated and biocemented KS are shown in Fig. 2.25.

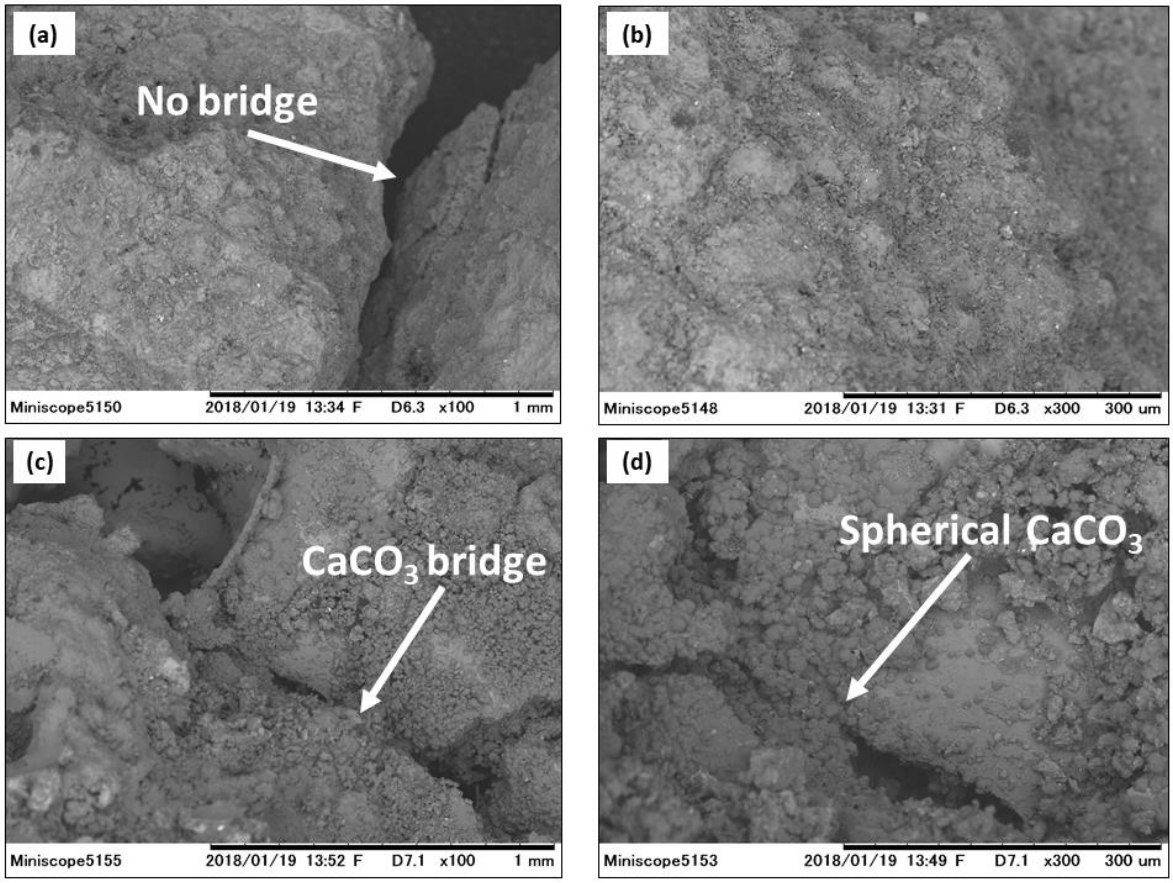

Fig. 2.25: SEM images of (a) untreated KS at x100 magnification, (b) untreated KS at x300 magnification, (c) biocemented KS prepared by immersed method at x100 magnification, and (d) biocemented KS prepared by immersed method at x300 magnification

Fig. 2.25(a) and 2.25(b) showed that the untreated KS is rough and separated, with no particle bonding. However, the biocemented KS (Fig. 2.25(c) and Fig. 2.25(d)) had spherical $CaCO_3$ deposited on the surface and between the sand grains, which was confirmed by XRD analysis. The deposited, spherical $CaCO_3$ caused bridging, which further roughened the surface and decreased the pore space size by filling the voids between particles and causing particle binding. The decrease in pore space size has reported in a number of previous studies (Mujah et al., 2017; Ng et al., 2012; Rowshanbakht et al., 2016).

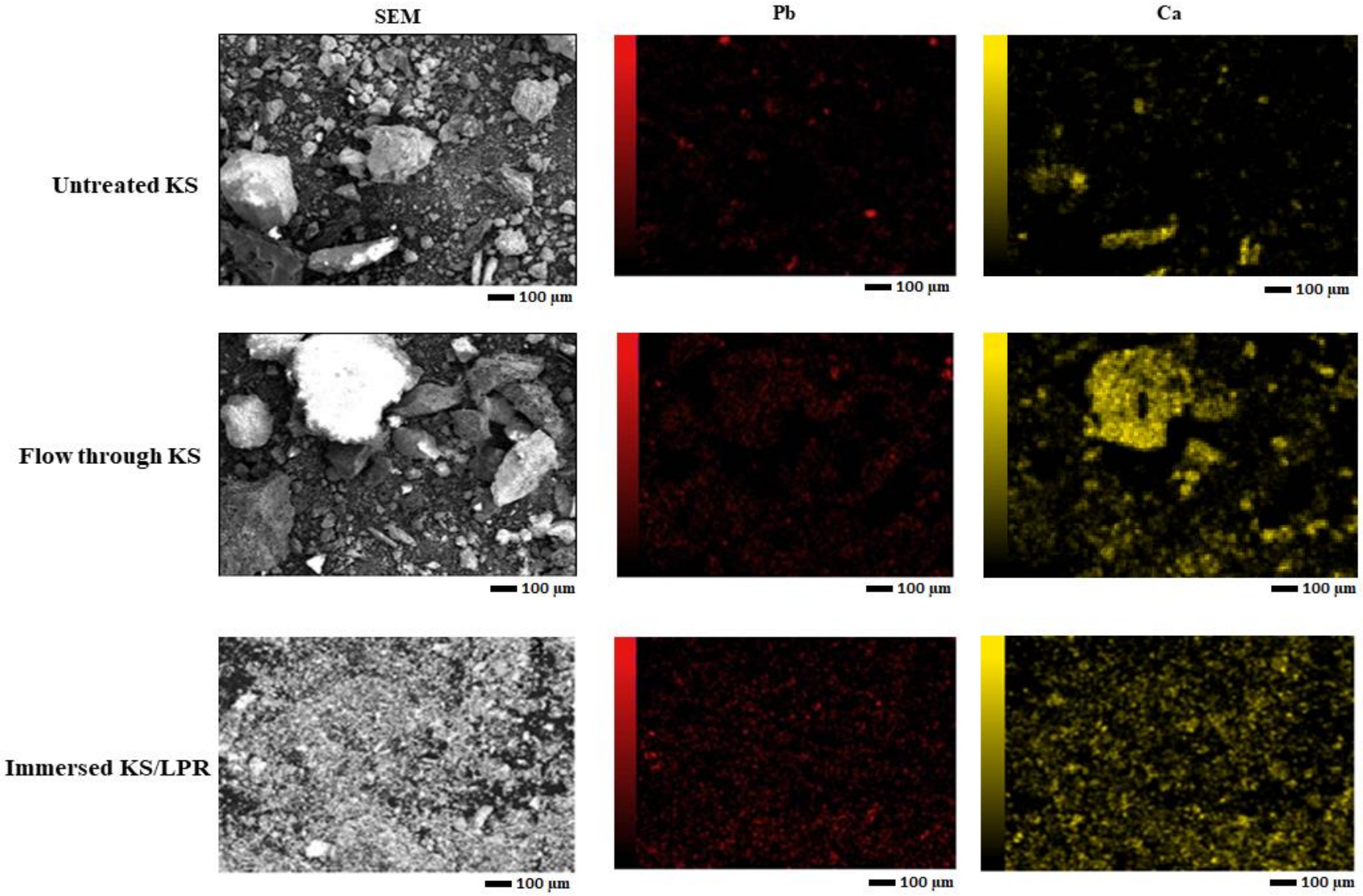

Fig. 2.26: SEM and EDS images of untreated and biocemented KS and KS/LPR

The EDS analysis revealed that untreated KS consisted mainly of C, O, S, Mg, Ca, Fe, Si, Zn, and Pb, whereas the biocemented KS and KS/LPR prepared by flow through and immersed methods consisted of C, O, S, Mg, Ca, Fe, Zn, Pb, Si, P, Na, Cl and Al. This composition is due to the heterogeneous nature of the orebody and subsequent MICP process during biocementation. The element composition is consistent with the minerals identified by XRD - quartz, hematite, goethite, magnetite, cerussite, and anglesite. Fig. 2.26 shows typical, representative EDS elemental mapping of Pb and Ca in untreated and biocemented KS and KS/LPR prepared by both the flow through and immersed methods. As shown, the presence of Ca and Pb in treated wastes is evident, which indicates that Pb, after treatment, was immobilized, that could result in the prevention of Pb migration out of the solid phase.

d. Leaching test results

The results of the leaching stability test results are shown in Fig. 2.27. After continuous leaching for 231 days, the concentrations of leached Pb^{2+} were below 0.001 mg/L for biocemented KS and KS/LPR prepared by the flow-through method. This means that leachability, which is the material's ability to release a contaminant from a solid phase into a contacting liquid, was prevented. Therefore, the results of the current study indicate that Pb from the biocemented monolith was negligible. Furthermore, it means that the stabilized mine waste was not influenced by contact with an eluent, binders and by the solubility of the contaminant (Bates and Hills 2015). These results indicate that Pb release from the biocemented monolith was negligible. Compared with stabilized materials which had a leachability of below 0.001 mg/L, the leachable concentrations of KS of 5.40 mg/L and that of KS/LPR of 7.87 mg/L Pb^{2+} was observed. This further reveal that biocementation can be used to prevent pollution of ecosystems whereby pollutants like heavy metals cannot be leached into ecosystems to raise background levels of these pollutants. The leachability test results confirm that the Pb^{2+} was effectively immobilized preventing toxic, water-soluble Pb from leaching out of the wastes. The water-soluble fraction of Pb is considered the most toxic fraction due to its potential to contaminate the food chain, surface water, and groundwater (Akbar et al. 2016; Tang et al. 2016; Yutong et al. 2016).

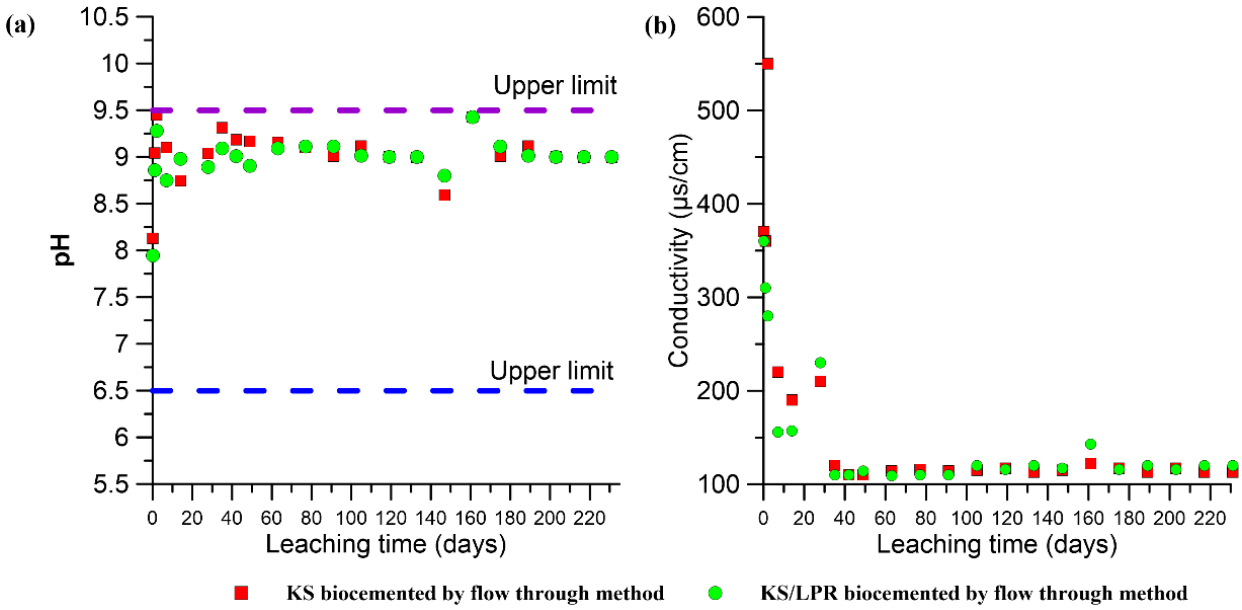

Fig. 2.27: Results of leaching test for biocemented KS and KS/LPR prepared by flow through method: (a) pH and (b) hydraulic conductivity

The pH values of the leachate from the biocemented KS and KS/LPR are shown in Fig. 2.27a. The biocemented KS and KS/LPR changed the initial pH of deionized water from pH 6.5 to a maximum pH of 9.5. The increased pH of the leachate, compared to the initial deionized water, could be due to the buffering capacity of the $CaCO_3$ in the biocemented material (Zhang et al. 2016b). The pH of the leachate was weakly alkaline and was within the bounds of the Zambia Environmental Management Agency (ZEMA) guidelines of 6.0 and 9.5 for effluent and wastewater discharge into the environment, indicated by the purple and blue lines in Fig. 2.27a (ZEMA 2013). The electrical conductivity of the leachate from the KS and KS/LPR is shown in Fig. 2.27b, ranging from 130 to 550 µS/cm. Schedule III 7(2) of the ZEMA (2013) guidelines for wastewater discharge into the environment is electrical conductivity of less than 4,300 µS/cm.

2.5.6 Strategy for biocementation of mine waste in Kabwe using *Pararhodobactor* sp

This chapter investigated the biocementation of Pb contaminated mine waste by *Pararhodobacter* sp. using MICP. The methodology adopted in this chapter takes into consideration the two parameters that are used for determining the degree of effectiveness of biocementation: strength and leach resistance (Malviya and Chaudhary, 2006). First, this study demonstrated that both biocemented KS and KS/LPR had increased strength, with maximum UCS of 8 MPa and of 4 MPa respectively. The results show that the flow through method for

biocementation is preferred. The increased strength of biocemented waste is attributed to the hydrolysis of urea and the precipitation of $CaCO_3$, which significantly reduced hydraulic conductivity compared to untreated wastes. Second, leachability of Pb^{2+} was below the detection limit of the ICP-AES (<0.001 mg/L for Pb) for biocemented KS and KS/LPR after leaching for 231 days. Furthermore, reduced slaking, and reduced water absorption capacity of the biocemented samples could limit the transport of oxygen and water through the wastes, thereby limiting mineral dissolution and transportation. On this basis, Pb contaminants in or on solid phases could have a reduced partition into water. Airborne transportation of Pb contaminated dust particles would be eliminated also as the biocemented wastes could not be dispersed by wind. Consequently, biocementation would reduce the risk of exposure to humans or biota. This result conforms with the results of a recent study by Wang et al. (2018), which found that MICP can alleviate cracking and wind erosion and can control the diffusion of dust from desert sand. The overall conceptual model for biocementing the Kabwe mine wastes in situ, based on the results of this study, is shown in Fig. 2.28.

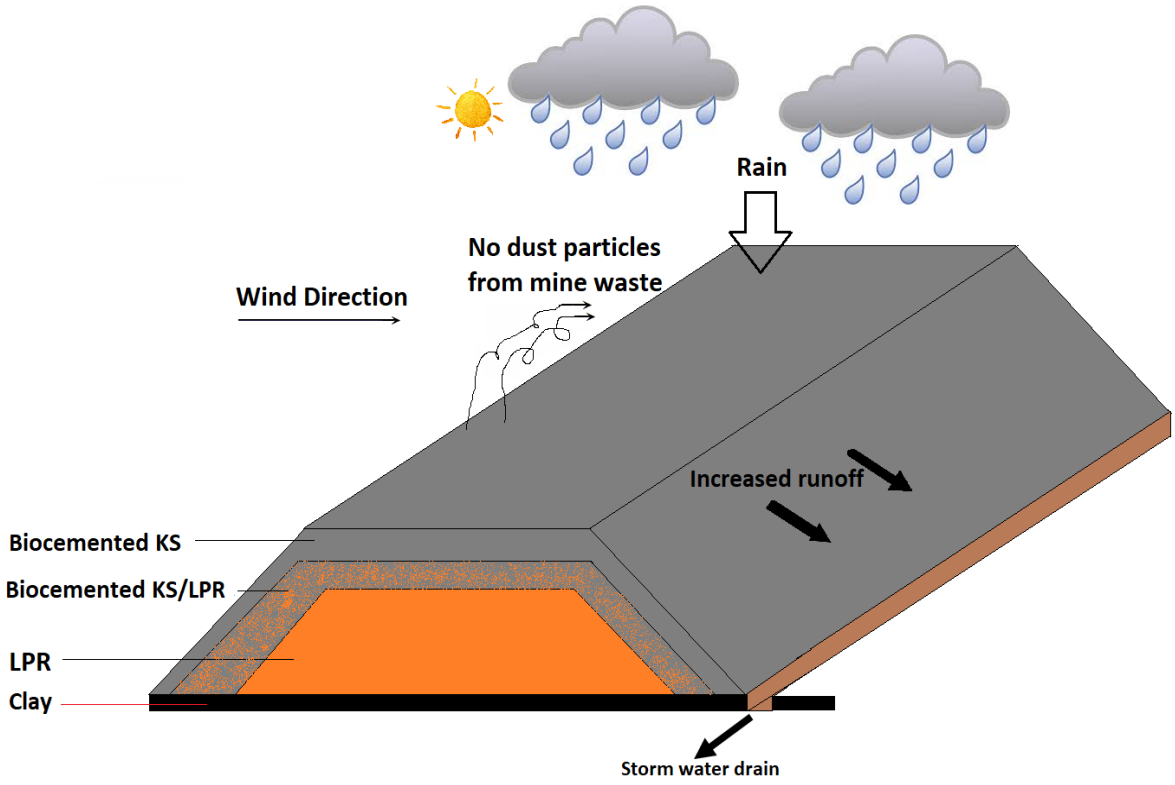

Fig. 2.28: Conceptual model for immobilization of Pb-contaminated mine wastes at Kabwe Mine site using MICP by *Pararhodobacter* sp.

2.6 Conclusion

In this chapter, demonstrated for the first time that Pb can be bioremediated by *Pararhodobacter* sp. and that the microorganism was capable of complete removal of Pb^{2+} during 6 h of incubation via elevation of the pH to alkaline conditions (8.0–9.1). SEM, EDS, and XRD further confirmed the transformation of toxic free Pb^{2+} ions to a more stable form of lead that bioprecipitated together with calcite or vaterite, which were predominant. Furthermore, syringe experiments revealed that UCS increased with increasing injection interval of bacteria, and the top part of the sample solidified more than the bottom. These results will facilitate the bioremediation of lead in both fine and coarse materials as an eco-friendly and sustainable method of heavy metal remediation.

This research promotes the utilization of biocementation as an alternative technique for effectively biocementing mine wastes. The results of this study show the transition of untreated kiln slag and leach plant residue to stabilize mine wastes with maximum strength values of 8 MPa for KS and 4 MPa for KS/LPR. The main mineral phases identified in the untreated KS and KS/LPR, composed of anglesite ($PbSO_4$) and cerussite ($PbCO_3$), were the main source of Pb in the environment in and around the Kabwe mine. These minerals were immobilized by the MICP process, which resulted in a less toxic and less permeable form of the KS and KS/LPR. Additionally, slaking tests revealed that biocemented KS and KS/LPR neither reacted nor disintegrated even after being subjected to five cycles of wetting and drying, which suggests that they could be stable and resist erosion by disruptive forces such as rain or wind. The water absorption coefficient was reduced significantly in the treated wastes, which would also improve resistance to water and wind erosion compared to untreated mine waste. Finally, leachable Pb^{2+} was below the detection limit after 231 days of continuous leaching. These results indicate that the use of MICP is effective, in situ heavy metal remediation method, with the potential for greater sustainability than other methods because it uses on-site materials which result in reduced cost and use of energy resources.

References

Achal, V., Pan, X., Lee, D.J., Kumari, D., Zhang, D., 2013. Remediation of Cr(VI) from chromium slag by biocementation. Chemosphere 93, 1352–1358. https://doi.org/10.1016/j.chemosphere.2013.08.008

Akbar, A., Sinegani, S., Monsef, M.J., 2016. Chemical speciation and bioavailability of cadmium in the temperate and semiarid soils treated with wheat residue. Environ. Sci. Pollut. Res. 23, 9750–9758. https://doi.org/10.1007/s11356-016-6171-x

Amarakoon, G.G.N.N., Kawasaki, S., 2018. Factors affecting sand solidification using MICP with *Pararhodobacter* sp. Mater. Trans. 59, 72–81. https://doi.org/10.2320/matertrans.M-M2017849

ASTM International, 2016. ASTM D4644 - 16 Standard test method for slake durability of shales and other similar weak rocks. https://doi.org/10.1520/D4644-16

ASTM International, 2013. ASTM C1585 - 13 Standard test method for measurement of rate of absorption of water by hydraulic-cement concretes. https://doi.org/10.1520/C1585-13

ASTM International, 2003. ASTM D5084 - 03 Standard test methods for measurement of hydraulic conductivity of saturated porous materials using a flexible wall permeameter. https://doi.org/10.1520/D5084-03

Bates, E., Hills, C., 2015. Stabilization and solidification of contaminated soil and waste: A manual of practice.

Begum, A., Harikrishna, S., Khan, I., 2009. Analysis of heavy metals in water, sediments and fish samples of Madivala lakes of Bangalore, Karnataka.pdf. Int. J. ChemTech Res. 1, 245–249.

Bhuiyan, M.A.H., Parvez, L., Islam, M.A., Dampare, S.B., Suzuki, S., 2010. Heavy metal pollution of coal mine-affected agricultural soils in the northern part of Bangladesh. J. Hazard. Mater. 173, 384–392. https://doi.org/10.1016/j.jhazmat.2009.08.085

Blacksmith, I., 2013. The worlds worst 2013: the top ten toxic threats. Zurich. https://doi.org/10.1017/CBO9781107415324.004

Chen, X., Guo, H., Cheng, X., 2017. Heavy metal immobilisation and particle cementation of tailings by biomineralisation. Environ. Geotech. 1–7. https://doi.org/10.1680/jenge.15.00068

Cheng, L., Cord-Ruwisch, R., 2014. Upscaling effects of soil improvement by microbially induced calcite precipitation by surface percolation. Geomicrobiol. J. 31, 396–406. https://doi.org/10.1080/01490451.2013.836579

Cheng, L., Cord-Ruwisch, R., Shahin, M.A., 2013. Cementation of sand soil by microbially

induced calcite precipitation at various degrees of saturation. Can. Geotech. J. 50, 81–90. https://doi.org/10.1139/cgj-2012-0023

Danjo, T., Kawasaki, S., 2016. Microbially induced sand cementation method using *Pararhodobacter* sp. strain SO1, inspired by beachrock formation mechanism. Mater. Trans. 57, 428–437. https://doi.org/10.2320/matertrans.M-M2015842

Demirci, E.E., Sahin, R., 2014. Effect of strength class of concrete and curing conditions on capillary water absorption of self-compacting and conventional concrete. Int. J. Civ. Environ. Eng. 8, 1191–1198.

Dhami, N.K., Reddy, M.S., Mukherjee, A., 2016. Significant indicators for biomineralisation in sand of varying grain sizes. Constr. Build. Mater. 104, 198–207. https://doi.org/10.1016/j.conbuildmat.2015.12.023

Eryürük, K., Yang, S., Suzuki, D., Sakaguchi, I., Akatsuka, T., Tsuchiya, T., Katayama, A., 2015. Reducing hydraulic conductivity of porous media using $CaCO_3$ precipitation induced by *Sporosarcina pasteurii.* J. Biosci. Bioeng. 119, 331–336. https://doi.org/10.1016/j.jbiosc.2014.08.009

González-Muñoz, M.T., Rodriguez-Navarro, C., Martínez-Ruiz, F., Arias, J.M., Merroun, M.L., Rodriguez-Gallego, M., 2010. Bacterial biomineralization: new insights from *Myxococcus*-induced mineral precipitation. Geol. Soc. London, Spec. Publ. 336, 31–50. https://doi.org/10.1144/SP336.3

Govarthanan, M., Lee, K.J., Cho, M., Kim, J.S., Kamala-Kannan, S., Oh, B.T., 2013. Significance of *Autochthonous Bacillus* sp. KK1 on biomineralization of lead in mine tailings. Chemosphere 90, 2267–2272. https://doi.org/10.1016/j.chemosphere.2012.10.038

Hammarstrom, J.M., Seal, R.R., Meier, A.L., Kornfeld, J.M., 2005. Secondary sulfate minerals associated with acid drainage in the eastern US: Recycling of metals and acidity in surficial environments. Chem. Geol. 215, 407–431. https://doi.org/10.1016/j.chemgeo.2004.06.053

Hukue, M., Kato, Y., Nakamura, T., Moriyama, N., 2001. A method for determining carbonate content for soils and evaluation of the results. Japanese Geotech. Soc. 49, 2669. in *Japanese*

International Society for Rock Mechanics, 2015. The ISRM suggested methods for rock characterization, testing and monitoring: 2007-2014. Springer International Publishing, Cham. https://doi.org/10.1007/978-3-319-07713-0

Kang, C.H., Oh, S.J., Shin, Y., Han, S.H., Nam, I.H., So, J.S., 2015. Bioremediation of lead by

ureolytic bacteria isolated from soil at abandoned metal mines in South Korea. Ecol. Eng. 74, 402–407. https://doi.org/10.1016/j.ecoleng.2014.10.009

Kribek, B., Nyambe, I.A., Njamu, F., Chitwa, G., Ziwa, G., 2009. Assessment of impacts of mining and mineral processing on the environment and human health in selected regions of the Central and Copperbelt Provinces of Zambia. Report No. RP/3/2008 for years 2008-2010. Lusaka.

Li, M., Cheng, X., Guo, H., 2013. Heavy metal removal by biomineralization of urease producing bacteria isolated from soil. Int. Biodeterior. Biodegradation 76, 81–85. https://doi.org/10.1016/j.ibiod.2012.06.016

Li, M., Cheng, X., Guo, H., Yang, Z., 2015. Biomineralization of carbonate by *Terrabacter Tumescens* for heavy metal removal and biogrouting applications. J. Environ. Eng. C4015005–C4015005. https://doi.org/10.1061/(ASCE)EE.1943-7870.0000970.

Li, X., Peng, W., Jia, Y., Lu, L., Fan, W., 2016. Bioremediation of lead contaminated soil with *Rhodobacter sphaeroides*. Chemosphere 156, 228–235. https://doi.org/10.1016/j.chemosphere.2016.04.098

Lopez-Arce, P., Doehne, E., Greenshields, J., Benavente, D., Young, D., 2009. Treatment of rising damp and salt decay: the historic masonry buildings of Adelaide, South Australia. Mater. Struct. Constr. 42, 827–848. https://doi.org/10.1617/s11527-008-9427-1

Mugwar, A.J., Harbottle, M.J., 2016. Toxicity effects on metal sequestration by microbially-induced carbonate precipitation. J. Hazard. Mater. 314, 237–248. https://doi.org/10.1016/j.jhazmat.2016.04.039

Mwandira, W., Nakashima, K., Kawasaki, S., 2017. Bioremediation of lead-contaminated mine waste by *Pararhodobacter* sp. based on the microbially induced calcium carbonate precipitation technique and its effects on strength of coarse and fine grained sand. Ecol. Eng. 109, 57–64. https://doi.org/10.1016/j.ecoleng.2017.09.011

Naik, M.M., Dubey, S.K., 2013. Lead resistant bacteria: Lead resistance mechanisms, their applications in lead bioremediation and biomonitoring. Ecotoxicol. Environ. Saf. 98, 1–7. https://doi.org/10.1016/j.ecoenv.2013.09.039

Natarajan, K.R., 1995. Kinetic Study of the Enzyme Urease from *Dolichos biflorus*. J. Chem. Educ. 72, 556–557. https://doi.org/10.1021/ed072p556

Nehrke, G., Van Cappellen, P., 2006. Framboidal vaterite aggregates and their transformation into calcite: A morphological study. J. Cryst. Growth 287, 528–530. https://doi.org/10.1016/j.jcrysgro.2005.11.080

Ng, W., Lee, M., Hii, S., 2012. An Overview of the factors affecting microbial-induced calcite

precipitation and its potential application in soil improvement. Int. J. Civil, Environ. Struct. Constr. Archit. Eng. 6, 188–194. https://doi.org/10.1007/s10853-012-6783-6

Nwuche, C.O., Ugoji, E.O., 2008. Effects of heavy metal pollution on the soil microbial activity. Int. J. Environ. Sci. Technol. 5, 409–414. https://doi.org/10.1007/BF03326036

Park, S.J., Park, Y.M., Chun, W.Y., Kim, W.J., Ghim, S.Y., 2010. Calcite-forming bacteria for compressive strength improvement in mortar. J. Microbiol. Biotechnol. 20, 782–788. https://doi.org/10.4014/jmb.0911.11015

Salifu, E., MacLachlan, E., Iyer, K.R., Knapp, C.W., Tarantino, A., 2016. Application of microbially induced calcite precipitation in erosion mitigation and stabilisation of sandy soil foreshore slopes: A preliminary investigation. Eng. Geol. 201, 96–105. https://doi.org/10.1016/j.enggeo.2015.12.027

Shafii, R.-N., Clough, W., 1982. The influence of cementation on the static and dynamic behavior of sands. Stanford, California, California.

Stocks-Fischer, S., Galinat, J.K., Bang, S.S., 1999. Microbiological precipitation of $CaCO_3$. Soil Biol. Biochem. 31, 1563–1571. https://doi.org/10.1016/S0038-0717(99)00082-6

Tang, W., Shan, B., Zhang, H., Zhu, X., Li, S., 2016. Heavy metal speciation, risk, and bioavailability in the sediments of rivers with different pollution sources and intensity. Environ. Sci. Pollut. Res. 23, 23630–23637. https://doi.org/10.1007/s11356-016-7575-3

Tembo, B.D., Sichilongo, K., Cernak, J., 2006. Distribution of copper, lead, cadmium and zinc concentrations in soils around Kabwe town in Zambia. Chemosphere 63, 497–501. https://doi.org/10.1016/j.chemosphere.2005.08.002

U.S. EPA, 2017. Leaching Environmental Assessment Framework (LEAF) how-to guide understanding the leaf approach and how and when to use it.

Wang, Z., Zhang, N., Ding, J., Lu, C., Jin, Y., 2018. Experimental study on wind erosion resistance and strength of sands treated with microbial-induced calcium carbonate precipitation. Adv. Mater. Sci. Eng. 2018, 1–10. https://doi.org/10.1155/2018/3463298

Weatherburn, M.W., 1967. Phenol-hypochlorite reaction for determination of ammonia. Anal. Chem. 39, 971–974. https://doi.org/10.1021/ac60252a045

Yabe, J., Nakayama, S.M.M., Ikenaka, Y., Muzandu, K., Ishizuka, M., Umemura, T., 2011. Uptake of lead, cadmium, and other metals in the liver and kidneys of cattle near a lead-zinc mine in Kabwe, Zambia. Environ. Toxicol. Chem. 30, 1892–1897. https://doi.org/10.1002/etc.580

Yabe, J., Nakayama, S.M.M., Ikenaka, Y., Yohannes, Y.B., Bortey-Sam, N., Kabalo, A.N., Ntapisha, J., Mizukawa, H., Umemura, T., Ishizuka, M., 2018. Lead and cadmium

excretion in feces and urine of children from polluted townships near a lead-zinc mine in Kabwe, Zambia. Chemosphere 202, 48–55. https://doi.org/10.1016/j.chemosphere.2018.03.079

Yutong, Z., Qing, X., Shenggao, L., 2016. Distribution, bioavailability, and leachability of heavy metals in soil particle size fractions of urban soils (northeastern China). Environ. Sci. Pollut. Res. 23, 14600–14607. https://doi.org/10.1007/s11356-016-6652-y

ZEMA, 2013. Limits for effluent and wastewater - Licencing Regulations 7(2) Third schedule.

Zhang, Yongyong, Zhang, S., Wang, R., Cai, J., Zhang, Yuge, Li, H., Huang, S., Jiang, Y., 2016. Impacts of fertilization practices on pH and the pH buffering capacity of calcareous soil. Soil Sci. Plant Nutr. 62, 432–439. https://doi.org/10.1080/00380768.2016.1226685

CHAPTER 3 SOLIDIFICATION OF SAND BY INDIGENOUS UREOLYTIC BACTERIA FOR CAPPING MINE WASTE TO CONTROL METALLIC DUST

3.1 Introduction

Kabwe Mine was a Pb and Zn mine that commenced its operations in 1902 until its closure in 1994. Apart from lead and zinc, it also produced silver, manganese, cadmium, vanadium, and titanium in smaller quantities (Mufinda, 2015). Due to the extraction of different minerals, several mineral processing techniques were used resulting in the production of different types of mine waste dumps that have resulted in soil pollution and waste that is a source of airborne dust (Fig. 3.1(a)).

In response to the concern of dust emanating from the mine wastes in Kabwe, remediation methods such as the revegetation of the waste dump by metallophytes were proposed and implemented, but subsequently failed because the plants failed to grow (Leteinturier et al., 2001). Additionally, mining waste has not been re-processed due to probably the cost of metal recovery (BMR Group PLC, 2019). A promising technique to prevent metallic dust from becoming airborne in-situ is the immobilization of these wastes by microbially induced calcium carbonate precipitation (MICP) using ureolytic bacteria (Achal et al., 2013; Chen et al., 2017; Kim and Lee, 2018; Mwandira et al., 2017; Nam et al., 2016; Zhu et al., 2016). The proposed use of MICP to cap mine wastes would eliminate both dust generation and water infiltration, restoring the contaminated site. Although many ureolytic bacteria have been isolated, continued isolation and identification of more novel species, especially those that are indigenous to the area, is indispensable.

Such an investigation, involving the isolation and identification of effective microorganisms for biotechnological applications, represents a sustainable approach to remediation, eliminating the current environmental problems without significantly changing the local ecological integrity.

3.2 Objectives

The objectives of this Chapter were to use MICP method to biocement sand using Pb tolerant bacteria isolated from Kabwe to prevent air-blown dust from the mine site and the specific objectives were to:

(i) Isolate Pb-resistant ureolytic bacteria from contaminated waste at Kabwe mine site;

(ii) The determination Ca^{2+}/urea concentration for solidification; and

(iii) The use of the bacteria to biocement sand.

3.3 Materials and methods

3.3.1 Soil sample collection

The soil was sampled from the abandoned Kabwe mine site of Central Province, Zambia (15°27′–17°28′ S latitude and 23°06′–25°33′ E longitude). The mine waste was exported from Zambia under approval No. RCT 7686229, and the import was also permitted by Plant Protection Station, Ministry of Agriculture, Forestry and Fisheries, Japan under the approval No. 29-836. The samples were transported from the site to the laboratory in a cooler box. Table 3.1 shows the soil sampling locations and shown in Figure 3.1a.

Table 3.1: Soil sampling locations, Kabwe, Zambia

	GPS Coordinates (UTM)	
	Easting	Northings
KBZ 1	653938.00	8400702.00
KBZ 2	653665.00	8400156.00
KBZ 3	654773.00	8401455.00
KBZ 4	654318.87	8402297.32

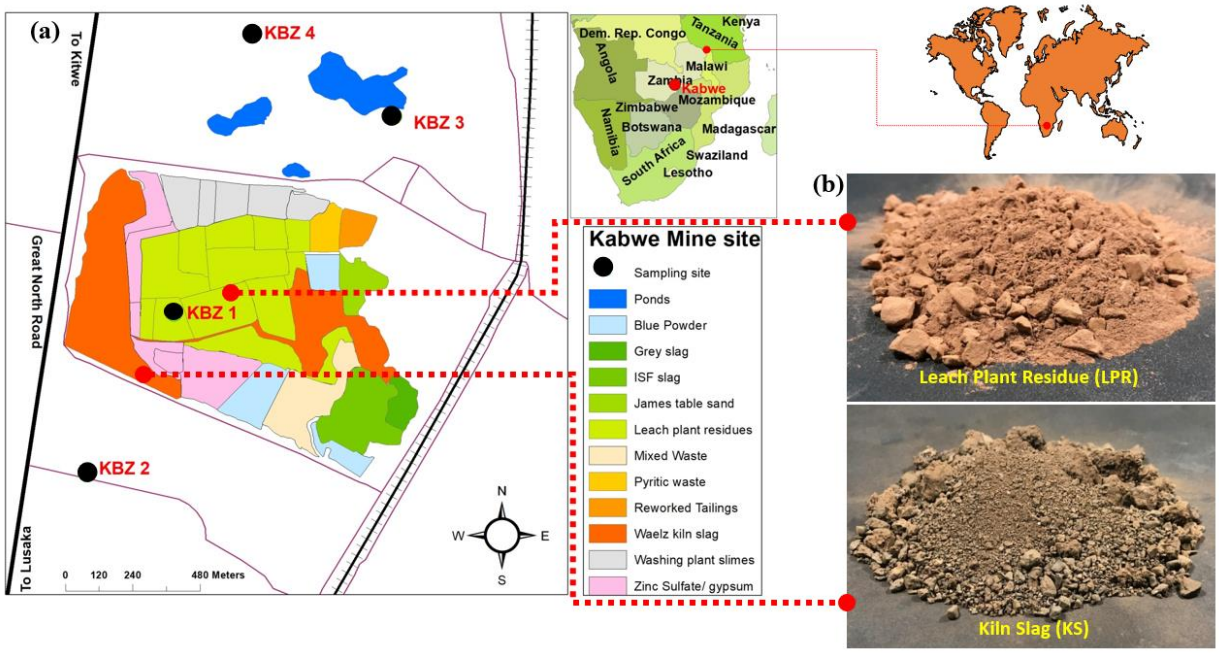

Fig. 3.1 (a) Location of soil sampling sites and the different mine wastes at the abandoned mine, Kabwe, Zambia (b) Appearance of leach plant residues and kiln slag.

3.3.2 Reagents and equipment used

a) Equipment

Same equipment and reagents used in Chapter 2 were used in this study.

b) Media

NH4 YE media was used which composed of 20 g/L yeast extract; 10 g/L di-ammonium sulfate $(NH_4)_2SO_4$; 0.13 M Tris buffer (pH = 8.0); and 20 g/L agar amended with Pb.

3.4 Experimental methods

3.4.1 Bacteria isolation from soil

Bacteria were isolated by placing 1 g of soil in a 15 mL sterile centrifuge tube and adding 10 mL of sterile water, followed by vigorous shaking by hand. Samples were diluted 10- to 10,000-fold using sterile water and plated on NH4 YE agar medium agar amended with Pb (II)) to isolate Pb-resistant strains as illustrated Fig. 3.2. The plates were incubated at 30 °C for 72 h.

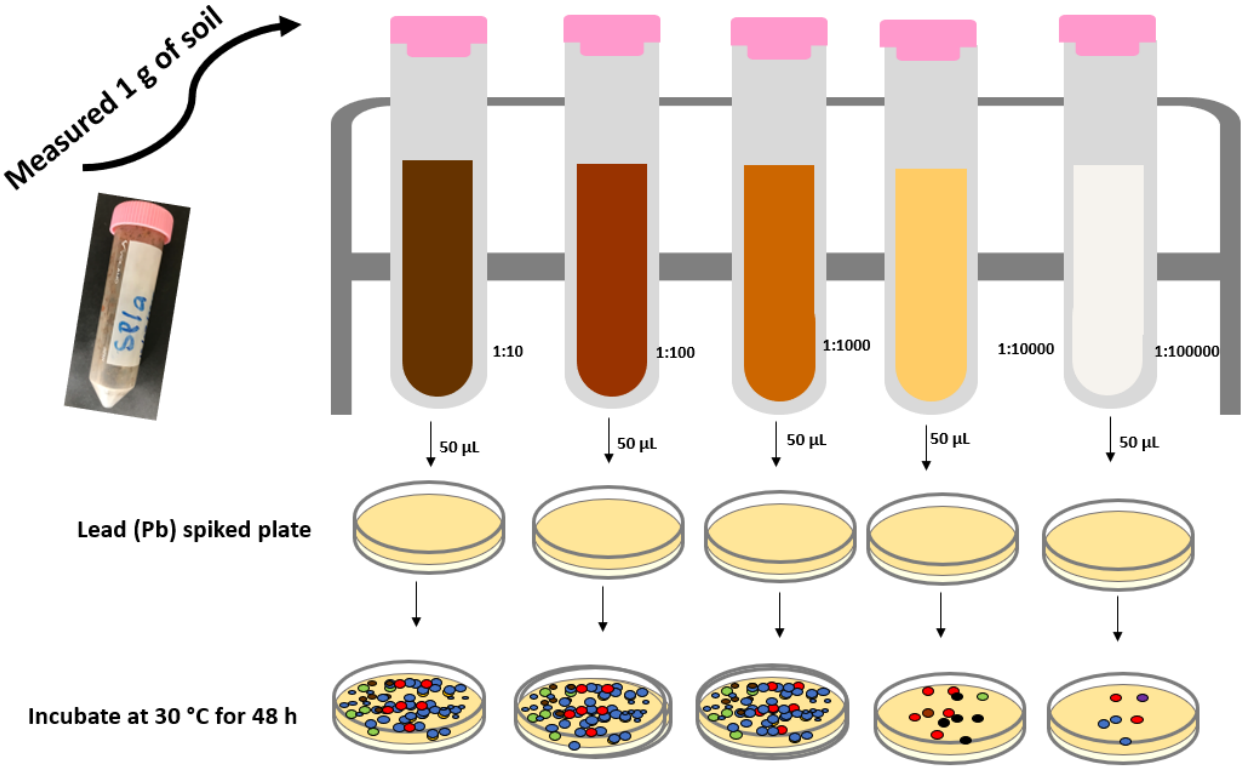

Fig. 3.2: Isolation for Pb tolerant strains from soil by serial dilutions

3.4.2 Cresol red screening for ureolytic bacteria

The grown serial diluted colonies were isolated based on color, shape, and morphology. These colonies were further screened until a pure culture was achieved by platting single colonies after plate streaking. Finally, the isolated colonies were screened by mixing with 20 mL of cresol red solution (25 g/L urea and 0.4 g/L cresol red) and left standing at 45 °C for 2 h. After 2 h, the samples that changed their color to purple were selected (Fig. 3.3).

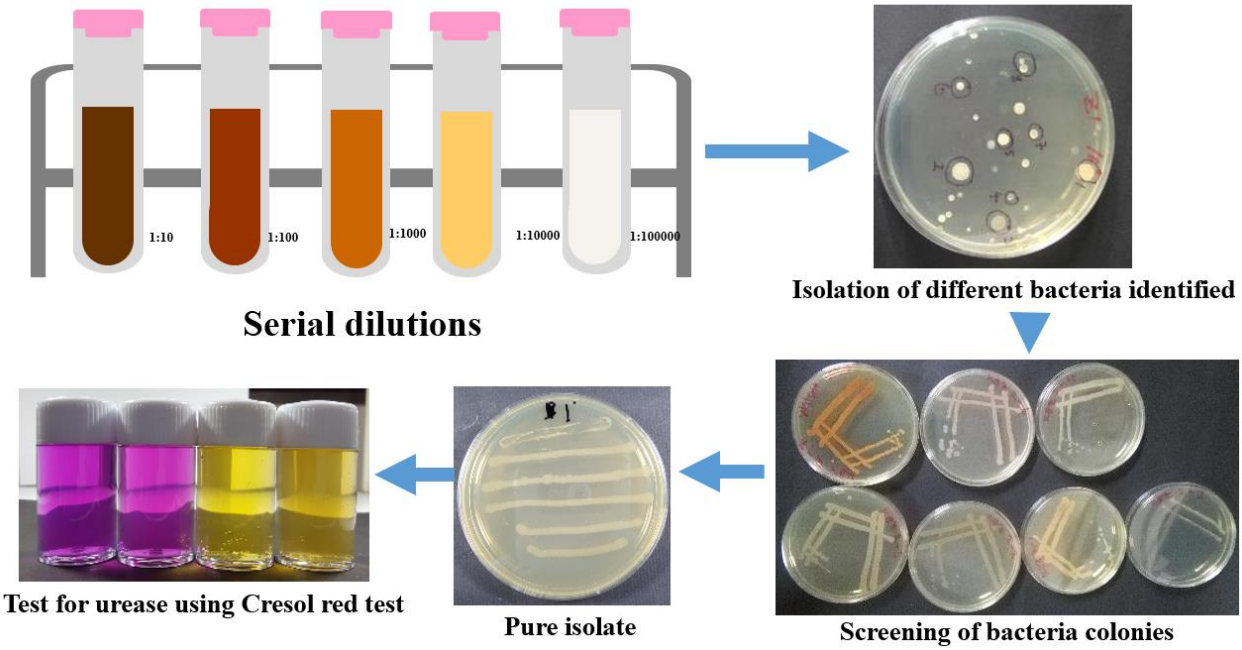

Fig. 3.3: Procedure used for cresol red screening for ureolytic bacteria

3.4.3 Molecular identification of Pb-resistant bacteria

The Pb-resistant isolate was identified by 16S rRNA sequence analysis as illustrated in Fig. 3.4. Step one 1 was to use cresol red to identify ureolytic bacteria. Step 2 was DNA extracts were amplified using two sets of primers targeting the 16S rRNA region specific for almost all bacterial 16S sequences: primers F9 (5'- GAGTTTGATCCTGGCTCAG -3') and R1451 (5'- AAGGAGGTGATCCAGCC -3'). The PCR amplification cycle consisted of an initial denaturation step of 5 min at 94 °C, followed by 25 cycles of 1 min at 94 °C, 2 min at 60 °C, and 1 min at 72 °C and a final extension step of 30 min at 72 °C. The amplicons were separated by gel electrophoresis and the resulting DNA bands were extracted and purified using the FastGene™ PCR extraction Kit following the manufacturer's instructions (Nippon Genetics Co. Ltd, Tokyo, Japan). Step 3 the extracted DNA was sent to Eurofins Genomics laboratory (Eurofins Genomics, Tokyo, Japan) for DNA sequencing. Step 4 and 5 was to subject the DNA to phylogenetic analysis was conducted by

TechnoSuruga Laboratory (TechnoSuruga Laboratory Company Ltd, Tokyo Japan), which used the BLAST algorithm to find related sequences in the GeneBank Database, DNA Data Bank of Japan and the European Molecular Biology Laboratory.

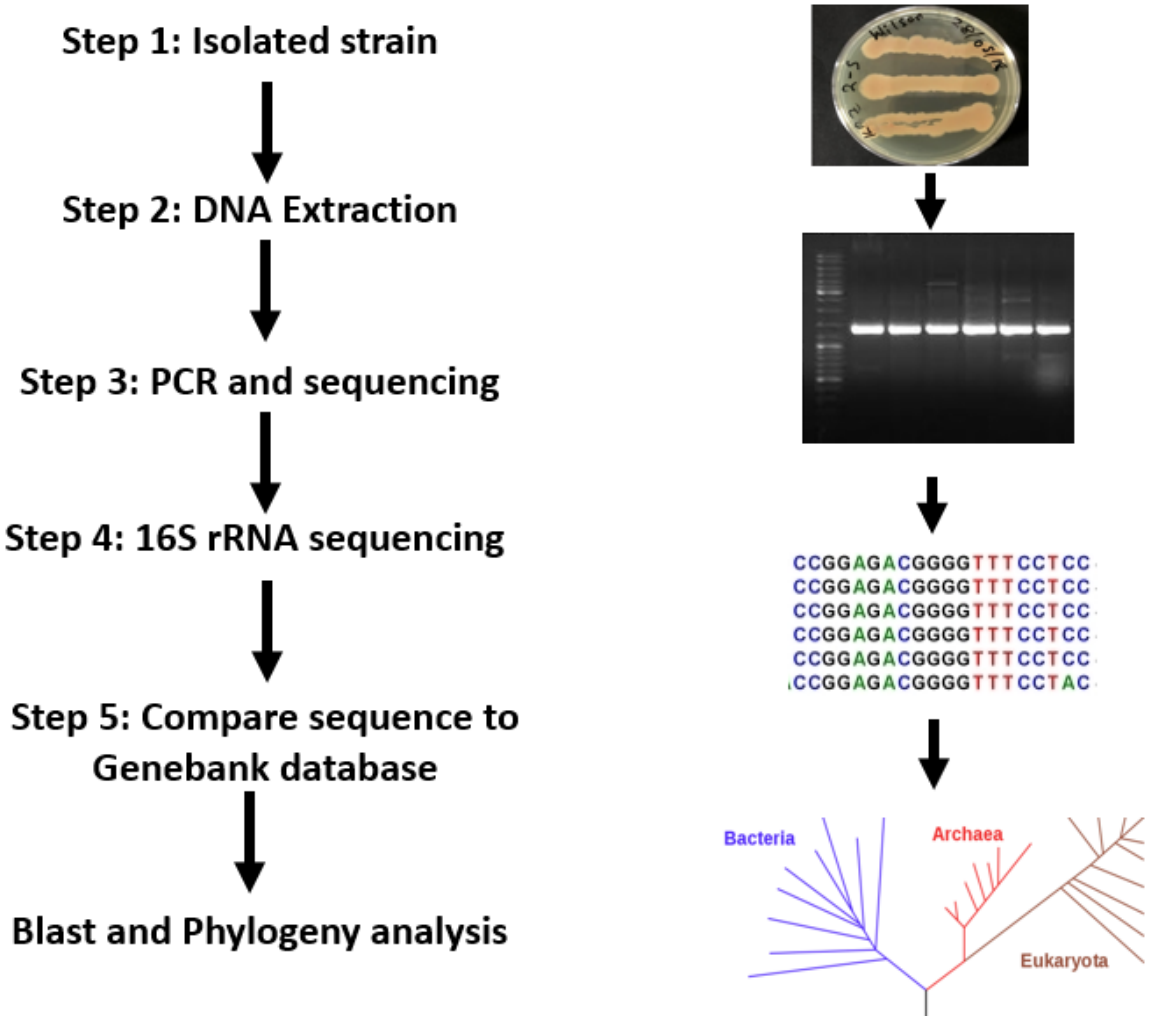

Fig. 3.4: Steps followed in molecular identification of Pb resistant ureolytic bacteria

3.4.4 Effect of Pb on microbial growth and urease activity of isolates

The same procedure used in Chapter 2 Subsection 2.4.1 and 2.4.2 were used to determine the effect of Pb on microbial growth and urease activity of isolates.

3.4.5 Determination of the Ca^{2+}/urea concentration for solidification

Bioprecipitation experiments were carried out to determine the Ca^{2+}/urea concentrations required for solidification. The bacterial isolate was precultured for 24 h in 5 mL NH4 YE medium, then 1 mL of preculture was inoculated into 100 mL of NH4 YE medium to grow the main culture at 30 °C for 24 h with continuous aeration at 160 rpm. The bacterial suspension was then added to

different equimolar concentrations of $CaCl_2$ and urea (0.1 M, 0.3 M, 0.5 M, 0.75 M, and 1.0 M). The mixtures were subsequently incubated for 24 h at 30 °C with shaking (160 rpm) and then centrifuged (15,000 rpm for 5 min) to collect the precipitate.

3.4.6 Evaluation of biocemented sand

The same procedures outlined in Chapter 2 were used to evaluated using the following parameters:

i. Estimated UCS using penetrometer;
ii. Hydraulic conductivity;
iii. SEM/XRD analysis; and
iv. Calcium carbonate content.
v. Colony-forming units (CFU) were calculated according to Equation 3.1

$$\frac{CFU}{mL} = \frac{\text{Number of colonies} \times \text{Dilution factor}}{\text{Volume of culture plated}} \qquad 3.1$$

3.5 Results and discussion

3.5.1 Isolation of ureolytic bacteria

Ureolytic bacteria were isolated based on the color change of the cresol red solution after urea hydrolysis. Colonies that changed the color of the solution from yellow to purple were selected. The color change is observed due to urea hydrolysis that causes the pH of the medium to rise. Of the thirty-five isolates from Kabwe, only four isolates, identified as *Oceanobacillus profundus* KBZ 1-3, Psychrobacillus sp. KBZ 2-2, *Oceanobacillus profundus* KBZ 2-3, and *O. profundus* KBZ 2-5 were found to produce urease and tolerated Pb, and were screened. Fig. 3.5 shows the sample ID, colonies on a plate, name of the isolated strain and their respective biosafety level. Biosafety level 1 applies to bacteria which are low-risk microbes that pose little to no threat of infection in healthy adults (*Laboratory biosafety manual Third edition*, 2004). *O. profundus* KBZ 1-3 and *O. profundus* KBZ 2-5 were selected for subsequent experiments because they were Pb-resistant and capable of biocementation. Fig. 3.6 shows the neighbor-joining phylogenetic tree of *O. profundus* KBZ 1-3 and *O. profundus* KBZ 2-5, which were isolated from the leach plant residue mine waste and near the wastewater pond, respectively.

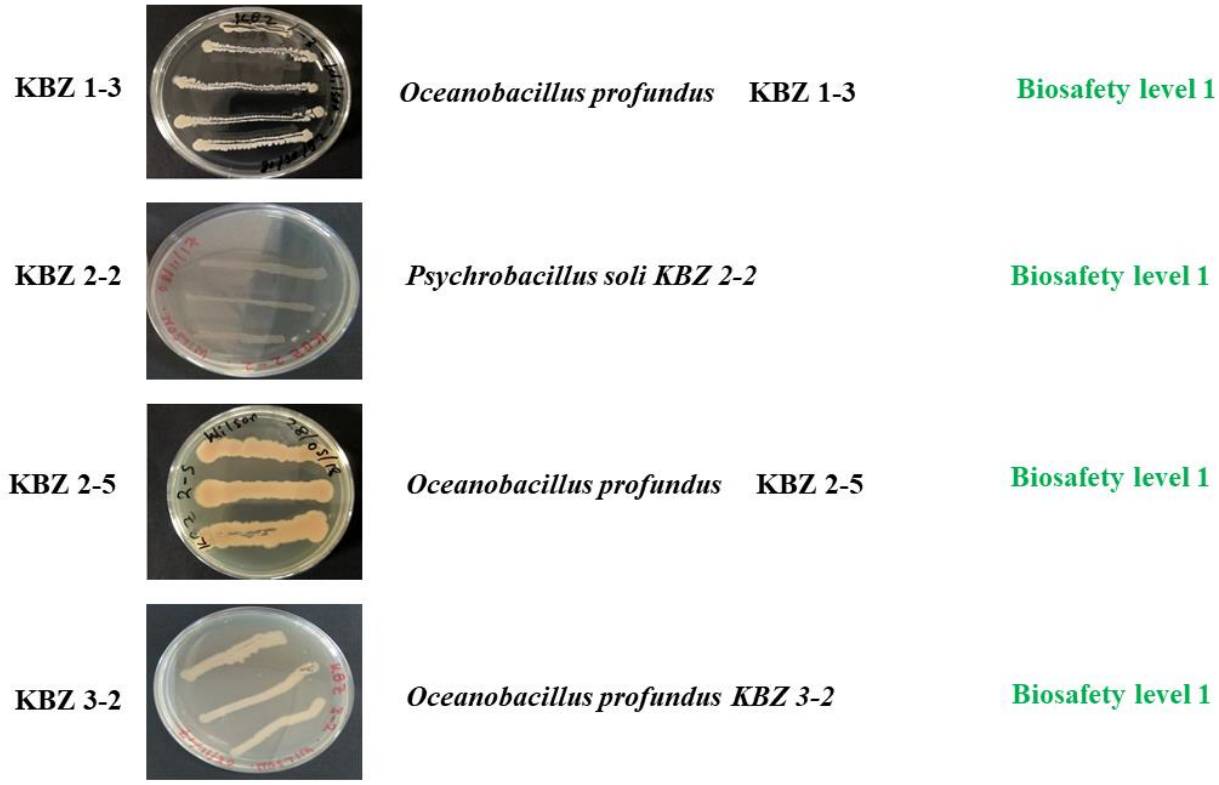

Fig. 3.5: Sample ID, isolated colonies on an agar plate, name of the isolated strain and their respective biosafety level

Both *O. profundus* 1-3 and *O. profundus* KBZ 2-5 are gram-positive, motile, aerobic, rod-shaped (0.2-0.4 µm and 0.5-0.6 µm respectively) and are classified as biosafety level 1 bacteria. The genus *Oceanobacillus* has been previously isolated from wastewater (Nam et al., 2008), Korean food (Whon et al., 2010), deep-sea sediment core samples (Yu et al., 2014) and human gut (Lagier et al., 2015).

According to literature, there are no reports indicating their potential application in biotechnology, bioremediation nor biosorption. Therefore, *O. profundus* KBZ 1-3 and *O. profundus* KBZ 2-5 isolated from Kabwe waste samples represent a novel *Oceanobacillus* species that is being applied for the first time in a bioremediation study.

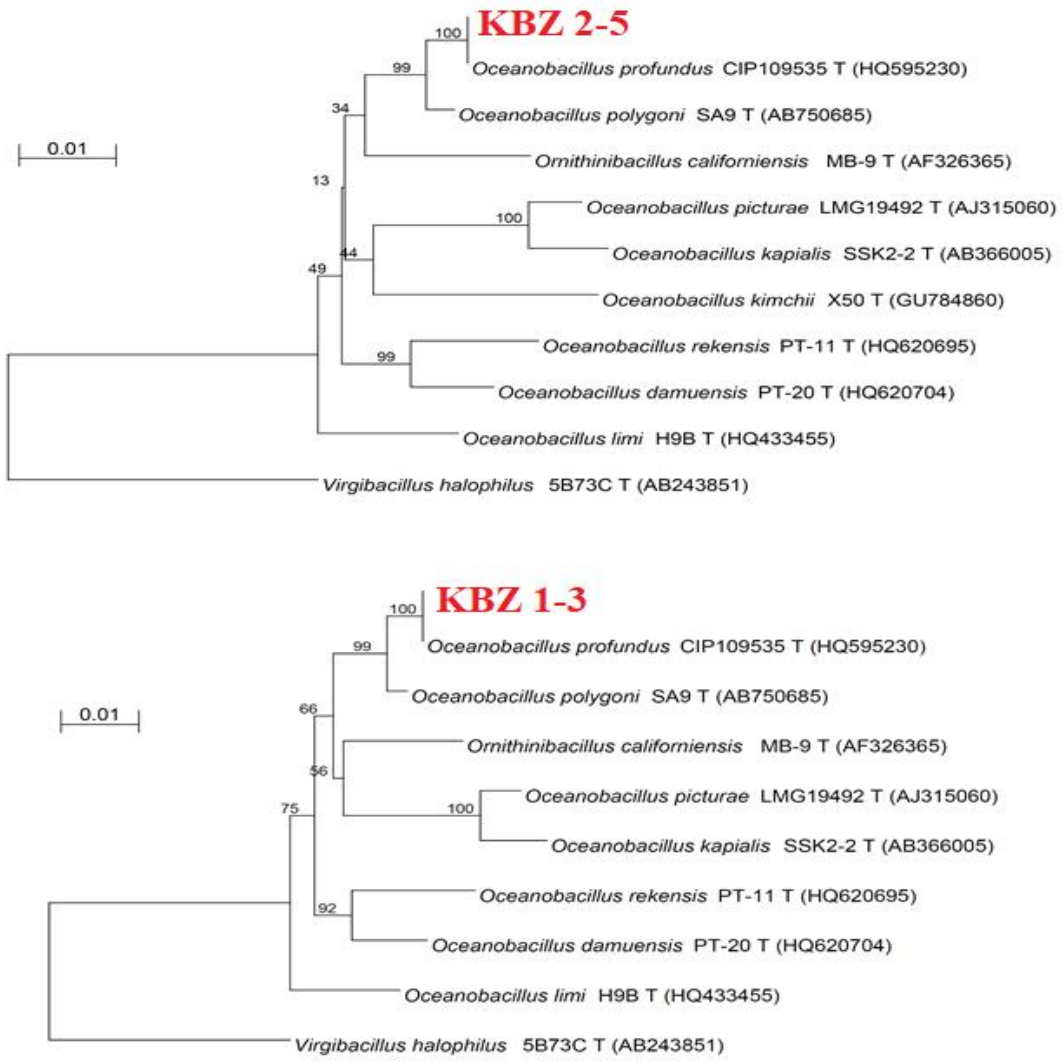

Fig. 3.6: Neighbor-joining phylogenetic tree based on 16s rRNA gene sequence of strains *O. profundus* KBZ 1-3, and *O. profundus* KBZ 2-5, type strains of *Oceanobacillus* species and related taxa

3.5.2 Effect of Pb on microbial growth and urease activity of isolates

Since the isolates are intended to be used in a heavily Pb-contaminated environment, the bacteria were tested for the effect of Pb (II) in aqueous solutions. Fig. 3.7 shows the effects of Pb on both microbial growth and urease activity of *O. profundus* KBZ 1-3 and *O. profundus* KBZ 2-5. Both bacteria displayed similar growth patterns, i.e., increased growth in Pb-free media and slight growth retardation in the presence of 50 mg/L Pb. Therefore, the effects of Pb on microbial growth were minimal, likely because these bacteria were isolated from a Pb-contaminated site. Similar results have been reported from previous research at an abandoned mine in South Korea (Kang et al., 2015).

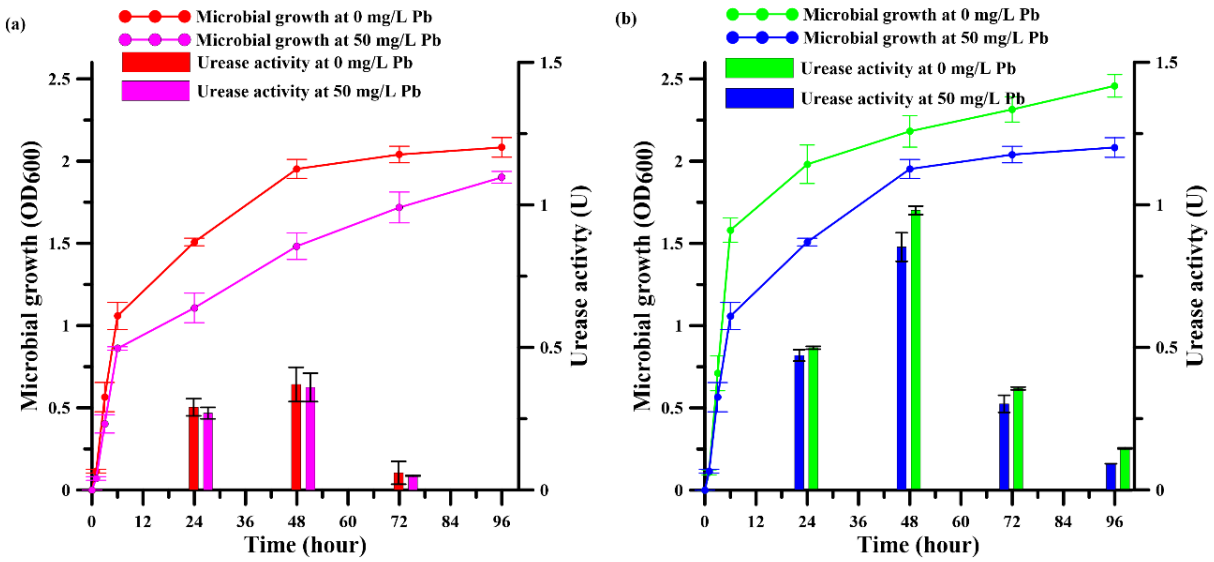

Fig. 3.7: Microbial growth and urease activity of (a) *O. profundus* KBZ 1-3, and (b) *O. profundus* KBZ 2-5. Error bars indicate standard deviations of three independent replicates. (U=µmol urea hydrolyzed/min)

The effect of Pb on urease activity was studied because it is crucial in MICP-mediated bioremediation. As shown in Fig. 3.7, the urease activity *O. profundus* KBZ 2-5 is higher than that of *O. profundus* KBZ 1-3; both bacteria expressed the highest urease activity after 48 h incubation with only appreciable levels at 24 h and 72 h. Only *O. profundus* KBZ 2-5 maintained the enzyme activity until 96 h. The urease activities of both isolates were not significantly affected by Pb, probably because they were isolated from a Pb -contaminated site. Higher urease activity is very important in MICP-mediated processes because it has a significant impact on the rate of carbonate production that consequently precipitates as $CaCO_3$. The results clearly showed increased growth and urease activity by *O. profundus* KBZ 1-3 and *O. profundus* KBZ 2-5 in the absence and presence of Pb. Overall, both bacteria are suitable for the biocementation of mine waste contaminated with Pb because they are Pb-tolerant, with high growth and urease activities.

3.5.3 Determination of the Ca^{2+}/urea concentration required for solidification

Calcium and urea are the two most important ingredients for carrying out the MICP process. The urease enzyme produced from the bacteria hydrolyzes urea ($CO(NH_2)_2$) to ammonium (NH_4^+) and carbonate (CO_3^{2-}) ions, which leads to the precipitation of $CaCO_3$ in the presence of calcium ions (Ca^{2+}). Therefore, the tolerance to and the optimal concentrations of Ca and urea may vary from one bacterial species to another, requiring the determination of optimal conditions for *O. profundus* KBZ 1-3 and *O. profundus* KBZ 2-5. Fig. 3.8 shows the amount of precipitate formed

by both bacteria when the molar concentration ratio of Ca: urea = 1:1; equimolar concentrations, according to a previous study (Soga and Qabany, 2013).

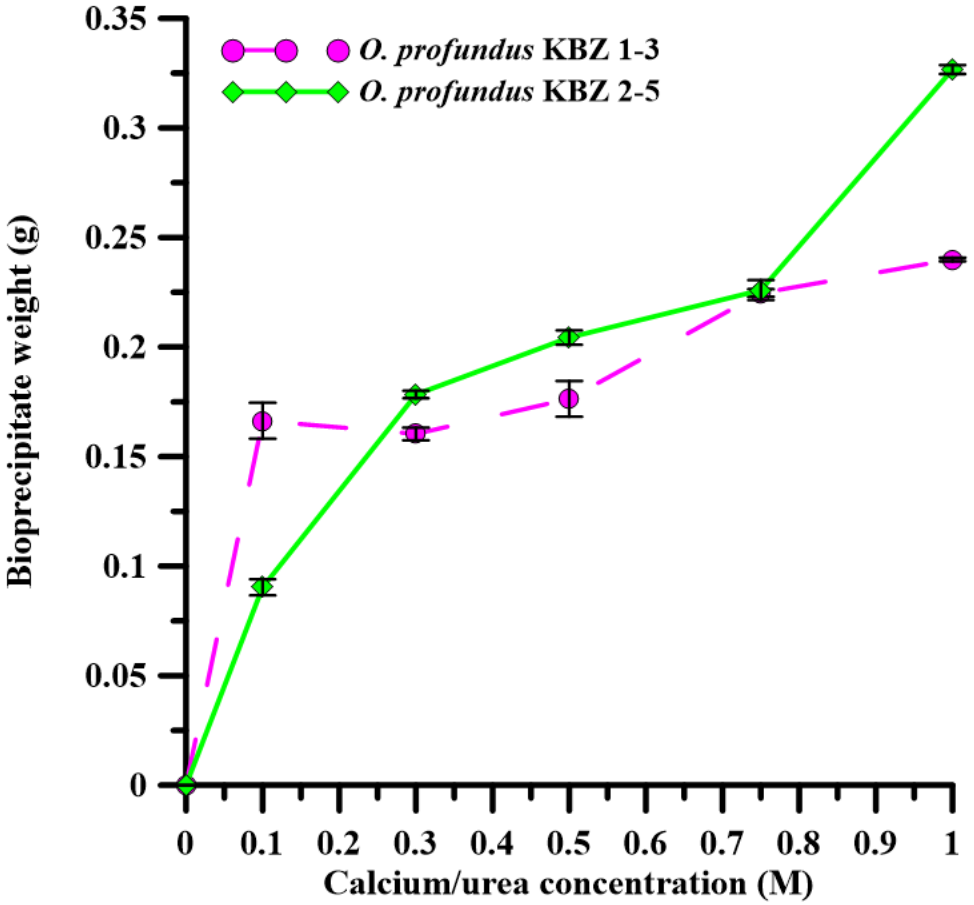

Fig. 3.8: Weight of $CaCO_3$ bioprecipitated by *O. profundus* KBZ 1-3 and *O. profundus* KBZ 2-5 at different equimolar concentrations of calcium and urea. Error bars indicate the standard deviation of three independent replicates.

As shown in Fig. 3.8, increasing the equimolar Ca and urea concentrations also increased the amount of precipitate. In this study, 0.5 M for Ca and urea was used. Previous studies have indicated that a low equimolar concentration in the solution should be used to ensure a uniform consistency of $CaCO_3$ precipitation (Mujah et al., 2017). Table 3.2 shows the conducive Ca/urea concentration of other ureolytic bacteria. Since a solution with low concentration may produce a more uniform precipitation pattern, even though higher concentrations produce higher amounts of $CaCO_3$ precipitate, a lower concentration was selected. In this study, both *O. profundus* KBZ 1-3 and *O. profundus* KBZ 2-5 produced the precipitation of spherical calcite crystals (Fig. 3.9). Calcite is the preferred form of $CaCO_3$ for biocementation because it is the most stable, compared to the other polymorphic forms such as aragonite and vaterite (Boulos et al., 2014). The two isolates precipitated

$CaCO_3$, which can be used as an inert covering for mine wastes. Capping is advantageous as a treatment technology because it is a permanent remedy that can also eliminate dust, thus addressing chronic risks of Pb poisoning to humans and other ecological receptors (Bellenfant et al., 2013; Johnson et al., 1992; Lottermoser, 2011).

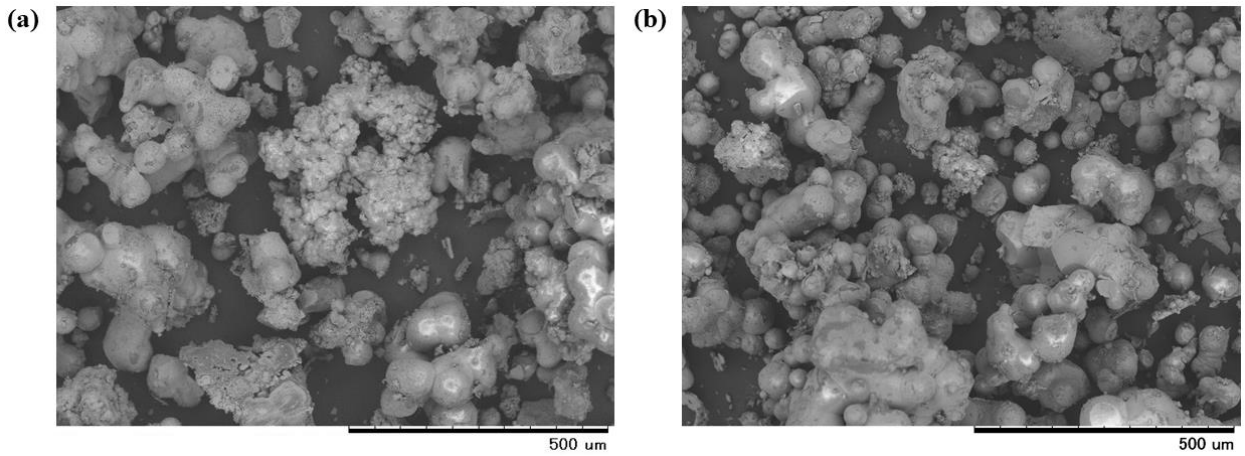

Fig. 3.9: SEM image of bioprecipitate by (a) *O. profundus* KBZ 1-3, and (b) *O. profundus* KBZ 2-5

Table 3.2: Comparison of the Ca/Urea concentration of this study and other ureolytic bacteria

Bacteria	Ca/Urea Concentration (M)	Reference
S. pasteurii	0.5/0.5	Whiffin et al., 2007
Pararhodobacter sp	0.5/0.5	Danjo and Kawasaki, 2015
L. xylanilyticus	1.0/1.0	Gowtham et al. 2019
Psychrobacillus sp	0.5/0.5	Gowtham et al. 2019
O. Profundus KBZ 1-3	0.5/0.5	This study
O. Profundus KBZ 2-5	0.5/0.5	This study

3.5.4 SEM and XRD analyses of solidified sand

To further confirm the role of MICP, biocemented samples were examined by SEM and XRD. Fig. 3.10 shows typical SEM images and the corresponding XRD patterns of the control (a) and biocemented sand (b, c). The control samples presented a typical morphology of sand and appeared as discrete particles, while the biocemented samples showed prominent crystalline

deposits on the surface and between sand particles. The SEM micrographs verify the effectiveness of the so-called bridging phenomenon mediated by MICP, i.e. the deposited $CaCO_3$ forms bridges between particles as part of the binding process (Mujah et al., 2017; Ng et al., 2012b; Rowshanbakht et al., 2016).

The XRD analysis revealed that the control specimens are composed of only quartz, while the biocemented sand includes calcite. Calcite is formed due to the ureolysis and subsequent precipitation of $CaCO_3$. The XRD results allowed us to conclude that MICP plays an important role in the solidification of sand.

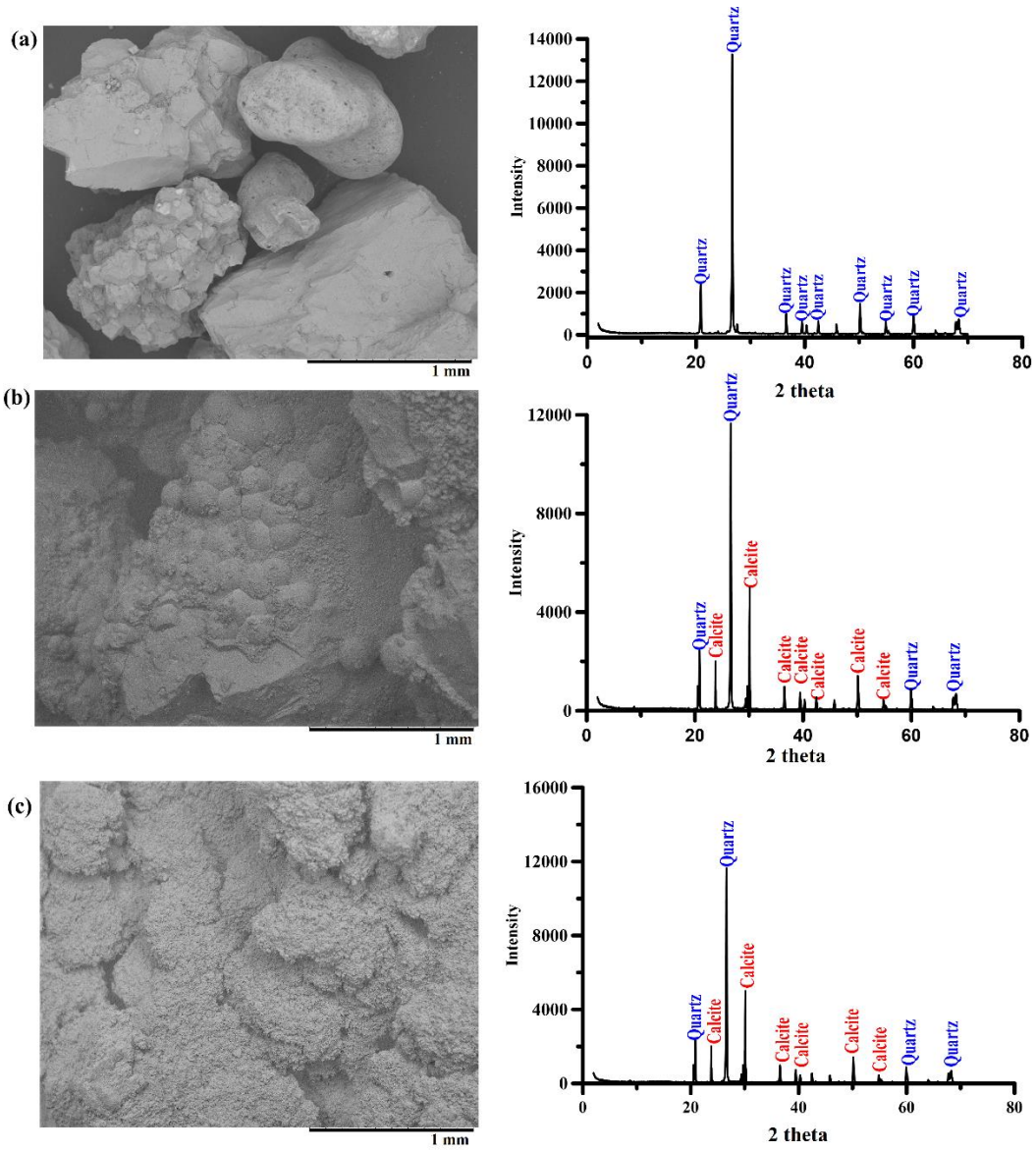

Fig. 3.10: SEM view and the corresponding XRD analysis comparing (a) control specimen, (b) biocemented sand prepared by the flow-through method using *O. profundus* KBZ 1-3, and (c) biocemented sand prepared by the flow-through method using *O. profundus* KBZ 2-5.

The major pathway for Pb to enter into the blood of humans and animals around the Kabwe mine site is through inhalation and injection of dust particles emanating from the abandoned mine wastes dumps, since the prevailing winds blow mostly from east (the mine site) to west (toward a large residential area) (Tembo et al., 2006; Yabe et al., 2011, 2013, 2015, 2018). Immobilizing the sand via MICP aggregates the sandy material, making it less susceptible to being blown by the wind. This significantly curtails the Pb exposure pathway to humans and animals in and around the mine site. MICP using indigenous bacteria can be immediate and easily implemented because all the required materials such as sand, indigenous bacteria, nutrients, Ca source, and urea are locally available. Some researchers have proposed the use of alternative locally available nutrients and Ca sources such as lactose mother liquor (Achal et al., 2009) and eggshells (Choi et al., 2016), which also demonstrates the flexibility of the process. In a similar way, many locally available resources required for capping, including the indigenous bacteria, can be made available that will not change the integrity of the local ecology.

3.5.5 CFU, UCS, and $CaCO_3$ content of biocemented sand

UCS was measured to characterize the strength of cemented sand. Fig. 3.11 and Fig. 3.13 shows the appearance biocemented sand at days 1, 7 and 14, while Fig. 3.14 and Fig. 3.15 shows the corresponding estimated values of CFU, UCS, and $CaCO_3$ at the top, middle, and bottom parts of the specimens. All control specimen had no strength while sand biocemented by *O. profundus* KBZ 1-3 under immersed and flow-through conditions had maximum estimated UCS values of 4 MPa and 1.7 Mpa (Fig. 3.13(c), (d)), corresponding to 19.98 % and 4.56 % $CaCO_3$ (Fig. 3.13(e), (f)), content and maximum bacterial count of 1×10^{-6} CFU/mL and 2.68×10^{-6} CFU/mL on day 14. The results indicated that both UCS and $CaCO_3$ content increased with treatment days with immersed condition showing greater strength at both day 7 and days 14. As shown in Fig 3.13 (a), the CFU/ml shown a uniform distribution throughout immersed method treatment compared to disproportionate distribution with the flow-through method (Fig 3.13 (b)). This could have been due to less contact time during the injection of bacterial suspension and cementation solution. Similar results were obtained when *O. profundus* KBZ 2-5 was used under both immersed and flow-through conditions. Maximum estimated UCS values of 5.7 MPa and 3.1 Mpa (Fig. 3.14(c), (d)), corresponding to 16.78 % and 2.54 % $CaCO_3$ content (Fig. 3.14(e), (f)), and maximum bacterial count of 1.3×10^{-6} CFU/mL and 2.9×10^{-6} CFU/mL on day 14. In comparison to the results of *O. profundus* KBZ 1-3, the results indicated that both CFU, UCS and $CaCO_3$ content increased with treatment days with immersed condition showing greater strength at both day 7 and days 14. Generally, for all cases,

the amount of $CaCO_3$ content in the immersed condition is greater than flow through condition due to differences in contact time.

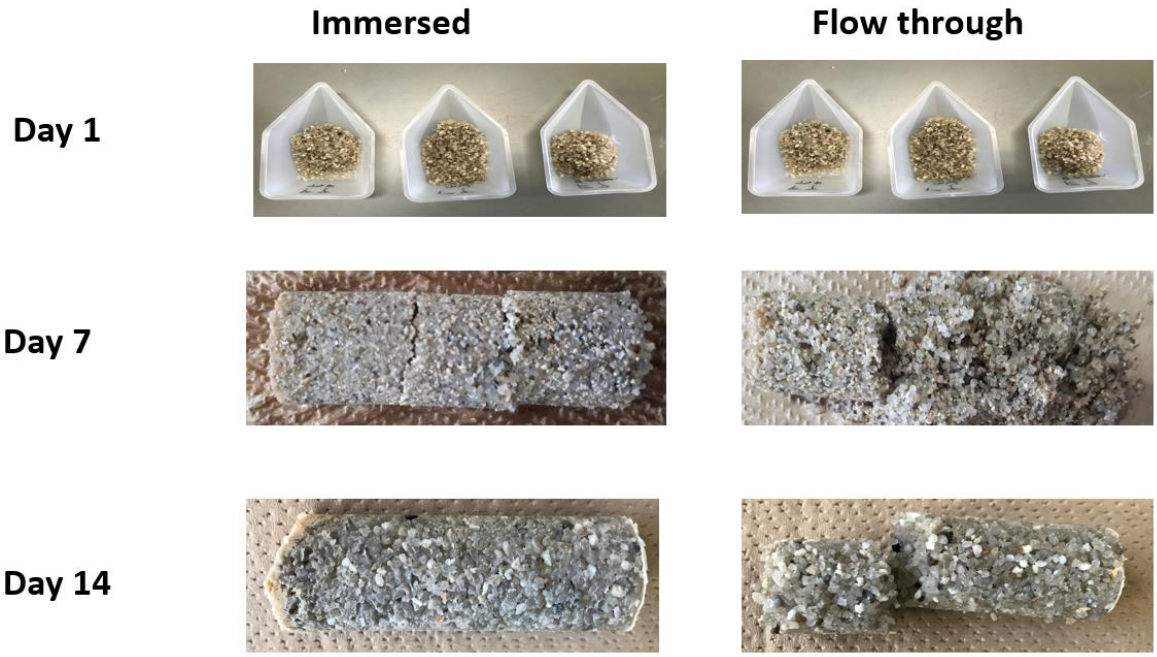

Fig. 3.11: Visualization of biocemented sand mediated by *O. profundus* KBZ 1-3 treated by both immersed and flow through treatment methods at day 1, 7 and 14 days

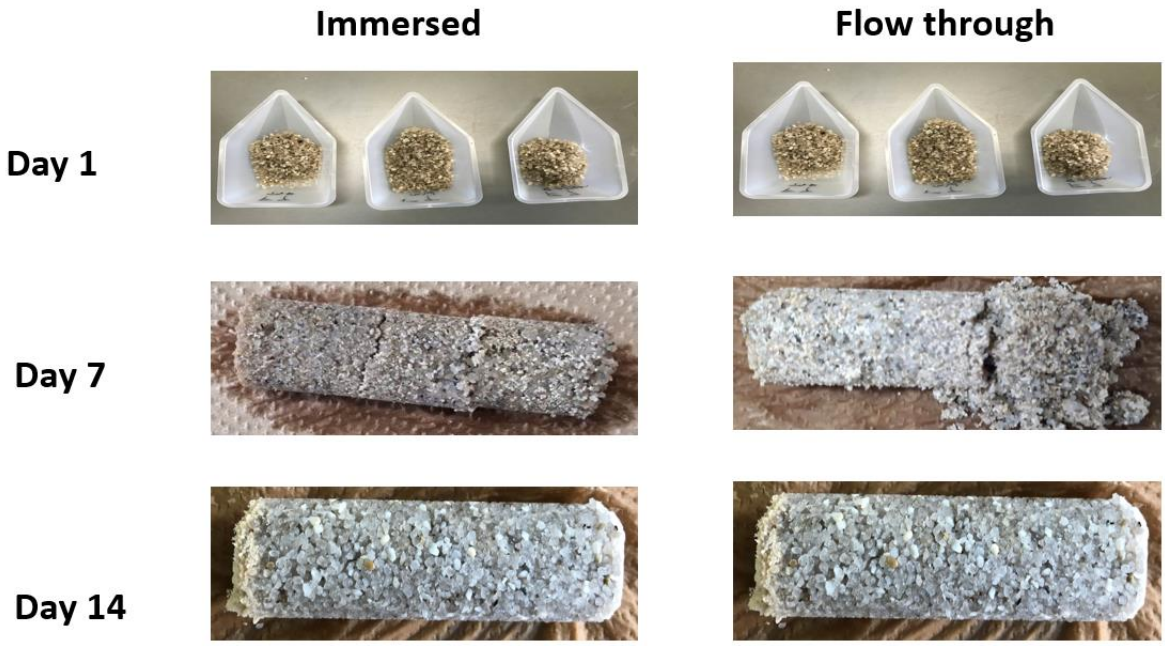

Fig. 3.12: Visualization of biocemented sand mediated by *O. profundus* KBZ 2-5 treated by both immersed and flow through treatment methods at day 1, 7 and 14 days.

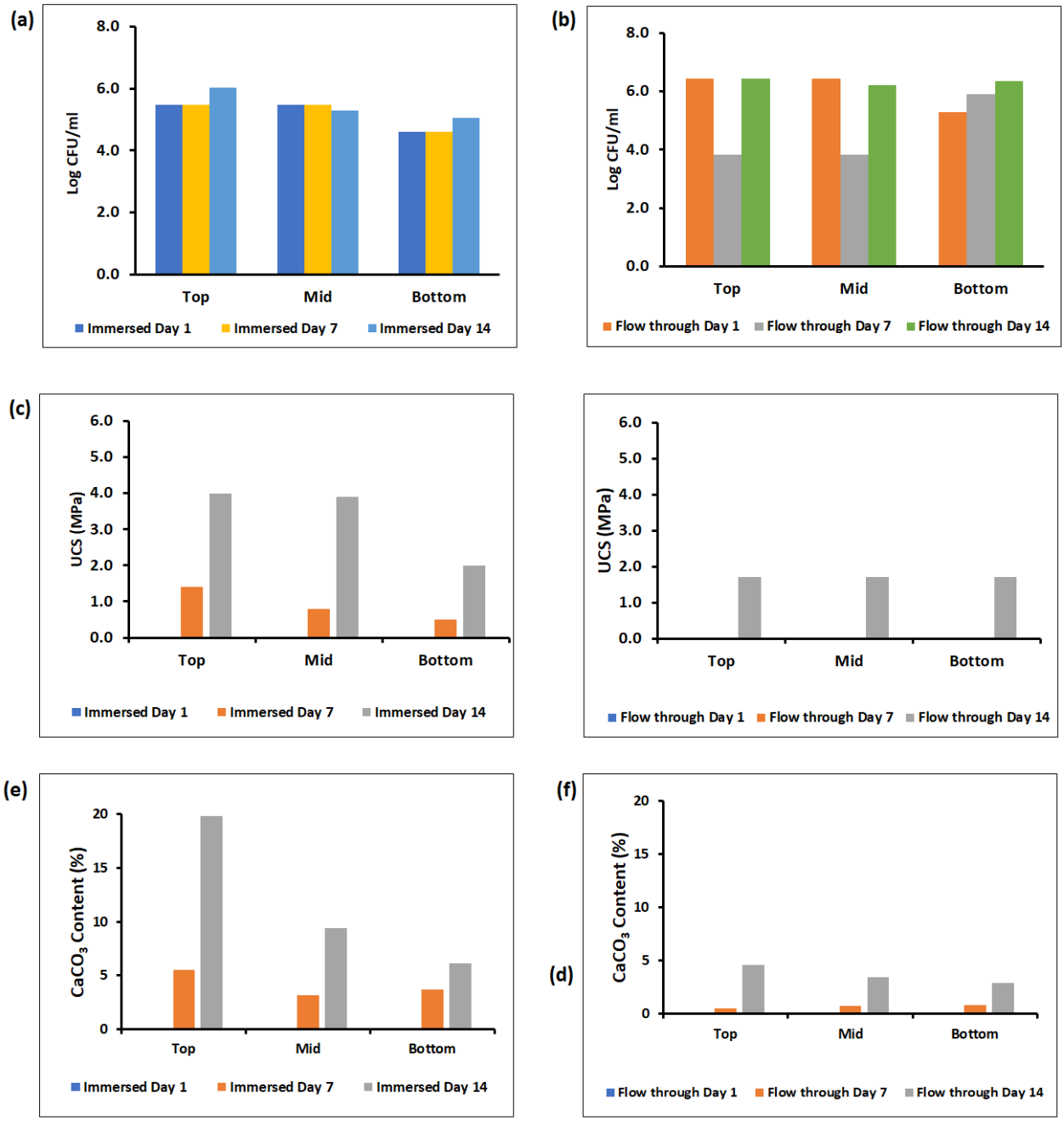

Fig. 3.13: Temporal variation of CFU/mL, UCS and $CaCO_3$ mediated by *O. profundus* KBZ 1-3 and *O. profundus* KBZ 1-3

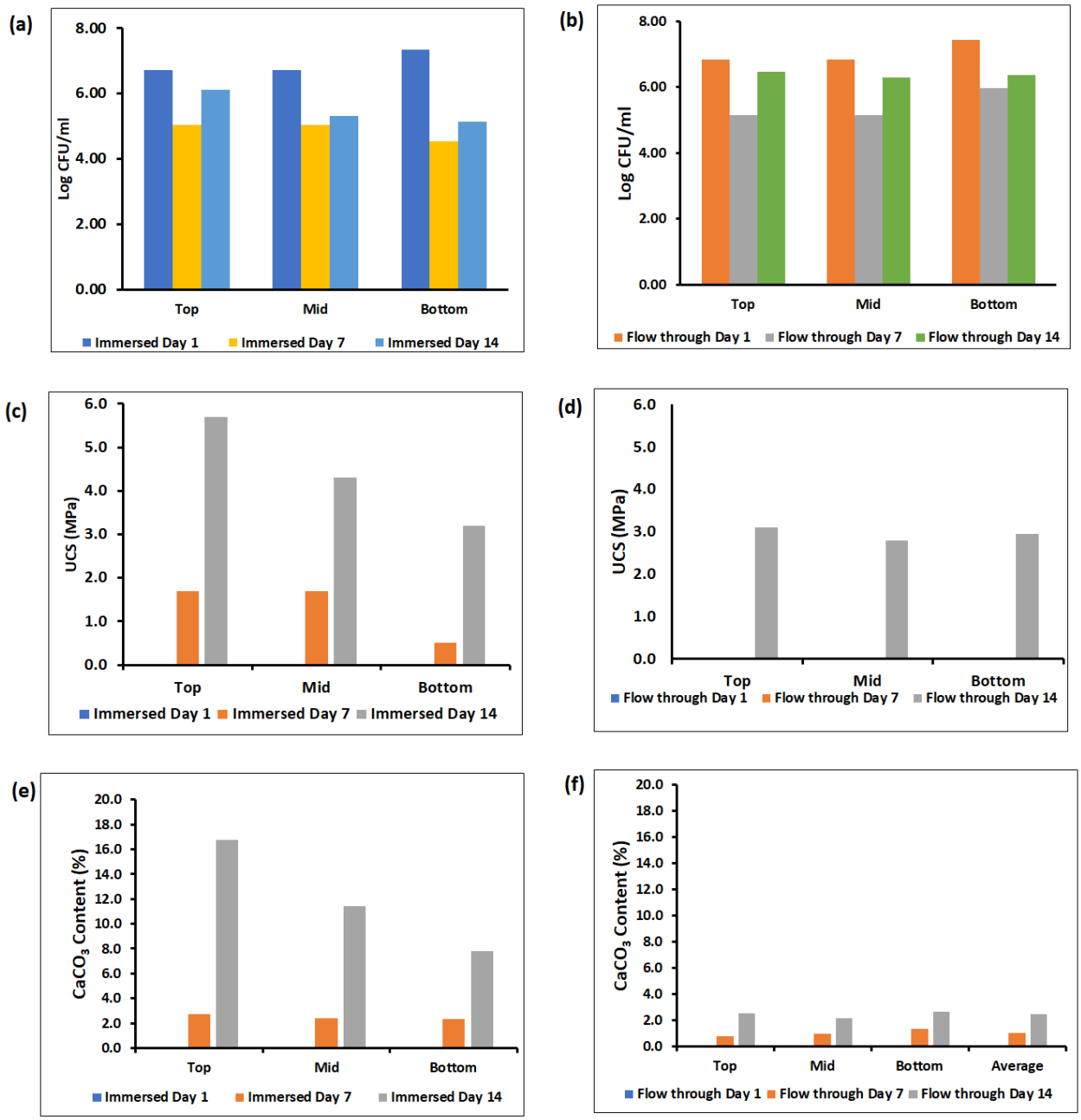

Fig. 3.14: Temporal variation of CFU/mL, UCS and $CaCO_3$ mediated by *O. profundus* KBZ 2-5

Since the difference in UCS was marginal, both bacteria may be useful for solidification. Additionally, biocemented sand by both immersed and flow-through cementation methods provided strength. Therefore, both types of injection methods can be used for solidifying sand. The results imply that the increased strength of biocemented sand has the potential to prevent the airborne transport of metallic dust by prevailing winds and to reduce infiltration; these benefits are similar to those of conventional cement, used worldwide for capping mining waste (Batchelor, 2006; Sobiecka, 2013). The UCS of biocemented sand increased with $CaCO_3$ which suggests that

$CaCO_3$ plays a significant role in the strength of sand provided the number of bacteria indicated by CFU, as elucidated by previous studies (Amarakoon and Kawasaki, 2018).

3.5.6 Hydraulic conductivity

Hydraulic conductivity is a measure of how easily water can pass through a material. During immobilization, reduced hydraulic conductivity is desired because it reduces the ability of water to contact contaminants, and therefore, reduces contaminant leaching rates. Hydraulic conductivity tests were performed for the sand before and after MICP treatment. Before treatment, the hydraulic conductivity was 1.4 $\times 10^{-3}$ m/s. Biocemented sand treated by the immersed and flow-through methods using *O. profundus* KBZ 1-3 reduced the permeability of sand to 9.6×10^{-8} m/s and 2.4×10^{-7} m/s, respectively. Similarly, *O. profundus* KBZ 2-5 reduced the water permeability of sand to 8.9×10−8 m/s and 2.5×10−7 m/s when treated by the immersed and flow-through methods, respectively. In all the cases, the hydraulic conductivity improved by more than three orders of magnitude for both immersed and flow-through methods. The reduced hydraulic conductivity achieved in this study has the potential to limit the entrance of water and oxygen into the dump, and hence reduce the leaching of heavy metals. This reduction in permeability is consistent with results of previous studies (Achal et al., 2013, Eryürük et al., 2015).

Other studies have proposed vegetation cover (Chehregani et al., 2009, Leteinturier et al., 2001) and synthetic cover (Fourie et al., 2010; Mazzieri et al., 2013) to cap mine wastes. Vegetation cover is desirable because like MICP, it reduces surface erosion and because a large proportion of percolating water is lost to the atmosphere through transpiration, reducing the concentrations of soluble heavy metals entering watercourses. However, this method would be difficult to implement in Kabwe, because vegetation growth is not possible at the site due to lack of nutrients and high levels of toxic trace elements at the site (Leteinturier et al., 2001). On the other hand, synthetic covers are uneconomical and expensive, especially compared to the MICP technique. Due to its originality and sustainability, MICP has recently gained much attention from researchers around the world as a replacement for conventional concrete and has been proposed for other geotechnical applications such as ground improvement (Salifu et al., 2016b), coastal erosion control (Khan et al., 2015), mine waste immobilization (Achal et al., 2013), self-healing concrete (Wiktor and Jonkers, 2011), and wastewater treatment (Torres-Aravena et al., 2018). Conventional physicochemical methods have already been tested to clean up the environment. However, most of these methods are costly, perform sub-optimally, and produce secondary sludge, making the cleanup process expensive and unsustainable, requiring large inputs of energy and large quantities of chemical reagents (Jena and Dey, 2016).

3.6 Conclusion

The abandoned Pb and Zn mine wastes in Kabwe mine continue to pose a serious threat to the quality of human health, water, and soil. In this chapter it has been shown that MICP mediated by indigenous ureolytic bacteria *Oceanobacillus profundus* KBZ 1-3 and KBZ 2-5 can be used to solidify sand, thus preventing dust formation and water infiltration. Both bacteria were able to tolerate Pb and mediate the formation of $CaCO_3$ bioprecipitate, which was confirmed to be calcite by XRD analysis. The biocemented sand achieved maximum UCS values of 3.1 MPa and 5.7 MPa, which are useful enough to prevent Pb dust particles from being blown away by prevailing winds and to prevent water erosion. Combined with a reduced hydraulic conductivity of 9.6×10^{-8} m/s and 8.9×10^{-8} m/s mediated by *Oceanobacillus profundus* KBZ 1-3 and KBZ 2-5, respectively, the process is expected to retard heavy metal leaching due to the lack of oxygen and water resulting from reduced infiltration.

References

Achal, V., Mukherjee, A., Basu, P.C., Reddy, M.S., 2009. Lactose mother liquor as an alternative nutrient source for microbial concrete production by Sporosarcina pasteurii. J. Ind. Microbiol. Biotechnol. 36, 433–438. https://doi.org/10.1007/s10295-008-0514-7

Achal, V., Pan, X., Lee, D.J., Kumari, D., Zhang, D., 2013. Remediation of Cr(VI) from chromium slag by biocementation. Chemosphere 93, 1352–1358. https://doi.org/10.1016/j.chemosphere.2013.08.008

Amarakoon, G.G.N.N., Kawasaki, S., 2018. Factors affecting sand solidification using MICP with *Pararhodobacter* sp. Mater. Trans. 59, 72–81. https://doi.org/10.2320/matertrans.M-M2017849

Batchelor, B., 2006. Overview of waste stabilization with cement. Waste Manag. 26, 689–698. https://doi.org/10.1016/j.wasman.2006.01.020

Bellenfant, G., Guezennec, Anne-Gwenaëlle Bodénan, F., D'Hugues, P., Cassard, D., 2013. Reprocessing of mining waste: combining environmental management and metal recovery? Mine Clos. 571–582.

BMR Group PLC, 2019. Tailings stockpiles [WWW Document]. URL http://www.bmrplc.com/tailings_stockpiles.php (accessed 1.25.19).

Boulos, R.A., Zhang, F., Tjandra, E.S., Martin, A.D., Spagnoli, D., Raston, C.L., 2014. Spinning up the polymorphs of calcium carbonate. Sci. Rep. 4, 1–6. https://doi.org/10.1038/srep03616

Chehregani, A., Noori, M., Yazdi, H.L., 2009. Phytoremediation of heavy-metal-polluted soils: Screening for new accumulator plants in Angouran mine (Iran) and evaluation of removal ability. Ecotoxicol. Environ. Saf. 72, 1349–1353. https://doi.org/10.1016/j.ecoenv.2009.02.012

Chen, X., Guo, H., Cheng, X., 2017. Heavy metal immobilisation and particle cementation of tailings by biomineralisation. Environ. Geotech. 1–7. https://doi.org/10.1680/jenge.15.00068

Choi, S., Wu, S., Chu, J., 2016. Biocementation for sand using an eggshell as calcium source. J. Geotech. Geoenvironmental Eng. 142, 2–5. https://doi.org/10.1061/(ASCE)GT.1943-5606.0001534.

Eryürük, K., Yang, S., Suzuki, D., Sakaguchi, I., Akatsuka, T., Tsuchiya, T., Katayama, A., 2015. Reducing hydraulic conductivity of porous media using $CaCO_3$ precipitation induced by *Sporosarcina pasteurii*. J. Biosci. Bioeng. 119, 331–336. https://doi.org/10.1016/j.jbiosc.2014.08.009

Fourie, A.B., Bouazza, A., Lupo, J., 2010. Improving the performance of mining infrastructure through the judicious use of geosynthetics. 9th Int. Conf. Geosynth. Brazil.

Gowthaman, S., Mitsuyama, S., Nakashima, K., Komatsu, M., Kawasaki, S., 2019. Biogeotechnical approach for slope soil stabilization using locally isolated bacteria and inexpensive low-grade chemicals: A feasibility study on Hokkaido expressway soil, Japan. Soils Found. https://doi.org/10.1016/j.sandf.2018.12.010

Jena, S., Dey, S.K., 2016. Heavy Metals. Am. J. Environ. Stud. 1, 48–60.

Johnson, M.S., Cooke, J.A., Stevenson, J.K.W., 1992. Revegetation of metalliferous wastes and and after metal mining, Mining and its Environmental Impact.

Kang, C.H., Oh, S.J., Shin, Y., Han, S.H., Nam, I.H., So, J.S., 2015. Bioremediation of lead by ureolytic bacteria isolated from soil at abandoned metal mines in South Korea. Ecol. Eng. 74, 402–407. https://doi.org/10.1016/j.ecoleng.2014.10.009

Khan, M.N.H., Amarakoon, G.G.N.N., Shimazaki, S., Kawasaki, S., 2015. Coral sand solidification test based on microbially induced carbonate precipitation using ureolytic bacteria. Mater. Trans. 56, 1725–1732. https://doi.org/10.2320/matertrans.M-M2015820

Kim, J.H., Lee, J.Y., 2018. An optimum condition of MICP indigenous bacteria with contaminated wastes of heavy metal. J. Mater. Cycles Waste Manag. 1–9. https://doi.org/10.1007/s10163-018-0779-5

Laboratory biosafety manual Third edition, 2004.

Lagier, J.C., Khelaifia, S., Azhar, E.I., Croce, O., Bibi, F., Jiman-Fatani, A.A., Yasir, M., Helaby, H. Ben, Robert, C., Fournier, P.E., Raoult, D., 2015. Genome sequence of *Oceanobacillus picturae* strain S1, an halophilic bacterium first isolated in human gut. Stand. Genomic Sci. 10, 1–9. https://doi.org/10.1186/s40793-015-0081-2

Leteinturier, B., Laroche, J., Matera, J., Malaisse., F., 2001. Reclamation of lead/zinc processing wastes at Kabwe, Zambia: a phytogeochemical approach. South Africa J. Sci. 97, 624–627.

Lottermoser, B.G., 2011. Recycling, reuse and rehabilitation of mine wastes. Elements 7, 405–410. https://doi.org/10.2113/gselements.7.6.405

Mazzieri, F., Di Emidio, G., Fratalocchi, E., Di Sante, M., Pasqualini, E., 2013. Permeation of two GCLs with an acidic metal-rich synthetic leachate. Geotext. Geomembranes 40, 1–11. https://doi.org/10.1016/j.geotexmem.2013.07.011

Mufinda, B., 2015. A History of Mining in Broken Hill (Kabwe): 1902-1929. University of the Free State. *Thesis*

Mujah, D., Shahin, M.A., Cheng, L., 2017. State-of-the-art review of biocementation by microbially induced calcite precipitation (MICP) for soil stabilization. Geomicrobiol. J. 34, 524–537. https://doi.org/10.1080/01490451.2016.1225866

Mwandira, W., Nakashima, K., Kawasaki, S., 2017. Bioremediation of lead-contaminated mine

waste by *Pararhodobacter* sp. based on the microbially induced calcium carbonate precipitation technique and its effects on strength of coarse and fine grained sand. Ecol. Eng. 109, 57–64. https://doi.org/10.1016/j.ecoleng.2017.09.011

Nam, I.H., Roh, S.B., Park, M.J., Chon, C.M., Kim, J.G., Jeong, S.W., Song, H., Yoon, M.H., 2016. Immobilization of heavy metal contaminated mine wastes using *Canavalia ensiformis* extract. Catena 136, 53–58. https://doi.org/10.1016/j.catena.2015.07.019

Nam, J.H., Bae, W., Lee, D.H., 2008. *Oceanobacillus caeni* sp. nov., isolated from a Bacillus-dominated wastewater treatment system in Korea. Int. J. Syst. Evol. Microbiol. 58, 1109–1113. https://doi.org/10.1099/ijs.0.65335-0

Ng, W., Lee, M., Hii, S., 2012. An overview of the factors affecting microbial-induced calcite precipitation and its potential application in soil improvement. World Acad. Sci. Eng. Technol. 62, 723–729.

Rowshanbakht, K., Khamehchiyan, M., Sajedi, R.H., Nikudel, M.R., 2016. Effect of injected bacterial suspension volume and relative density on carbonate precipitation resulting from microbial treatment. Ecol. Eng. 89, 49–55. https://doi.org/10.1016/j.ecoleng.2016.01.010

Salifu, E., MacLachlan, E., Iyer, K.R., Knapp, C.W., Tarantino, A., 2016. Application of microbially induced calcite precipitation in erosion mitigation and stabilisation of sandy soil foreshore slopes: A preliminary investigation. Eng. Geol. 201, 96–105. https://doi.org/10.1016/j.enggeo.2015.12.027

Sobiecka, E., 2013. Investigating the chemical stabilization of hazardous waste material (fly ash) encapsulated in Portland cement. Int. J. Environ. Sci. Technol. 10, 1219–1224. https://doi.org/10.1007/s13762-012-0172-1

Soga, A.A., Qabany, K., 2013. Effect of chemical treatment used in MICP on engineering properties of cemented soils. Géotechnique Volume 63, 331–339.

Tembo, B.D., Sichilongo, K., Cernak, J., 2006. Distribution of copper, lead, cadmium and zinc concentrations in soils around Kabwe town in Zambia. Chemosphere 63, 497–501. https://doi.org/10.1016/j.chemosphere.2005.08.002

Torres-Aravena, Á., Duarte-Nass, C., Azócar, L., Mella-Herrera, R., Rivas, M., Jeison, D., 2018. Can microbially induced calcite precipitation (MICP) through a ueolytic pathway be successfully applied for removing heavy metals from wastewaters? Crystals 8, 438. https://doi.org/10.3390/cryst8110438

Whon, T.W., Jung, M.-J., Roh, S.W., Nam, Y.-D., Park, E.-J., Shin, K.-S., Bae, J.-W., 2010. *Oceanobacillus kimchii* sp nov Isolated from a Traditional Korean Fermented Food. J. Microbiol. 48, 862–866. https://doi.org/10.1007/s12275-010-0214-7

Wiktor, V., Jonkers, H.M., 2011. Quantification of crack-healing in novel bacteria-based self-healing concrete. Cem. Concr. Compos. 33, 763–770. https://doi.org/10.1016/j.cemconcomp.2011.03.012

Yabe, J., Nakayama, S.M.M., Ikenaka, Y., Muzandu, K., Choongo, K., Mainda, G., Kabeta, M., Ishizuka, M., Umemura, T., 2013. Metal distribution in tissues of free-range chickens near a lead-zinc mine in Kabwe, Zambia. Environ. Toxicol. Chem. 32, 189–192. https://doi.org/10.1002/etc.2029

Yabe, J., Nakayama, S.M.M., Ikenaka, Y., Muzandu, K., Ishizuka, M., Umemura, T., 2011. Uptake of lead, cadmium, and other metals in the liver and kidneys of cattle near a lead-zinc mine in Kabwe, Zambia. Environ. Toxicol. Chem. 30, 1892–1897. https://doi.org/10.1002/etc.580

Yabe, J., Nakayama, S.M.M., Ikenaka, Y., Yohannes, Y.B., Bortey-Sam, N., Kabalo, A.N., Ntapisha, J., Mizukawa, H., Umemura, T., Ishizuka, M., 2018. Lead and cadmium excretion in feces and urine of children from polluted townships near a lead-zinc mine in Kabwe, Zambia. Chemosphere 202, 48–55. https://doi.org/10.1016/j.chemosphere.2018.03.079

Yabe, J., Nakayama, S.M.M., Ikenaka, Y., Yohannes, Y.B., Bortey-Sam, N., Oroszlany, B., Muzandu, K., Choongo, K., Kabalo, A.N., Ntapisha, J., Mweene, A., Umemura, T., Ishizuka, M., 2015. Lead poisoning in children from townships in the vicinity of a lead-zinc mine in Kabwe, Zambia. Chemosphere 119, 941–947. https://doi.org/10.1016/j.chemosphere.2014.09.028

Yu, C., Yu, S., Zhang, Z., Li, Z., Zhang, X.H., 2014. *Oceanobacillus pacificus* sp. nov., isolated from a deep-sea sediment. Int. J. Syst. Evol. Microbiol. 64, 1278–1283. https://doi.org/10.1099/ijs.0.056481-0

Zhu, X., Li, W., Zhan, L., Huang, M., Zhang, Q., Achal, V., 2016. The large-scale process of microbial carbonate precipitation for nickel remediation from an industrial soil. Environ. Pollut. 219, 149–155. https://doi.org/10.1016/j.envpol.2016.10.047

CHAPTER 4 ZINC AND LEAD REMOVAL FROM AQUEOUS SOLUTION BY METAL TOLERANT INDIGENOUS BACTERIA

4.1 Introduction

The contamination of water bodies by heavy metals has resulted in increased research on how to remove these toxic pollutants from the environment. The most investigated heavy metals include chromium (Cr), zinc (Zn), cadmium (Cd), mercury (Hg), lead (Pb), nickel (Ni), and arsenic (As) due to the significant public health and environmental risk they pose (Tchounwou et al., 2012). These heavy metals are introduced in the environment as a result of human activities such as mining (smelting, tailings, ore, and waste rock) and agriculture (fertilizers, pesticides, and herbicides) (Jena and Dey, 2016; Plumlee and Morman, 2011; Pourrut et al., 2011). Reverse osmosis, electrodialysis, ion exchange, precipitation, solvent extraction, and phytoremediation have mainly been used to decontaminate wastewater before being released into the natural environment, however, the cost of these technologies have challenges as they are extremely expensive and/or less effective (Ayangbenro and Babalola, 2017). In addition to these methods, biosorption has over the years emerged as one of the most promising alternatives to conventional heavy metal bioremediation method. Biosorption is the removal of heavy metal from aqueous solution by green biological materials such as bacteria (Khan et al., 2016), yeast (Rodríguez et al., 2018), algae (Anastopoulos and Kyzas, 2015), fungi (Prasad et al., 2013), or agricultural waste (Abdi and Kazemi, 2015). Even though many of these biomaterials have been isolated and identified, the isolation and identification of more and indigenously available biological materials are indispensable in sites heavily contaminated with heavy metals.

Therefore, this study was motivated to isolate novel Pb-tolerant indigenous bacteria strains from Pb contaminated soil and evaluate their ability to treat polluted water from Kabwe Mine. According to the authors' knowledge, this is the first study to isolate Pb resistant bacteria from Kabwe Mine Site for bioremediation purposes. Pb was selected for investigation because it is a pollutant that has led to significant health problems to those living in the vicinity (Yabe et al., 2015). Additionally, Pb was selected because the site where the bacterium was isolated has Pb contaminated due to abandoned mine which has polluted the flora and fauna of the area (Sracek et al., 2010). From previous investigations, it is evident that local population, soil,

water, and food is contaminated with Pb, leading Kabwe to be labeled as one of the 10 most polluted places on Earth in 2013 (Blacksmith, 2013). Therefore, isolation of indigenous bacteria strain is important because the isolated strain could possibly tolerate high heavy metal concentrations in different ways and may play a significant role in the restoration of a contaminated site as they are already adapted to the contaminated site and may potentially not change the local ecological niche.

4.2 Objective

The objectives of this Chapter were to use isolate metal tolerant bacteria for heavy metal removal from water and the specific objectives were to:

(i) The isolation of a novel Pb resistant bacterium from Pb contaminated soil at the Kabwe Mine Site in Kabwe, Zambia;

(ii) The determination of the effect of Pb and Zn on the isolated bacteria;

(iii) The determination of the accumulation and distribution of Pb and Zn accumulation in different cellular parts to elucidate the biosorption mechanism;

(iv) The evaluation of the efficiency of heavy metal removal using the isolation of a novel Pb resistant bacterium.

4.3 Materials and methods

4.3.1 Bacteria used

O. profundus KBZ 3-2 isolated from chapter 2 was used in this study.

4.3.2 Reagents and media

a) DAPI Nucleic Acid Stain, Molecular Probes, Invitrogen
b) Wheat germ agglutinin, Alexa Fluor® 633 conjugate, Molecular Probes, Invitrogen
c) Leadmium™ Green AM Dye, Molecular Probes, Invitrogen
d) LB (Luria-Bertani) media are two types of media (per liter) used in this study: 5 g/L yeast extract; 10 g/L Tryptone; 10 g/L Sodium Chloride; and 20 g/L Agar

4.3.3 Other equipment

a) Vibra-Cell™ (Sonics & Materials, Inc., Newtown, USA) was used for sonication.
b) Fourier Transform Infrared Spectroscopy (FTIR) was conducted using FTIR spectrometer JASCO 360 FTIR Spectrometer (Tokyo, Japan).

c) Freeze dryer (Eyela FDU-1200, Rikakikai Co. Ltd, Tokyo, Japan) was used for the preservation of biological preservation.

d) Spectral imaging confocal microscope (Nikon Confocal system A1Rsi, Nikon Instruments Inc.) shown in Fig. 4.1 was used for autofluorescence.

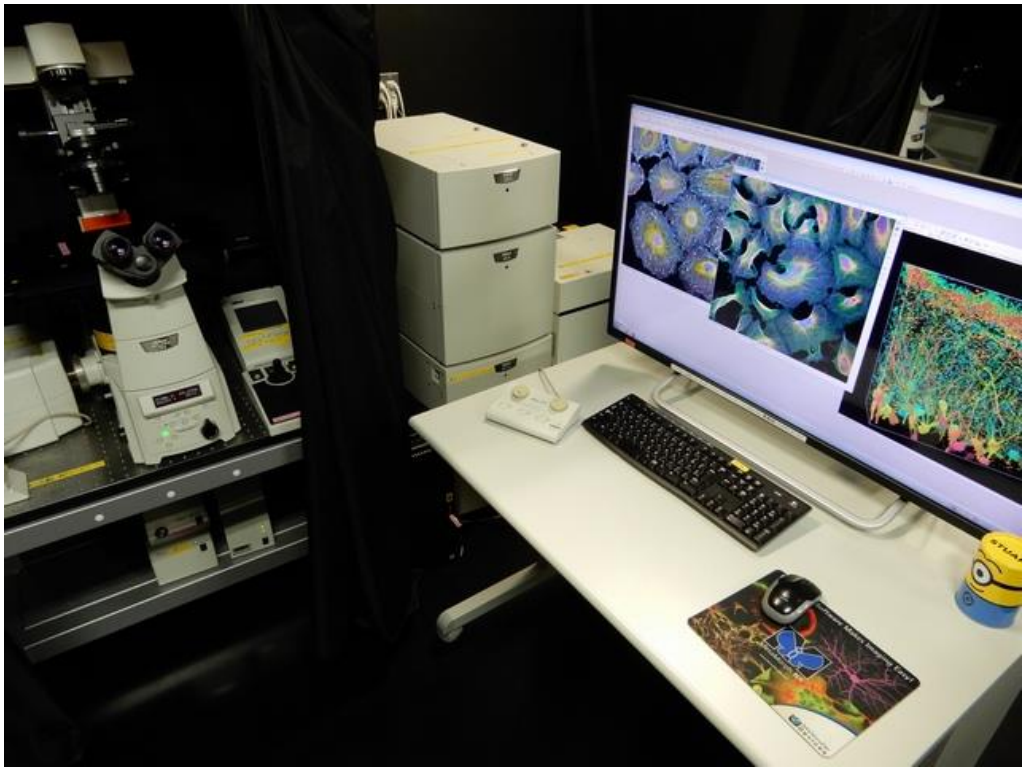

Fig. 4.1: Spectral imaging confocal microscope (*http://nic.es.hokudai.ac.jp/station1_e.html*)

4.4 Experimental methods

4.4.1 Pb and Zn stock solution preparation

Pb (II) and Zn (II) ion stock solutions were prepared by dissolving $PbCl_2$ and $ZnCl_2$ in distilled water. Dilutions were made to obtain the desired concentration. Prior to the use, the stock solution was filter sterilized through a sterilized 0.22 µm filter.

4.4.2 Effect of pH

pH 2 to pH 9 was used to determine the effect of pH adjusted using 1 M NaOH and 99.5 % concentrated nitric acid.

4.4.3 Effect of temperature

For the effect of temperature, after inoculation, samples were incubated at different temperature of 20 ºC, 25 ºC, 30 ºC, 35 ºC, and 40 ºC.

4.4.4 Effect of contact time

The effect of contact time on biosorption was studied allowing the biosorption to proceeded for 24 hours using a single metal solution containing ions with constant aeration in a shaker at 160 rpm at determined pH and temperature.

4.4.5 Determination of heavy metal removal efficiency

The removal efficiency was determined by allowing the biosorption to proceeded for 24 hours and then the sample was centrifuged at 10,000 rpm for 5 minutes and then filtered using a 0.45 µm filter. The filtrate was acidified by nitric acid to pH < 2 followed by measurement of the metal ion concentration by inductively coupled plasma atomic emission spectroscopy. The percentage removal of the metal ions in aqueous solution by the bacteria was calculated using Equation 4.1.

$$\text{Heavy metal removal percentage}(\%) = \frac{C_0 - C_1}{C_0} \qquad 4.1$$

Where C_0 is the initial concentration of the metal ion before treatment and C_1 is the final concentration of the solution after treatment.

4.4.6 Pb and Zn accumulation in different cellular parts

Pb and Zn accumulation in different cellular parts were determined according to literature (Sheng et al., 2016) as illustrated in Fig. 4.2. Briefly, cell pellets were harvested by centrifuge at 5,000 rpm for 10 mins. Pb and Zn concentration determined in the supernatant. Then the cell pellets were ultrasonicated in 5 mL Tris-HCl (10 mM, pH 8.0). Centrifugation was conducted at 8,000 rpm for 10 minutes. The supernatant was thereafter collected for analysis, in order to detect the cytoplasmic water-soluble Pb and Zn accumulation. The precipitate from centrifugation was then suspended in SDS extracting solution (5%, 10 mM, pH 8) before centrifuged at 8000 rpm for 10 minutes. The resulting supernatant was used for the determination of cellular soluble protein-bound Pb and Zn accumulation, while the obtained

precipitate was digested in 65% nitric acid solution to detect cell surface-bound Zn^{2+} and Pb^{2+} accumulation.

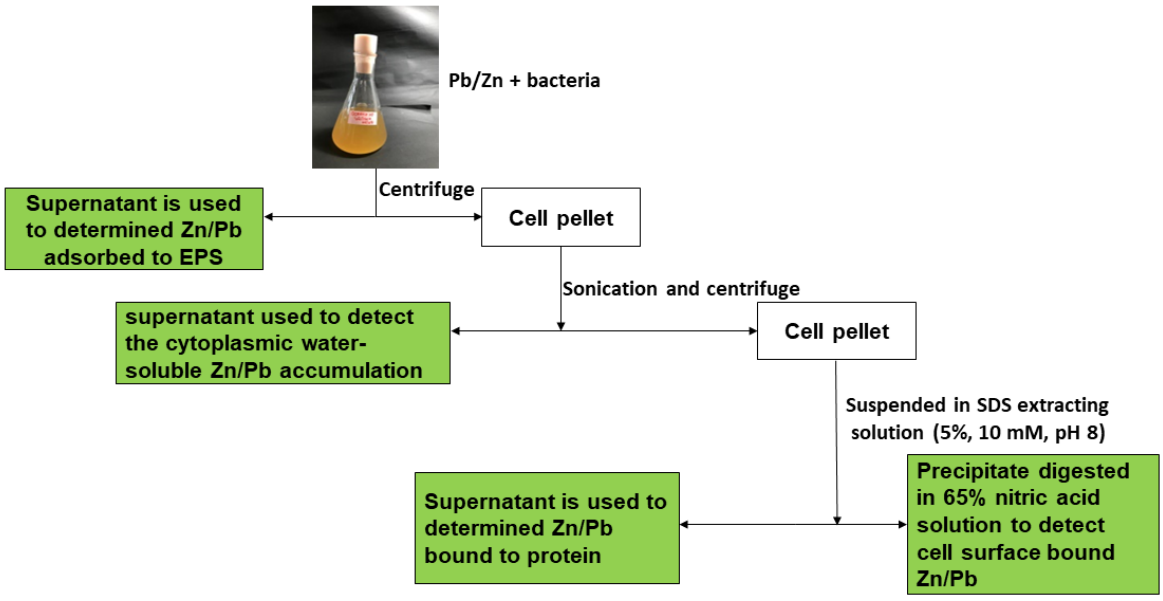

Fig. 4.2: Flow diagram for the partitioning of Pb in cellular parts

4.4.7 Characterization of biosorbent

a) FTIR analysis

Fourier Transform Infrared Spectroscopy (FTIR) was conducted for grown bacterium where, the bacterial cells were harvested by centrifugation at 5,000 rpm for 10 mins and washed three times with saline solution (0.9 % NaCl, pH 6.5). Then bacterial pellets were freeze-dried overnight, and their infrared spectra were recorded on an FTIR spectrometer in the region 4000-400/cm.

b) Composition of EPS

The protein content of the supernatant was determined by the Bradford protein assay with bovine serum albumin as the standard whereas the total carbohydrate content was determined by the phenol sulfuric acid method, using pure glucose as standard (Dubois et al., 1956).

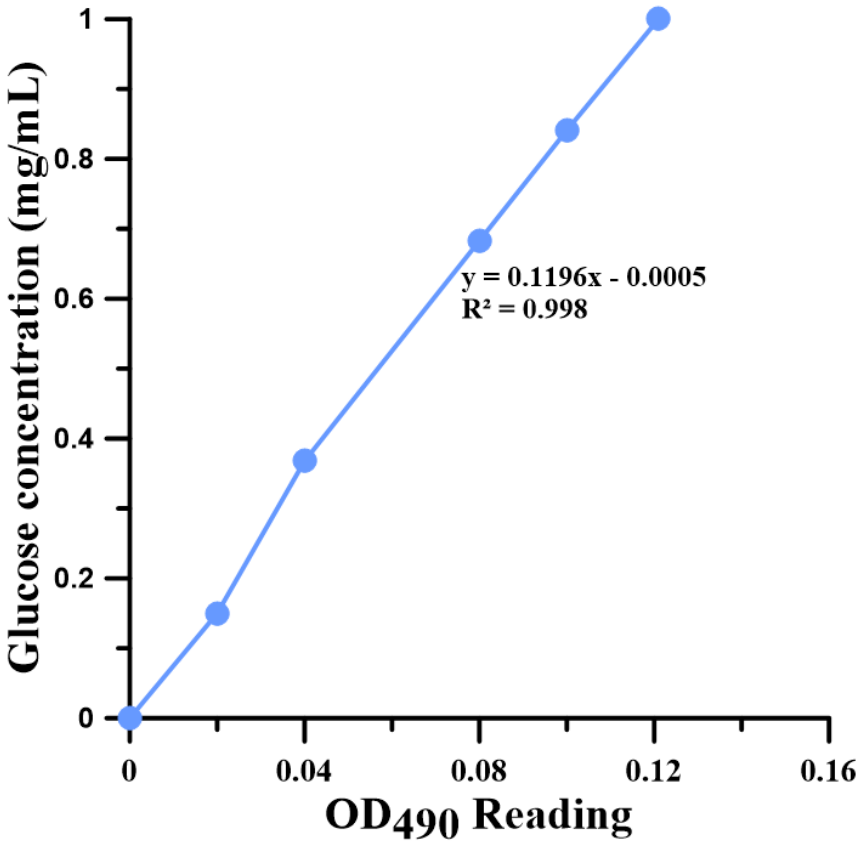

Fig. 4.3: Standard curve for the phenol-sulfuric acid method

c) Fluorescence microscopy

Confocal images were taken by a confocal laser scanning microscopy system (Nikon A1 and Ti-E) equipped with a Plan Apo VC x60 objective lens (NA 1.40, Nikon). Three different staining dyes were added to the sample sequentially to stain DNA (DAPI Nucleic Acid Stain, Molecular probes, Invitrogen), EPS (wheat germ agglutinin, Alexa Fluor® 633 conjugate, Molecular probes, Invitrogen), and Pb (II) (Leadmium™ Green AM Dye, Molecular probes, Invitrogen), respectively.

4.4.8 Biosorption isotherms

Biosorption was analyzed using the two widely accepted isotherm models of Langmuir and Freundlich adsorption isotherm models. The Langmuir biosorption model is shown in Equation 4.2, and its linearized form is shown in Equation 4.3.

$$Q_{eq} = \frac{Q_{\max}.K_L.C_{eq}}{1+K_L.C_{eq}} \qquad 4.2$$

$$\frac{C_{eq}}{Q_{eq}} = \frac{C_{eq}}{Q_{\max}} + \frac{1}{Q_{\max}.K_L} \qquad 4.3$$

Where Q_{eq} is the amount adsorbed (mg/g), C_{eq} is the equilibrium concentration of the adsorbate (mg/l), Q_{max} is the theoretical monolayer capacity (mg/g), and K_L = Langmuir constant.

The Freundlich biosorption model is shown in Equation 4.4, where K_f is the Freundlich constant, and n is the adsorption intensity constant. The linearized form of this model is indicated in Equation 4.5.

$$Q_{eq} = K_f.C_{eq}^{1/n} \qquad 4.4$$

$$\ln Q_{eq} = \ln K_f + \frac{1}{n}\ln C_{eq} \qquad 4.5$$

4.5 Results and discussion

4.5.1 Effect of pH

Fig. 4.4 shows the effect of pH on Pb^{2+} biosorption. Fig. 4.4 shows that at lower pH values of pH 2 and 3 the removal percentage of Pb^{2+} ions were as low as 85 % and 28 % removal of Pb and Zn respectively probably because of the influence on functional groups that lower pHs have on the binding onto the binding sites. Similar findings by earlier investigators have been attributed to protonation or poor ionization of functional group at low pH, inducing a weak complex affinity of the metal ions (Jnr and Harcourt, 2004; Pehlivan et al., 2012). However, at higher pH values, the binding efficiency increased because the functional groups were available.

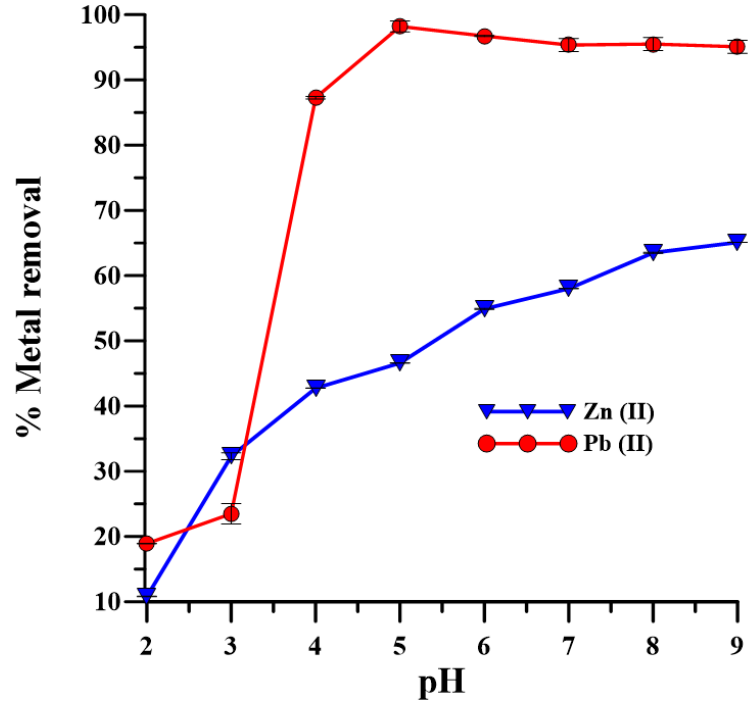

Fig. 4.4: Effect pH on biosorption by *O. Profundus* KBZ 3-2

4.5.2 Effect of temperature

Fig. 4.5 shows the effect of temperature variation. From these results, the biosorption temperature was determined to be 30 ºC. Therefore, the temperature of 30 ºC was chosen for all biosorption studies.

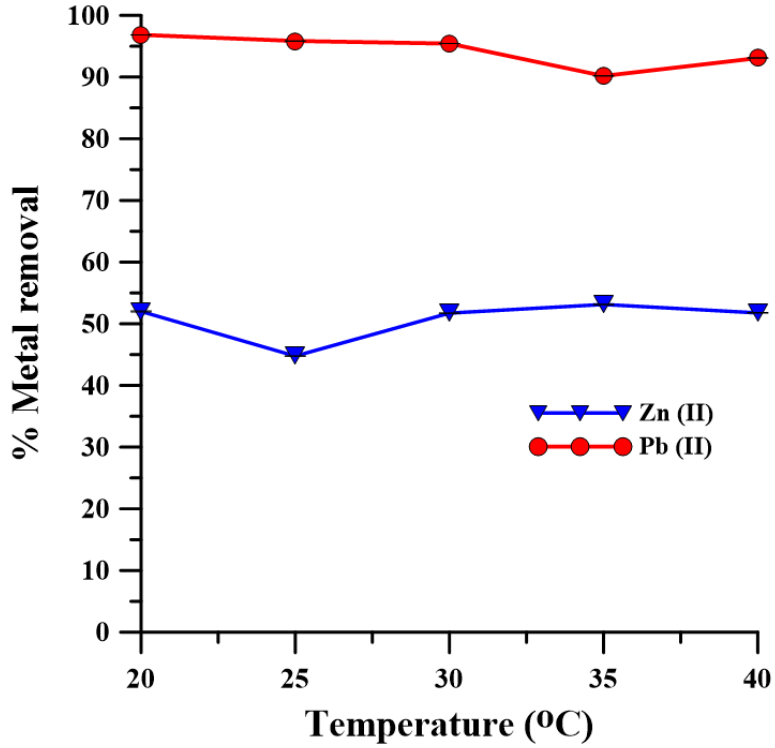

Fig. 4.5: Effect temperature on biosorption by *O. Profundus* KBZ 3-2

4.5.3 Effect of contact time

Fig. 4.6 shows the effect of contact time on the biosorption efficiency of Pb and Zn. Two phases of biosorption were observed which are the rapid initial biosorption rate of both Pb and Zn at the beginning of the batch experiment until 120 mins of contact time and then became constant and secondly a slower phase. These phases could have been due to the number of available biosorption sites. Initially, there were many vacant sites available for the Pb and Zn to adsorb to which were then later occupied and resulted in a slow phase. Therefore, the contact time for all the batch experiments was 120 mins.

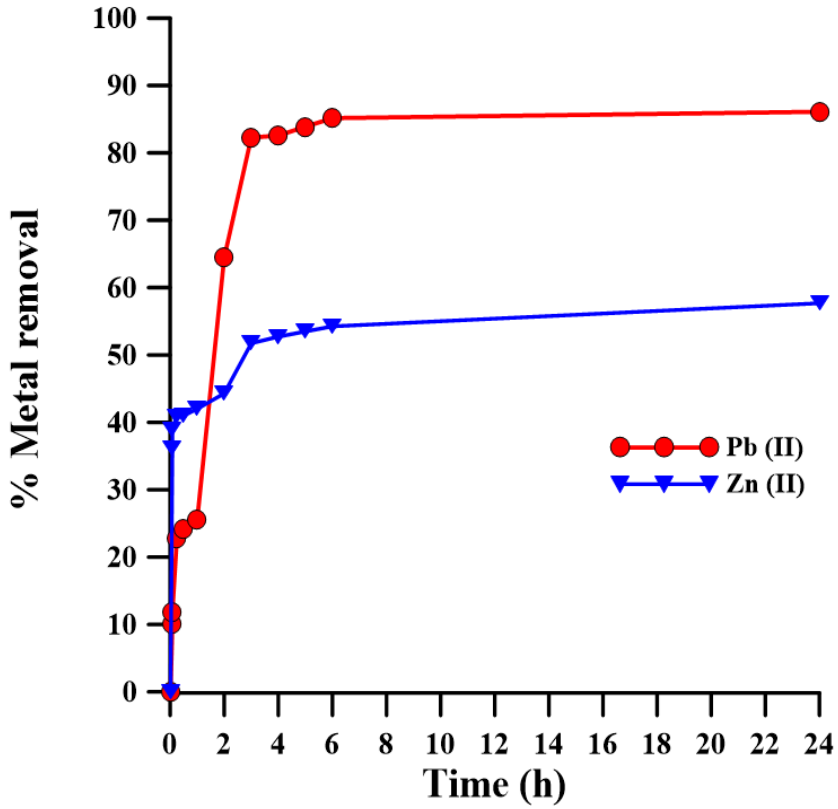

Fig. 4.6: Effect contact time on biosorption by *O. Profundus* KBZ 3-2

4.5.4 Pb and Zn accumulation in different cellular parts

To understand the possible mechanism by which Pb and Zn are removed by the isolate, a mass balance on the concentration trends among the different cellular parts of the bacteria was investigated. The different cellular parts investigated were extracellular polymeric substance (EPS), cytoplasm, cell protein, and cell surface of *O. Profundus* KBZ 3-2 and the results are shown in Fig. 4.7.

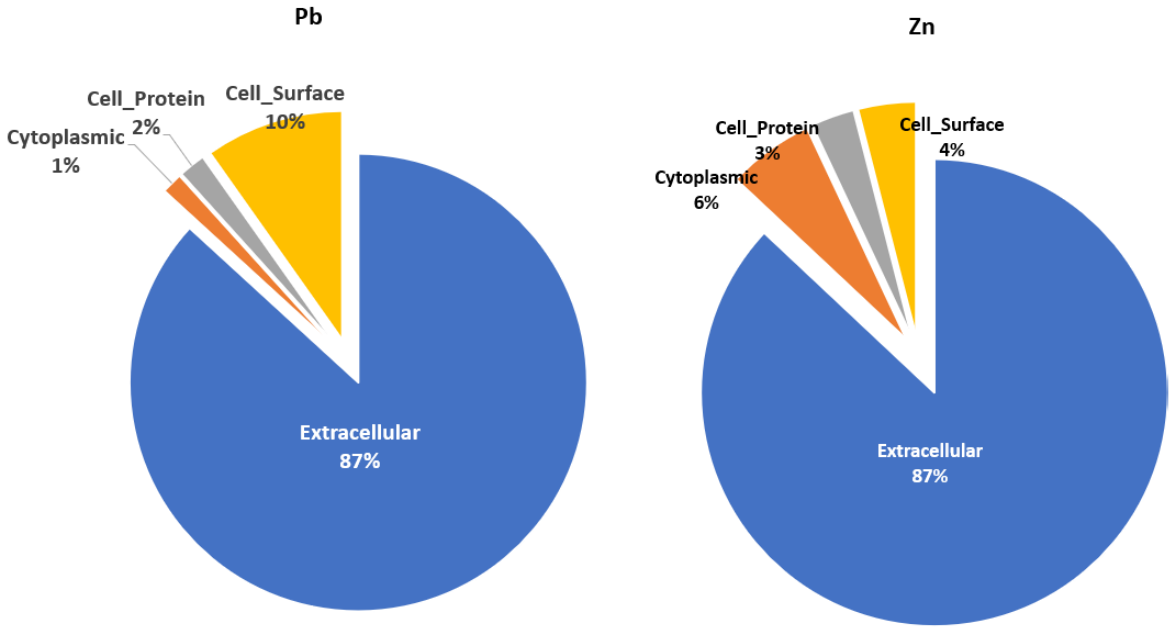

Fig. 4.7: Accumulation of (a) Pb and (b) Zn in different cellular parts of *O. Profundus* KBZ 3-2 at determined biosorption conditions

The highest concentration of Pb was found in the EPS (87%), cell protein (2 %), cytoplasm (1 %), and cell surface (10 %). Conversely, the highest concentration of Zn was found in the EPS (87%), cell protein (3 %), cytoplasm (6 %), and cell surface (1%). This result entails that the bacteria release EPS in the soluble phase which helps with heavy metal complexation. Previous studies have investigated the composition of EPS and mainly of nucleic acid, proteins, glycoproteins, and glycolipids (Pal and Paul, 2008). Therefore, the possible mechanism of Pb and Zn sequestration by *Oceanobacillus Profundus* KBZ 3-2 occurs by soluble EPS being actively secreted by bacteria to defend itself from toxins thereby binding the Zn and Pb ions from solutions consequently detoxification occurs (More et al., 2014; Shi et al., 2017). Binding of Pb and Zn to EPS immobilizes the metals and prevents the entry into the cell hence the little amount of Pb^{2+} detection inside the cell.

4.5.5 Characterization of biosorbent

a) FTIR

Fig. 4.8 shows the FTIR analysis of the *O. Profundus* KBZ 3-2 freeze-dried biomass. The sharp peak at 1634 cm^{-1} representative of a C=N bond which represented Amide I found in proteins. Additionally, the sharp peak at 3259 cm^{-1} is representative of an N-H bond represents amide A, typically found in proteins. Peaks 1555 cm^{-1} and 1200 cm^{-1} C-O bonds were identified

as phenols. The biosorption of Pb and Zn was, therefore, mainly due functional groups identified by amide groups (C=N and N-H bonds) typically found in proteins; and C-O bonds identified as phenols that were identified to be responsible for complexation with heavy metals. Protein and carbohydrates strong affinity for heavy metals

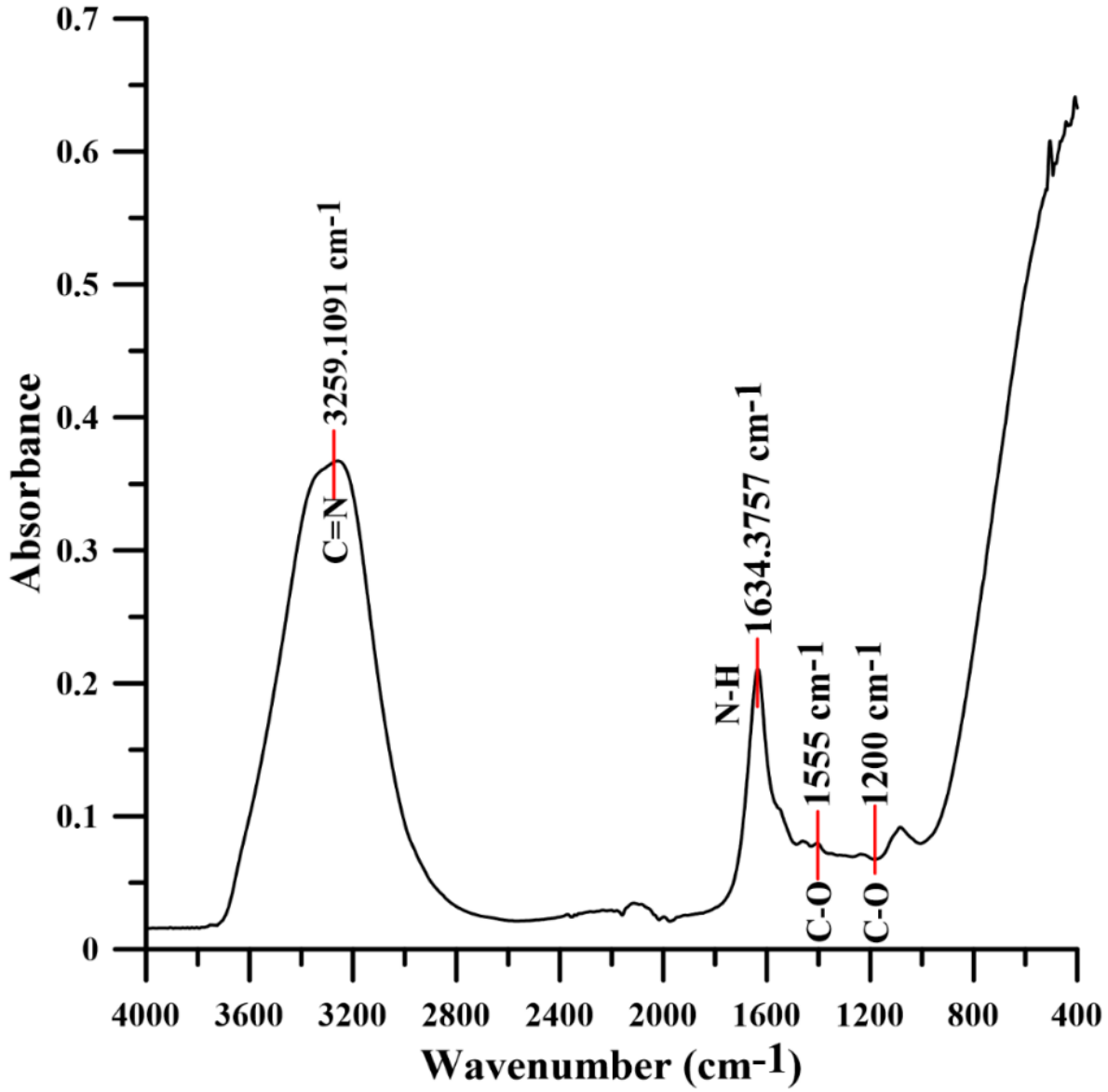

Fig. 4.8: FTIR analysis of *O. Profundus* KBZ 3-2 biomass

b) Composition of EPS

The ESP is the main component that is responsible for metal sequestration in our study, the composition of EPS was determined. The EPS had 104.9 µg/L of protein compared to 679.3 µg/L of carbohydrates. Typical the EPS mainly consists of water, protein, polysaccharides, DNA, uronic acid and humic acid (Nouha et al., 2018; Shi et al., 2017; Tourney and Ngwenya,

2014). However, in this study, only protein and polysaccharides were determined because proteins and carbohydrates are the most significant components that contribute the carboxyl (-COOH) and hydroxyl (-OH) functional groups which are negatively charged, and this charge gives them the ability to bind to heavy metals. This suggests that the secretion of the protein and carbohydrates by *O. Profundus* KBZ 3-2 are responsible for the Pb and Zn detoxification via metal chelation-complexation.

c) Fluorescence microscopy analysis

The results of the fluorescent microscopy are shown in Fig. 4.9 indicating the live cells (blue), lectin-conjugate EPS dye (red), and the Pb-specific fluorescent probe (green). The local correlation and visualization among live bacteria, EPS and the heavy metal confirming the sequential extraction of metal ion on the different cellular parts (Fig. 4.7). The signal of live cells was spatially associated with lectin-conjugate EPS dye indicating that the EPS was synthesized by the cells. As can be observed the cells are surrounded by the EPS. Additionally, the signal for the Pb-specific fluorescent probe was found to be mostly enriched in the EPS matrix. This association confirms results that protein and carbohydrates secrete by the strain are responsible for the heavy metal detoxification via metal chelation-complexation. This further suggests that the secretion of the protein and carbohydrates by *O. Profundus* KBZ 3-2 are responsible for the Pb and Zn detoxification via EPS-metal chelation-complexation.

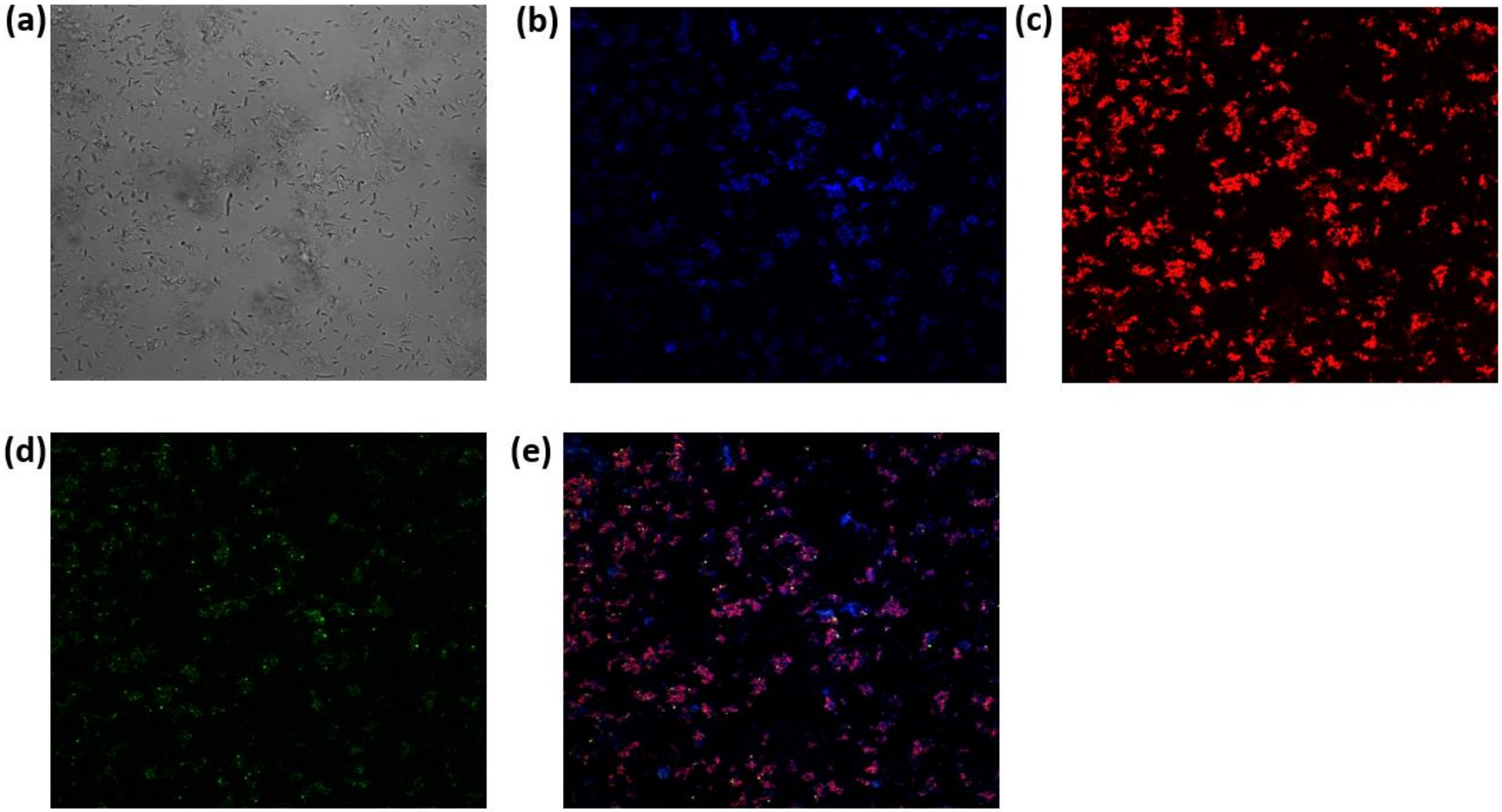

Fig. 4.9: Images of fluorescence microscopy with color corresponding to (a) Bright light microscopy of bacteria (b) Live cells indicated by blue DNA binding dye (c) EPS indicated red by lectin-conjugate (d) Pb indicated green (e) Overlay of live bacterial cells, EPS and Pb

4.5.6 Biosorption isotherms

Fig. 4.10(a) and 4.10(b) show that the amount of Pb and Zn adsorbed increased with increasing dose. This implies effective bioremediation, albeit at different extents, with Pb adsorption being significantly more effective. Fig. 4.10(c) and 4.10(d) shows respectively the Langmuir and Freundlich isotherms of *O. Profundus KBZ 3-2* biomass for metal ion system of Pb and Zn. Different concentrations were used, ranging from 1 – 5 mg/L Zn^{2+} and 5 – 50 mg/L of Pb^{2+}. Comparing the coefficients of determination of the Langmuir and Freundlich isotherms, it was determined that the latter isotherm best fit the data for both Pb and Zn. An adsorption system that fits with the Freundlich model is indicative of an adsorbent with a heterogeneous surface, with stronger binding sites being preferentially occupied (Saadi et al., 2015). The linear fit of the Pb^{2+} and Zn^{2+} data gave a slope (1/n) value of 0.027 and 0.4756, respectively, and thus an adsorption intensity constant (n) of 37.037 and 2.102, respectively. When a 1/n value is equal to unity, linear adsorption occurs which would cause identical adsorption energies for all sites; therefore, the deviation of the 1/n value, in this case, means that the adsorption energies differ at different sites. This is reinforced by the finding that Pb and Zn are present at different parts, with a distinct preference for the EPS matrix (Gautam et al., 2017). An adsorption intensity constant greater than 1 is indicative of high energetic interaction between the adsorbent and the adsorbate (Casarin et al., 2016), and suggests favorable adsorption. A plausible mechanism for the adsorption is through complexation and chelation of Pb and Zn onto the functional groups present in the biomass, corroborated by the fluorescence microscopy analysis.

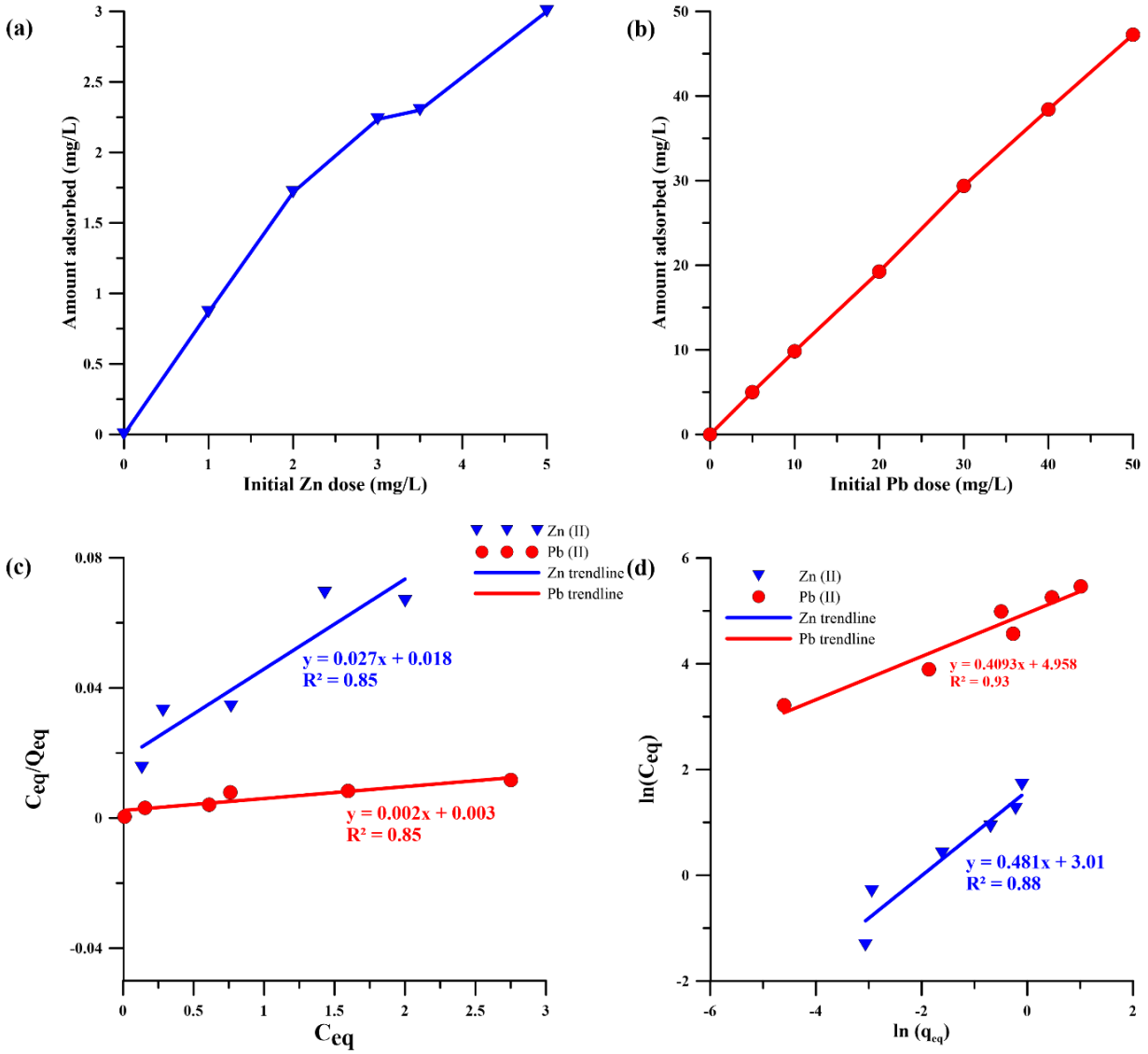

Fig. 4.10: *O. Profundus* KBZ 3-2 adsorption isotherms for Pb and Zn; (a) Langmuir isotherm (b) Freundlich isotherm.

4.5.7 Removal of heavy metal from polluted groundwater from Kabwe mine by *O. Profundus* KBZ 3-2

Demonstration of applicability of *O. Profundus* KBZ 3-2 to remove heavy metal from water waste tested by using contaminated water from Kabwe mine. Groundwater was abstracted from one of the boreholes. Groundwater collected from Kabwe mine represents a realistic background for metal ions and samples were collected and treated by biosorbent. All the metal

ions were below the detection limit of ICP-AES except Zn which was in excess (Table 4.1). The bacteria would be useful as a final polishing biosorbent before the discharge of the water into the natural environment.

Table 4.1: Heavy metal removal from contaminated water from study area by *O. Profundus* KBZ 3-2 (BDL- Below Detection Limit)

Element	Before (mg/L)	After (mg/L)	WHO Limit (mg/L)
Pb	2.29	BDL	0.01
Zn	1,348	432	2
Ni	0.923	BDL	0.07
Cu	12.27	0.274	2

4.6 Conclusion

The study isolated and identified a novel strain of bacteria, *O. profundus* KBZ 3-2, from lead contaminated soil at the Kabwe Mine Site in Zambia capable for heavy metal removal from water. The biosorption was determined to be pH 6.5, temperatureb30 ºC, and 120 min contact time. Beyond 120 minutes, the limited sites for biosorption cause adsorption to become constant. The proposed mechanism of biosorption was through chelation-complexation on the present functional groups on the EPS of the biomass, such as the amide groups and phenols. This was corroborated by a mass balance calculation of concentration trends of Pb and Zn. This result was corroborated by adsorption isotherm modeling, which ascertained the Freundlich model as best fitting for both Pb and Zn. *Oceanobacillus profundus* KBZ 3-2 as a biosorbent is highly efficient and has great potential in upscaling its biosorption purpose for bioremediation at the Kabwe Mine site.

References

Abdi, O., Kazemi, M., 2015. A review study of biosorption of heavy metals and comparison between different biosorbents. J. Mater. Environ. Sci. 6, 1386–1399.

Anastopoulos, I., Kyzas, G.Z., 2015. Progress in batch biosorption of heavy metals onto algae. J. Mol. Liq. 209, 77–86. https://doi.org/10.1016/j.molliq.2015.05.023

Ayangbenro, A.S., Babalola, O.O., 2017. A new strategy for heavy metal polluted environments: A review of microbial biosorbents. Int. J. Environ. Res. Public Health 14. https://doi.org/10.3390/ijerph14010094

Blacksmith, I., 2013. The worlds worst 2013: The Top ten toxic threats. Zurich. https://doi.org/10.1017/CBO9781107415324.004

Bong, C.W., Alfatti, F.M., Zam, F.A., Obayashi, Y., Suzuki, S., 2010. The effect of zinc exposure on the bacteria abundance and proteolytic activity in seawater. Interdiscip. Stud. Environ. Chem. Responses to Contam. 57–63.

Casarin, J., Gonçalves, C., Coelho, G.F., 2016. Adsorption of Metallic Ions Cd^{2+}, Pb^{2+}, and Cr^{3+} from water samples using Brazil Nut shell as a low-cost biosorbent, in: Smart Materials for Waste Water Applications. pp. 311–334.

Dubois, M., Gilles, K.A., Hamilton, J.K., Rebers, P.A., Smith, F., 1956. Colorimetric method for determination of sugars and related substances. Anal. Chem. 28, 350–356. https://doi.org/10.1021/ac60111a017

Gautam, R.K., Sani, S., Chattopadhyaya, M.C., 2017. Functionalized magnetic nanoparticles for environmental remediation, Materials Science and Engineering: Concepts, Methodologies, Tools, and Applications. https://doi.org/10.4018/978-1-5225-1798-6.ch028

Jena, S., Dey, S.K., 2016. Heavy Metals. Am. J. Environ. Stud. 1, 48–60.

Jnr, M.H., Harcourt, P., 2004. Studies on the effect of pH on the sorption of Pb^{2+} and Cd^{2+} ions from aqueous solutions by *Caladium bicolor* (Wild Cocoyam) biomass. Electron. J. Biotechnol. 7, 313–323. https://doi.org/10.2225/vol7-issue3-fulltext-8

Kelly, J.J., Häggblom, M.M., Tate, R.L., 2003. Effects of heavy metal contamination and remediation on soil microbial communities in the vicinity of a zinc smelter as indicated by analysis of microbial community phospholipid fatty acid profiles. Biol. Fertil. Soils 38, 65–71. https://doi.org/10.1007/s00374-003-0642-1

Khan, Z., Rehman, A., Hussain, S.Z., Nisar, M.A., Zulfiqar, S., Shakoori, A.R., 2016. Cadmium

resistance and uptake by bacterium, *Salmonella enterica* 43C, isolated from industrial effluent. AMB Express 6. https://doi.org/10.1186/s13568-016-0225-9

More, T.T., Yadav, J.S.S., Yan, S., Tyagi, R.D., Surampalli, R.Y., 2014. Extracellular polymeric substances of bacteria and their potential environmental applications. J. Environ. Manage. 144, 1–25. https://doi.org/10.1016/j.jenvman.2014.05.010

Nouha, K., Kumar, R.S., Balasubramanian, S., Tyagi, R.D., 2018. Critical review of EPS production, synthesis and composition for sludge flocculation. J. Environ. Sci. (China) 66, 225–245. https://doi.org/10.1016/j.jes.2017.05.020

Pal, A., Paul, A.K., 2008. Microbial extracellular polymeric substances: central elements in heavy metal bioremediation. Indian J. Microbiol. 48, 49–64. https://doi.org/10.1007/s12088-008-0006-5

Pehlivan, E., Altun, T., Parlayici, S., 2012. Modified barley straw as a potential biosorbent for removal of copper ions from aqueous solution. Food Chem. 135, 2229–2234. https://doi.org/10.1016/j.foodchem.2012.07.017

Plumlee, G.S., Morman, S.A., 2011. Mine wastes and human health. Elements 7, 399–404. https://doi.org/10.2113/gselements.7.6.399

Pourrut, B., Shahid, M., Dumat, C., Winterton, P., Pourrut, B., Shahid, M., Dumat, C., Winterton, P., Pinelli, E., Uptake, L., 2011. Lead uptake, toxicity, and detoxification in plants. Rev. Environ. Contam. Toxicol. 213, 113–136. https://doi.org/10.1007/978-1-4419-9860-6

Prasad, a S.A., Varatharaju, G., Anushri, C., Dhivyasree, S., 2013. Biosorption of Lead by *Pleurotus florida* and *Trichoderma viride* 3, 66–78.

Rodríguez, I.A., Cárdenas-González, J.F., Juárez, V.M.M., Pérez, A.R., Zarate, M. de G.M., Castillo, N.C.P., 2018. Biosorption of heavy metals by *Candida albicans*. Adv. Bioremediation Phytoremediation. https://doi.org/10.5772/intechopen.72454

Saadi, R., Saadi, Z., Fazaeli, R., Fard, N.E., 2015. Monolayer and multilayer adsorption isotherm models for sorption from aqueous media Monolayer and multilayer adsorption isotherm models for sorption. https://doi.org/10.1007/s11814-015-0053-7

Sheng, Y., Wang, Y., Yang, X., Zhang, B., He, X., Xu, W., Huang, K., 2016. Cadmium tolerant characteristic of a newly isolated *Lactococcus lactis* subsp. lactis. Environ. Toxicol. Pharmacol. 48, 183–190. https://doi.org/10.1016/j.etap.2016.10.007

Shi, Y., Huang, J., Zeng, G., Gu, Y., Chen, Y., Hu, Y., Tang, B., Zhou, J., Yang, Y., Shi, L., 2017.

Exploiting extracellular polymeric substances (EPS) controlling strategies for performance enhancement of biological wastewater treatments: An overview. Chemosphere 180, 396–411. https://doi.org/10.1016/j.chemosphere.2017.04.042

Sracek, O., Veselovský, F., Kříbek, B., Malec, J., Jehlička, J., 2010. Geochemistry, mineralogy and environmental impact of precipitated efflorescent salts at the Kabwe Cu-Co chemical leaching plant in Zambia. Appl. Geochemistry 25, 1815–1824. https://doi.org/10.1016/j.apgeochem.2010.09.008

Tchounwou, P.B., Yedjou, C.G., Patlolla, A.K., Sutton, D.J., 2012. Heavy metal toxicity and the environment. EXS 101, 133–64. https://doi.org/10.1007/978-3-7643-8340-4_6

Tourney, J., Ngwenya, B.T., 2014. The role of bacterial extracellular polymeric substances in geomicrobiology. Chem. Geol. 386, 115–132. https://doi.org/10.1016/j.chemgeo.2014.08.011

Yabe, J., Nakayama, S.M.M., Ikenaka, Y., Yohannes, Y.B., Bortey-Sam, N., Oroszlany, B., Muzandu, K., Choongo, K., Kabalo, A.N., Ntapisha, J., Mweene, A., Umemura, T., Ishizuka, M., 2015. Lead poisoning in children from townships in the vicinity of a lead-zinc mine in Kabwe, Zambia. Chemosphere 119, 941–947. https://doi.org/10.1016/j.chemosphere.2014.09.028

CHAPTER 5 DEVELOPMENT OF METALLOTHIONEIN-CELLULOSE BASED BIOSORBENT FOR THE REMOVAL OF PB (II) AND ZN (II) FROM WATER

5.1 Introduction

Cellulose and metallothioneins (MTs) are respectively the most abundant polymer on earth (Belgacem and Gandini, 2008) and most ubiquitous cysteine-rich proteins present in bacteria (Shi et al., 1992), mammals (Dziegiel et al., 2016) and plants (Banuelos and Terry., 1999). Pure cellulose has not gained any use as biosorbents due to the low adsorption capacity and variable stability (Hokkanen et al., 2016). This has led researchers to exploit strategies to modify cellulose via grafting (Wojnárovits et al., 2010) and direct chemical modification which has shown to remove toxic trace elements in water, however, these processes require huge energy cost and reagents (Fakhre and Ibrahim, 2018). Additionally, MTs have traditionally being explored and investigated to increase toxic metal binding capacity, tolerance or accumulation of bacteria and plants (Care et al., 2015; Nguyen et al., 2013; Seker and Demir, 2011; Steffens, 1990). Despite these advances researchers continue to investigate and propose conventional water treatment methods such as chemical precipitation (Kurniawan et al., 2006), biochemical reactors (Rosca et al., 2016), electrolytic recovery (Shim et al., 2014), adsorption (Pinto et al., 2011), coagulation and flocculation (El Samrani et al., 2008), ion exchange (Dąbrowski et al., 2004), reverse osmosis (Cui et al., 2014), constructed wetlands (Vymazal, 2014), and nanotechnology (Al-saad et al., 2012) despite the abundant renewable resources. Many of these conventional technologies have high operational costs (Mahamuni and Adewuyi, 2010) due to the chemicals used, high energy consumption (Al-Karaghouli and Kazmerski, 2013) and high handling costs for sludge disposal (Yang et al., 2015).

To address this challenge, here propose to treat water using cellulose by harnessing and combining the capability of MTs to bind metal ion via cellulose-binding domains (CBM). The biosorbent was constructed from a protein fusion of MT from *Synechococcus elongatus*

PCC 7942 (Shi et al., 1992) that bind N-terminally to CBM from *C. thermocellum* (Hong et al., 2007) using cellulose as a base material as illustrated in Fig 5.1. Cellulose was chosen as a base for immobilizing the protein because it is abundant, natural, inexpensive, chemically inert, rigid and a renewable source of organic compounds on the planet (Belgacem and Gandini, 2008). Additionally, MT was chosen because they are a group of well-preserved structures of proteins that act as antioxidants, and they are distributed among all living organisms containing sulfhydryl group (Babula et al., 2012; Freisinger, 2011; Maret, 2011; Mejáre and Bülow, 2001; Vašák and Meloni, 2011). The sulfhydryl group plays a major role in binding toxic trace elements (Carpenè et al., 2007; Maret, 2011). Lead (Pb) and Zinc (Zn) were used in this study because both elements are toxic to human health affecting neurodevelopment and carcinogen respectively hence the need for their removal from water (World Health Organization, 2017) at the abandoned Kabwe mine site.

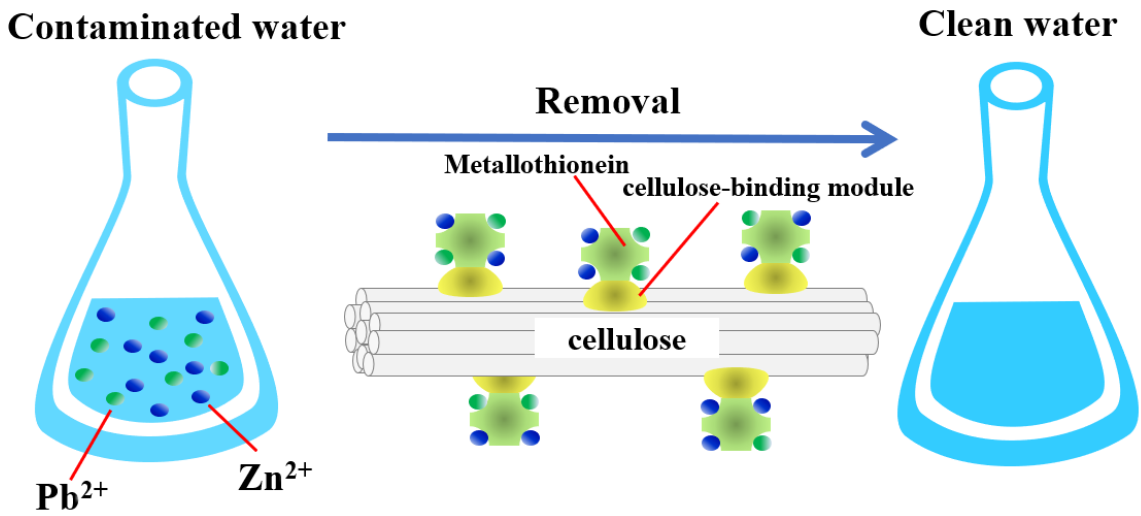

Fig. 5.1: Illustration of the genetic organization of cellulose-MT-CBM from heavy metal removal from water

5.2 Objectives

The specific objectives of this study were to:

(i) To construct a cellulose-MT-CBM biosorbent;

(ii) Determine the effect of pH, temperature, contact time and initial concentration of Pb (II) and Zn (II) on biosorption;

(iii) Exam the recyclability of cellulose-MT-CBM biosorbent; and

(iv) Study the biosorption isotherm and propose the adsorption mechanism.

5.3 Materials and methods

5.3.1 Materials

a) Plasmid vector and host bacteria

pET15b(+) vector was used as an expression vector using the multi cloning site was used to insert the gene of interest (Fig. 5.2). *Escherichia coli* DH5α was used as the host strain for plasmid amplification with *Escherichia coli* BL21(DE3) was used as a host in protein expression.

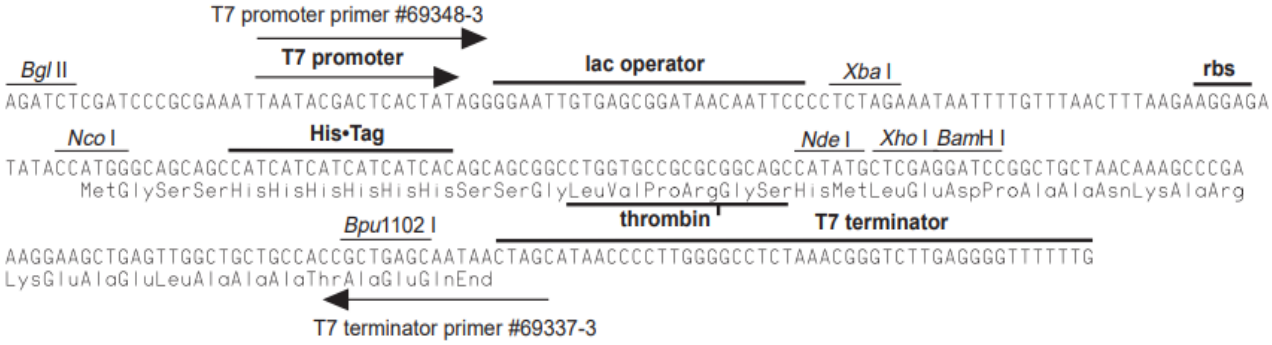

Fig. 5.2: Multi cloning region of the pET15b(+) vector

b) Restriction enzymes and reagents for PCR

Restriction enzymes XhoI and NdeI (Takara Bio Inc., Tokyo, Japan) were used to linearize the vectors in conjunction with CutSmart enzyme (Takara Bio Inc., Tokyo, Japan). The overlap polymerase chain reaction (PCR) has been conducted into 2 steps. Both of PCR

step used Primestar max DNA polymerase in the reaction. KAPA2G polymerase was used in colony PCR with T7 promoter and T7 terminator.

c) Gel electrophoresis and SDS-PAGE analysis

The agarose gel was prepared in a 1xTAE buffer. The gel was prepared into 2 concentrations, 1.5% for DNA fragments less than 1000 base pairs whereas 1% for DNA greater than 1000 base pairs. Midori green dye was used as a staining agent for PCR products in a ratio of 10:1 ratio. The reference DNA ladder was also stained with Midori green at 5:1 ratio. DNA and plasmid purification were conducted using a FastGene gel/PCR extraction kit (NIPPON Genetics Co. Ltd.) and FastGene Plasmid extraction kit (NIPPON Genetics Co. Ltd., Tokyo, Japan), respectively (Fig. 5.3).

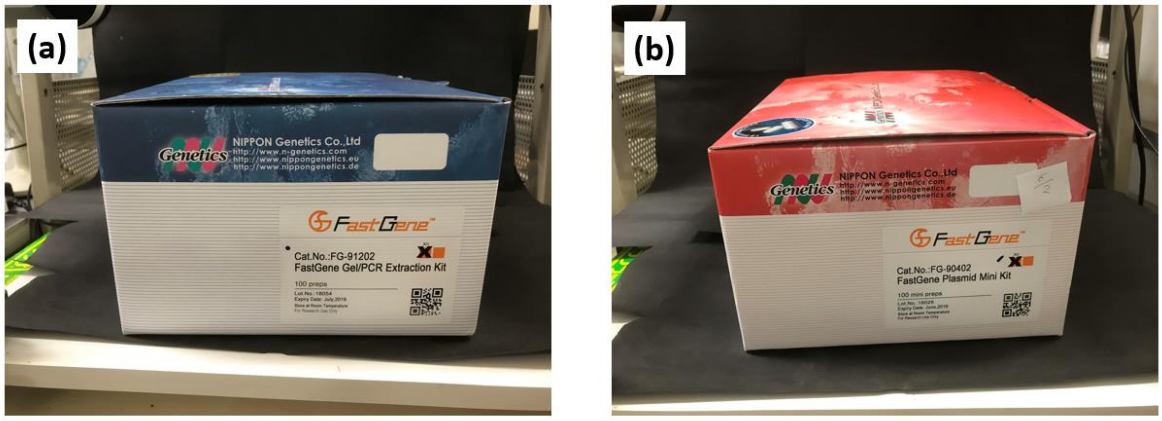

Fig. 5.3: (a) FastGene gel/PCR extraction kit (b) FastGene Plasmid extraction kit

d) Cellulose materials

Two types of cellulose were used for the adsorption of analysis of protein: Class I and Class II. The Class I cellulose included Whatman Paper No. 1 Microcrystalline cellulose whereas Class II was Amorphous regenerated cellulose (RAC) Prepared using Phosphoric acid or 1-Ethyl-3-methylimidazolium diethyl phosphate (Fig 5.4).

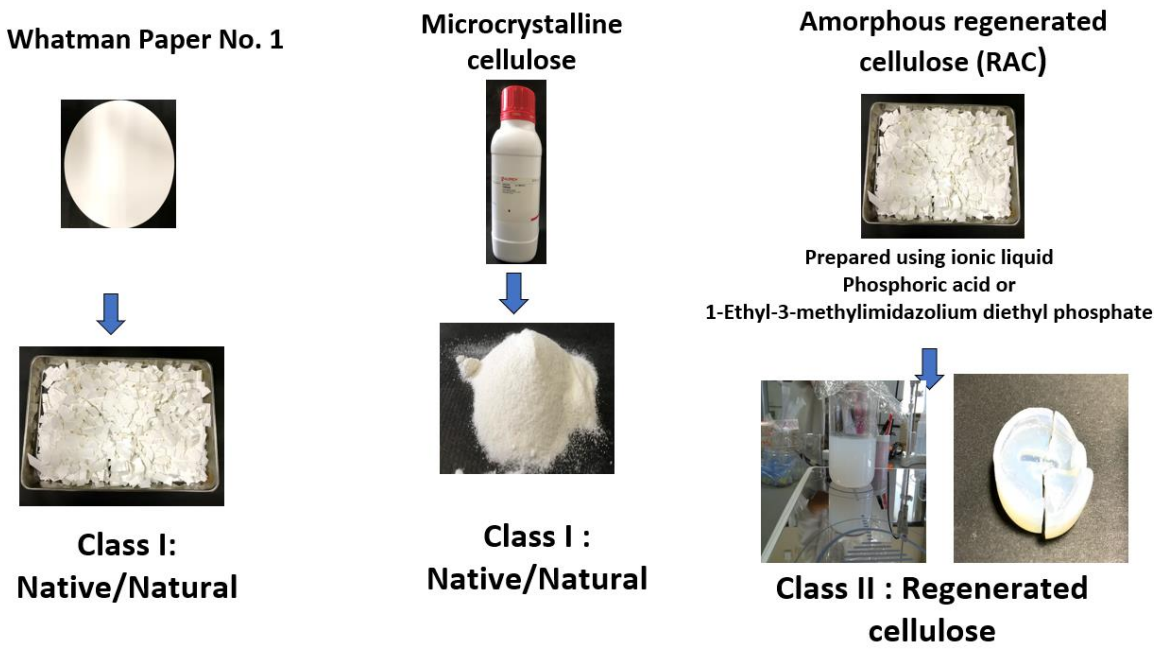

Fig. 5.4: Types of cellulose materials used

e) In-Fusion HD Cloning Kit

In-Fusion HD Cloning Kits are designed for fast, directional cloning of one or more fragments of DNA into any vector.

5.3.2 Equipment

a) Electrophoresis equipment

Marine 22 electrophoresis equipment was used for DNA separation (Fig. 5.5).

Fig. 5.5: Horizontal gel electrophoresis equipment

b) SDS page equipment

SDS PAGE equipment was used for protein separation (Fig. 5.6).

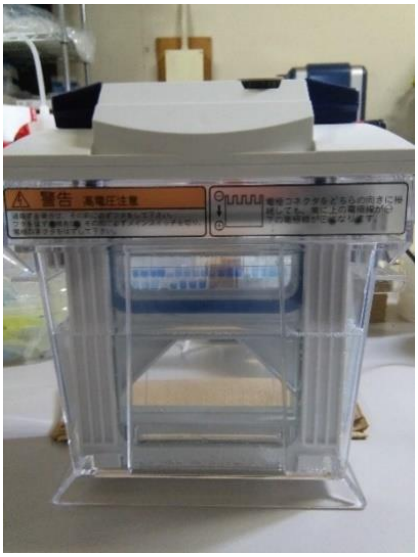

Fig. 5.6: Vertical gel electrophoresis equipment

c) Freeze dryer

Freeze dryer (Eyela FDU-1200, Rikakikai Co. Ltd, Tokyo, Japan) was used for the preservation of biological preservation (Fig. 5.7).

Fig. 5.7: Freeze Dryer

d) Heating block

The heating block was used for heating DNA during transformation and when conducting protein separation during SDS PAGE analysis (Fig. 5.8).

Fig. 5.8: Heating block

e) PCR Machine

PCR Machine equipment was used to amplify segments of DNA via PCR (Fig. 5.9).

Fig. 5.9: PCR equipment

f) Ultrasonication equipment

Vibra-Cell™ VCX 130 (Sonics & Materials, Inc., Newtown, USA) was used for ultrasonication to lyse cell pellets for protein extraction from genetically modified cells (Fig. 5.10).

Fig. 5.10: Ultrasonication equipment

g) Fourier Transform Infrared Spectroscopy (FTIR)

Fourier Transform Infrared Spectroscopy (FTIR) identifies chemical bonds in a molecule by producing an infrared absorption spectrum (Fig. 5.11).

Fig. 5.11: FTIR spectrometer with an attenuated total reflectance (ATR) attachment

h) X-ray photoelectron spectroscopy

X-ray photoelectron spectroscopy (XPS) measurements were performed in JPS-9200 Photoelectron Spectrometer (Joel Ltd.) to explore the oxidation states of Pb and Zn on the biosorbent using monochromatic Mg Kα radiation. Additionally, in order to compensate for surface charges effects, binding energies were calibrated using C 1s at 284.80 eV.

5.4 Experimental methods

5.4.1 Plasmid construction

The schematic representations of the three different types of fusion proteins are illustrated in Fig. 5.12 and the oligonucleotide primers listed in Table 5.1. Metallothionein (MT) gene from *Synechococcus elongatus* PCC 7942 and the cellulose-binding module (CBM) gene from genomic DNA of *C. thermocellum* NBRC 103400 with primer set Cfw_1 and Crv_2.

a) MT-CBM plasmid construction

To construct MT-CBM infusion was conducted using the In-Fusion HD Cloning Kit to form MT-CBM complex (primer overlap set OL_MTCfw 2 and OL_MTCrv 3 and infused with primer set IFfw_1 and IFrv_4). The MT-CBM amplicon was then inserted into a pET15b (+) vector digested with restriction enzymes NdeI/XhoI to form pET15(+)-MT-CBM. PCR was performed using PrimeSTAR® HS DNA Polymerase.

b) MT-CBM-MT plasmid construction

To construct MT-CBM-MT infusion was conducted using the In-Fusion HD Cloning Kit to form MT-CBM-MT complex (primer overlap set MT_fw and CBM_rv and infused with primer set IFfw_1 and MTpET15b_rv). The MT-CBM amplicon was then inserted into a pET15b (+) vector digested with restriction enzymes NdeI/XhoI to form pET15(+)-MT-CBM-MT.

c) MT-MT-CBM plasmid construction

To construct MT-MT-CBM infusion was conducted using the In-Fusion HD Cloning Kit to form MT-MT-CBM complex (primer overlap set MTMT_fw and MTMT_rv and infused with primer set IFfw_1 and CBMpET15b_rv). The MT-CBM amplicon was then inserted into a pET15b (+) vector digested with restriction enzymes NdeI/XhoI to form pET15(+)-MT-MT-CBM.

Table 5.1: Nucleotide sequences of primers used in this study

Primer	Nucleotide sequence (5' to 3')
Cfw_1	CCGGTATCAGGCAATTTGAAGGTTGAATTCTACAA
Crv_2	GCCACCGGGTTCTTTACCCCATACAAGAACACCGT
OL_MTCfw_2	GCAACTGTCATGGCCCGGTATCAGGCAATTTGAAG
OL_MTCrv_3	CTTCAAATTGCCTGATACCGGGCCATGACAGTTGC
IFfw_1	AGGAGATATACCATGACGAGTACCACCTTAGTGAA
IFrv_4	CAGCCGGATCCTCGATCAGCCACCGGGTTCTTTAC
MT_fw	ACGAGTACCACCTTAGTGAAGTGCGCTTGTGAGCC
CBM rv_2	GCCACCGGGTTCTTTACCCCATACAAGAACACCGT
MTpET15b_rv	CAGCCGGATCCTCGATCAGCCATGACAGTTGCAAC
MTMT_fw	GGTATCAGGCAATTTGAAGACGAGTACCACCTTAG
MTMT_rv	CTAAGGTGGTACTCGTCTTCAAATTGCCTGATACC
CBMpET15b_rv	CAGCCGGATCCTCGATCAGCCATGACAGTTGCAAC

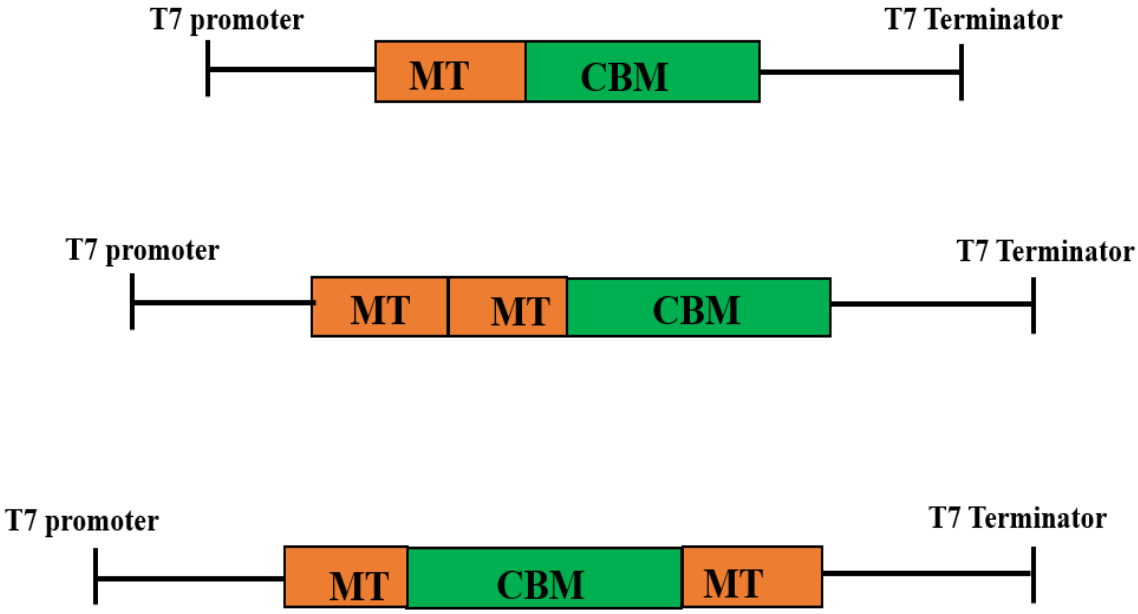

Fig. 5.12: Schematic representation of constructs in this study

5.4.2 Plasmid transformation and protein expression

Transformation of constructed plasmid was done by incubating the mixture of 1 µL of the constructed plasmid and 30 µL of *Escherichia coli* DH5α strain on ice for 30 minutes and then heat shocked at 42 °C using heat block for 30 seconds and placed on ice for 5 min again. The mixture was then plated on LB-AMP agar plate at 37 °C overnight. PCR colony was performed using a KAPA2G Fast Multiplex PCR Kit under PCR cycling conditions: 94 °C, 1 min; followed by 35 cycles of 98 °C, 5 sec; 55 °C, 5 sec; and 72 °C, 40 sec. After PCR was complete, 5 µl of each reaction was subjected to electrophoresis on a 1% agarose gel.

To express the protein, the plasmid was hosted by *Escherichia coli* BL21(DE3) strain. After which, the transformed bacteria were grown at 37 °C in LB medium with 100 mg/L of ampicillin while monitoring its absorbance at 600 nm. When the absorbance of the media reached 0.45, the expression of the protein was induced by adding 1 mmol/L final concentration of isopropyl b-D-1- thiogalactopyranoside (IPTG) to the medium. Once IPTG was added, the culturing temperature was reduced to 15 °C and allowed to continue growing for 24 h. The bacterial cells expressing the proteins were harvested by centrifugation at 5000

rpm for 10 min and lysed by sonication. The resulting supernatant was recovered and used for biosorption studies.

5.4.3 Determination of protein binding ability to cellulose and metal ion

To immobilize the protein to cellulose, Whatman filter paper No. 1 was cut into rectangular pieces and then submerged into the free MT-CBM protein supernatant for 2 h to form the cellulose-MT-CBM biosorbent. The schematic diagram of the process flow for the biosorption of protein to cellulose and consequently metal removal is illustrated in Fig. 5.13

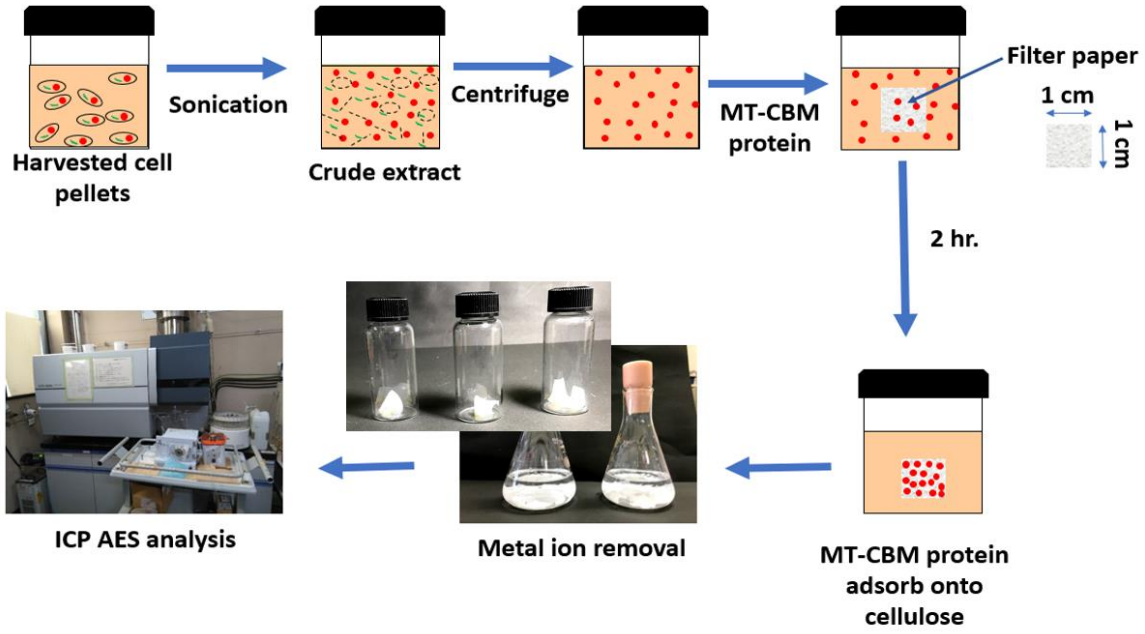

Fig. 5.13: Process flow for the immobilization of protein to cellulose and consequently metal analysis

5.4.4 Determination of the effect of pH, temperature, contact time and initial concentration on biosorption

Pb and Zn ions were used to understand the effect of pH and temperature, initial metal ion concentration from 10 mg/L to 80 mg/L were investigated on the biosorbent. To determine the effect of pH on biosorption, pH 2 to pH 9 was used and the pH of the aqueous

solution was adjusted using 1 M NaOH and 99.5 % concentrated nitric. The point of zero charge (pzc) of was determined by the pH drift method (Nasiruddin Khan and Sarwar, 2007). The effect of temperature was investigated at 15 ºC, 25 ºC, 35 ºC, and 50 ºC. The removal efficiency was determined by allowing the biosorption to proceeded for 60 min and then the sample was centrifuged at 10 000 rpm for 5 min and then filtered using a 0.45 µm filter. The filtrate was acidified by nitric acid to pH < 2 followed by measurement of the metal ion concentration by inductively coupled plasma atomic emission spectroscopy.

5.4.5 Characterization of biosorbent by FTIR

After freeze-drying, pure cellulose and cellulose-MT-CBM were subjected to ATR Fourier transform infrared spectroscopy (FTIR) and had their infrared spectra were recorded on an FTIR spectrometer JASCO 360 FTIR Spectrometer in the region 4000-400/cm.

5.4.6 Recyclability of cellulose-MT-CBM biosorbent

To determine the recoverability and reusability of the biosorbent, 2 g of cellulose-MT-CBM biosorbent was placed in 30 mL syringe tubes and a 10 mL of raw protein was adsorbed onto the cellulose kept at 25 ºC in an incubator for 1 h. The column was washed three times with deionized water and then either Pb or Zn aqueous solution was allowed to percolate through the column and collect the filtrate for metal analysis. In order to desorb the metal ions, the column was tested with 20 mM EDTA buffer. After desorption, the column was rinsed with deionized water prior to reuse. The reusability of the sorbent was tested for seven times.

5.4.7 Adsorption isotherm model

Biosorption was analyzed using Langmuir biosorption isotherm model. The Langmuir biosorption model is shown in Equation 4.2 and 4.3 in subsection 4.4.8.

5.5 Results and discussion

5.5.1 Verification of plasmid constructions, protein expression and protein binding ability to cellulose

Of the three plasmids construct only the MT-CBM and MT-CBM-MT were successfully constructed. The MT-MT-CBM construct was unsuccessful probably due to overlapping during PCR. To verify the correct construction of the nucleotide sequences of target genes MT (165 base pairs), CBM (483 base pairs) and complex MT-CBM (648 base pairs) and MT-CBM-MT (813 base pairs) were each verified in the expression vector by DNA sequencing (Eurofins Genomics, Tokyo, Japan). Fig. 5.14 shows the result of SDS-PAGE analysis for the protein expressed in *E. coli* BL21(DE3) and the biosorption of the protein to cellulose. Fig. 5.14(a) shows that the MT-CBM protein was successfully expressed and had a molecular weight of 23.1 kDa. This SDS-PAGE result show protein express was successful in the soluble phase. To verify the ability of the MT-CBM immobilization onto cellulose, the protein was subjected to adsorption onto cellulose and complete adsorption was achieved after 2 hours of immobilization as shown in Fig. 5.14(b) with the disappearance of the MT-CBM protein band. However, the ability of the MT-CBM-MT to immobilize onto cellulose was unsuccessful and therefore only the MT-CBM construct was discussed in this Chapter. This result showed that MT-CBM can bind to cellulose in a single-step purification. This result is consistent with previous studies where the CBM binds to cellulose material (Yunus and Tsai, 2015). The cellulose-based biosorbent herein referred to as cellulose-MT-CBM was used for subsequent studies.

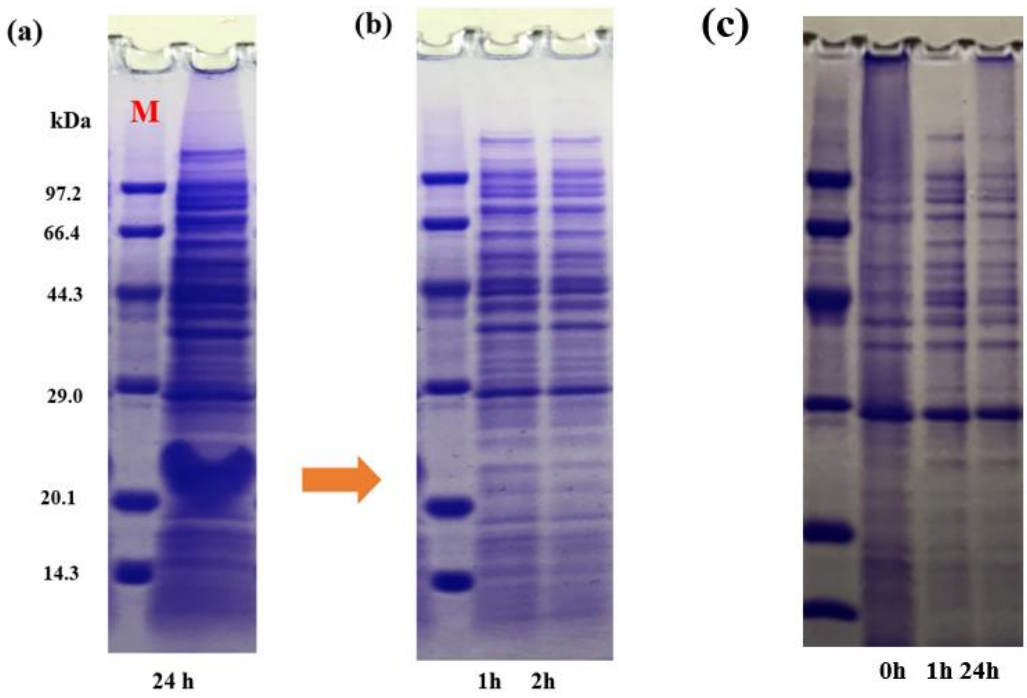

Fig. 5.14: (a) SDS PAGE showing the successful expression of the MT-CBM protein in the soluble phase (b) SDS PAGE of the biosorption of the MT-CBM protein to cellulose at different time intervals (1 h, 2 h and 3 h) (c) SDS PAGE of the biosorption of the MT-MT-CBM protein to cellulose at different time intervals (1 h, 2 h and 24 h)

To further investigate and confirm the biosorption of protein, cellulose was examined before and after adsorption of the MT-CBM protein by FTIR. Fig. 5.15 shows the FTIR spectra obtained for pure cellulose and cellulose-MT-CBM. It is evident that the pure cellulose material has no functional groups compared to the cellulose-MT-CBM. The broad and strong bands at 3251 cm^{-1} were attributed to amine (-NH) groups. The peaks at 1625 cm^{-1} were attributed to the stretching vibration of the amide group (C=O). The bands observed at 1302 cm^{-1} was assigned to C-O stretching of alcohols and carboxylic acids. This result further confirms that the MT-CBM protein adhered to the cellulose.

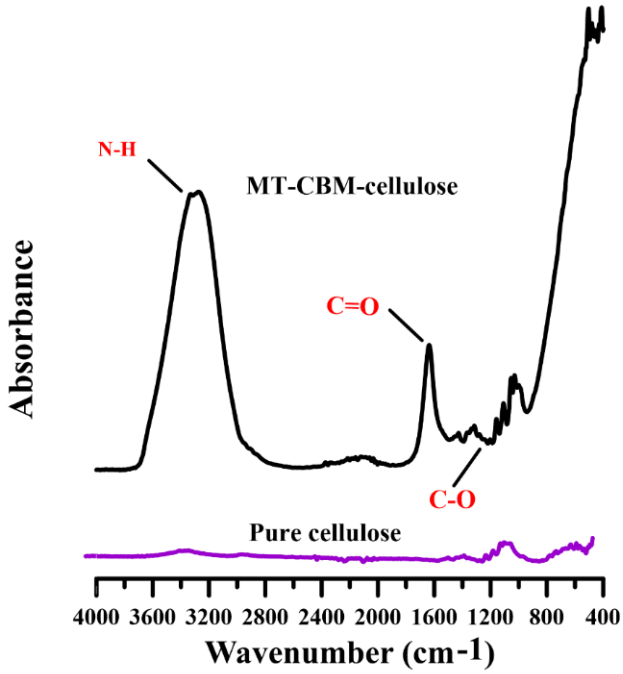

Fig. 5.15: FTIR analysis of pure cellulose (Whatman Paper No. 1) compared to cellulose-MT-CBM

5.5.2 Effect of pH, temperature, and contact time and initial concentration on biosorption

(a) Effect of pH

The results of the effect of pH are shown in Fig. 5.16. The influence of pH on the biosorption of Pb and Zn (II) indicated that the biosorption percentage of metal ions increases with increasing pH. From pH 2.0 to 7.0 the percentage removal of Pb (II) increased from 0.75 % to 93.96 % whereas Zn increased from 41.5 % to 91.94% and thereafter removal increased to 98 % to a maximum of 98 % at pH 9.0. This behavior is because pH changes metal solubility in solution which leads to dissociation of functional groups as observed by a similar study (Yunus and Tsai, 2015).

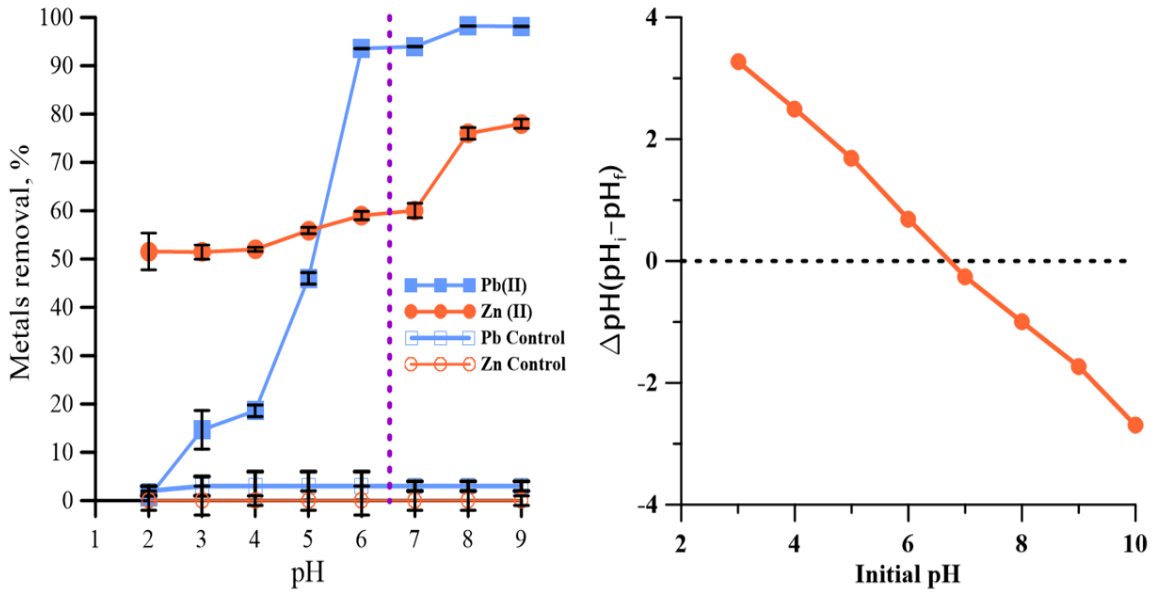

Fig. 5.16: Effect of pH (Initial metal ions were same - 20 mg/L at room temperature)

At lower pH, the binding sites are protonated and hence the metal ions are in solution and cannot access the binding sites on the cellulose-MT-CBM. However, when the pH is increased binding sites revert to being negatively charged and hence more favorable for sorption. As can be observed, the control had negligible biosorption capacity at all pH values due to lack of binding site. The determined pH 6.5 tarried with the pHpzc of the cellulose-MT-CBM because when the pH > pHpzc, the biosorption of Pb (II) and Zn (II) onto the biosorbents is favorable due to the presence of active negatively charged functional groups (the purple line indicates the pHpzc of the biosorbent) (Boström et al., 2005). The functional groups at pH 6.5 would, therefore, be negatively charged and be able to attract and sequester positively charged toxic trace elements.

(b) Effect of temperature

The effect of temperature was investigated for both Pb (II) and Zn (II) at 15 °C, 25 °C, 35 °C and 50 °C, and the obtained results are shown in Fig. 5.17. The biosorption capacity slightly increased as the temperature increased but insignificant. Both elements had high biosorption capacity at 25 °C, therefore, all subsequent experiments were conducted at room temperature.

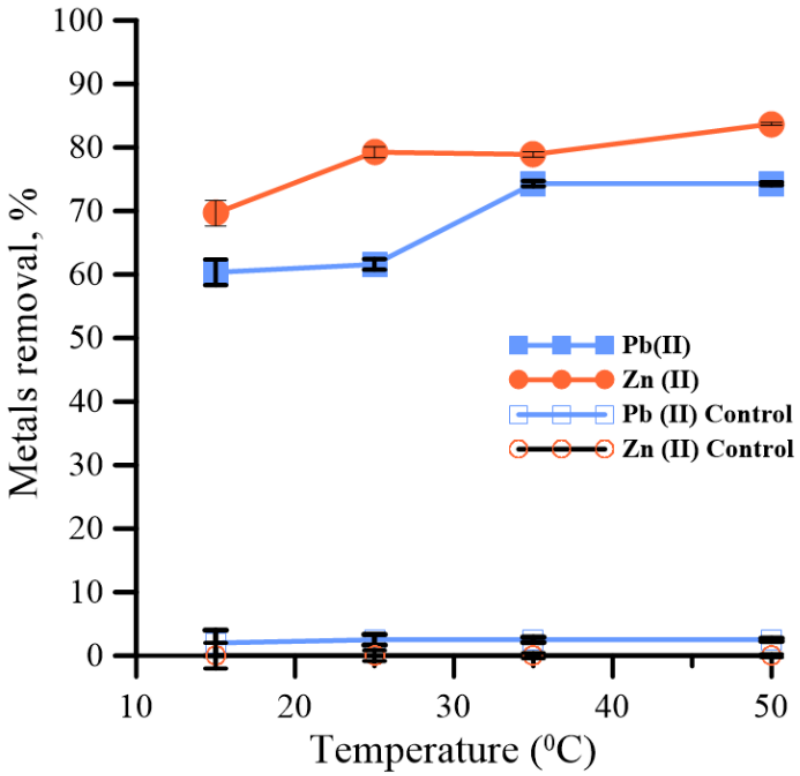

Fig. 5.17: Effect of temperature (Initial metal ions were same - 20 mg/L at pH 6.5)

(c) Effect of contact time

Contact time is an important factor affecting the efficiency of biosorption because it can provide valuable information on the mechanism of the biosorption process and kinetics. The effect of contact time on the biosorption capacity of cellulose-MT-CBM is shown in Fig. 5.18. It can be observed that the biosorption amount increases sharply in the first 5 minutes and that both elements had high biosorption capacity at around 20 min, therefore, all subsequent experiments were conducted at a contact time of 20 min. This behavior is typical of biosorbents as they have many empty binding sites which are gradually being filled and

saturation of metal-binding sites occurs. This rapid metal sorption is highly desirable for biosorbents for practical applications and has been reported by many researchers (Hassan and Awad, 2010; Jafari and Senobari, 2012; Pehlivan et al., 2012).

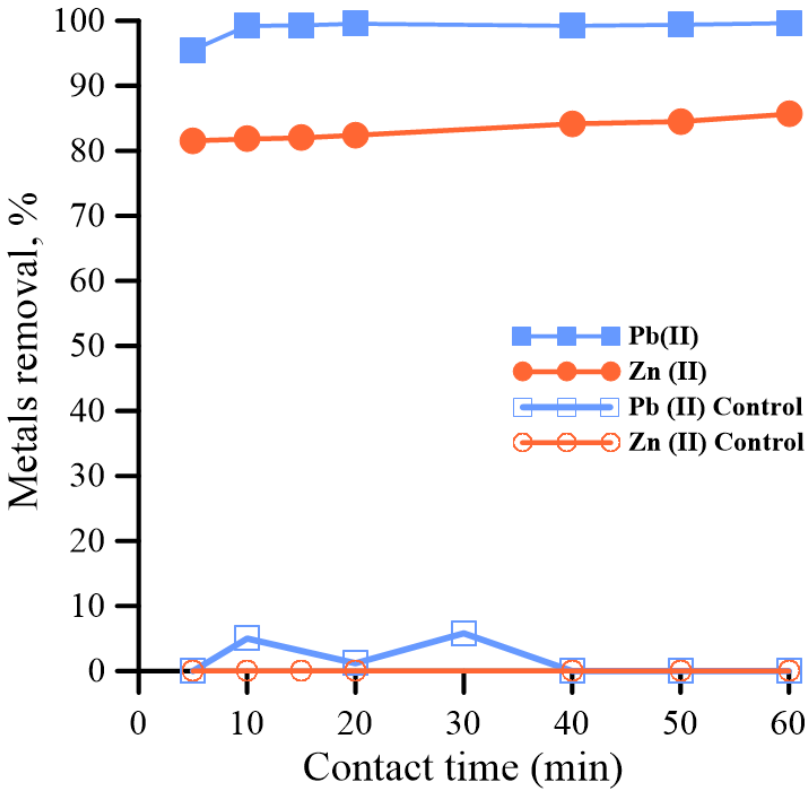

Fig. 5.18: Effect of contact time (Initial metal ions were same - 20 mg/L at pH 6.5)

(d) Effect of initial concentration

The results of the effect of initial concentration are shown in Fig. 5.19. The results show that when the initial Pb and Zn ion concentration was below 20 mg/L, the percentage removal was 100%.

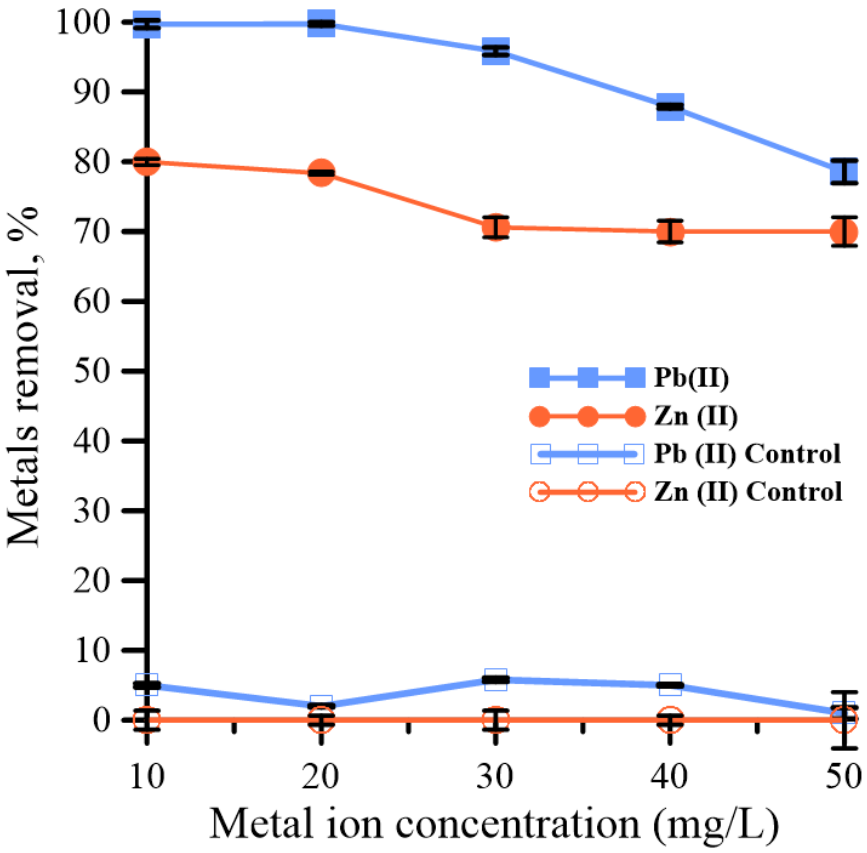

Fig. 5.19: Effect of initial concentration (pH 6.5 at room temperature)

At lower concentrations, all the metal ions present in the aqueous solution could possibly interact with the binding sites and thus the percentage biosorption was high and showed complete removal due to many available and free binding sites. Therefore, the cellulose-MT-CBM biosorbent seems to favor treatment of metal ions with concentrations below 20 mg/L as the removal was 100%. This could be probably that at higher concentrations than 20 mg/L of Pb (II) and Zn (II), slightly lower biosorption yield was observed attributed to the possible saturation of biosorption sites present in the cellulose-MT-CBM biosorbent. This is due to an increase in the number of ions competing for the limited available binding sites in the biosorbent.

5.5.3 Recyclability of cellulose-MT-CBM biosorbent

Recyclability of the cellulose-MT-CBM biosorbent was examined by reusing the same sorbent several times and results are shown in Fig. 5.20. The cellulose-MT-CBM was regenerated nine times and the bound Pb (II) and Zn (II) was desorbed by 20 mM EDTA. At cycle 4 and 7, the functionality could have been slightly lost. Recovery was restored by addition of MT-CBM protein to the cellulose. The results showed that the biosorbent would be usable for multiple metal sorption/desorption cycles without any significant loss in its efficiency compared to the control which had insignificant metal ions removal efficiency (Yunus and Tsai, 2015).

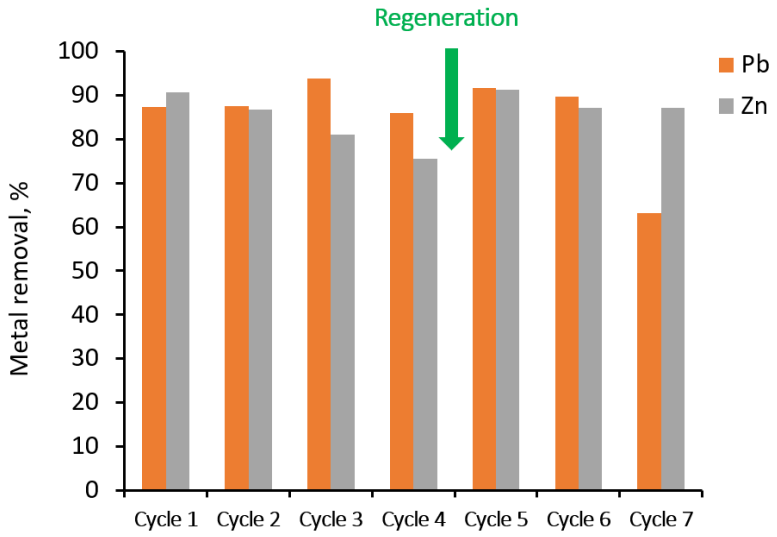

Fig. 5.20: Pb (II) and Zn (II) removal efficiency of Cellulose-MT-CBM at different cycles (Initial metal ions were same - 20 mg/L, pH = 6.5 at room temperature).

5.5.4 Adsorption mechanism

In order to elucidate the adsorption mechanism, XPS measurements of the biosorbent were performed to confirm the oxidation state(s) of Pb (II) and Zn (II) after it gets adsorbed onto the cellulose-MT-CBM biosorbent. In Figure 22, XPS wide scan spectra of cellulose-

MT-CBM before and after Pb (II) and Zn (II) adsorption depicted core levels of C1s, O1s, N1s, and Pb 4d and Zn 2p. Two new peaks at 141 and 136 eV appear after Pb (II) adsorption, which is attributed to the Pb 4f orbital whereas one new peak at 1022 eV attributed to the Zn 2p orbital. The results indicate that Pb (II) and Zn (II) were adsorbed on the biosorbent. The metal removal could be attributed to the formation of –N: •••Pb^{2+}/–N: •••Zn^{2+} complexes, in which a lone pair of electrons in the N atoms is donated to the shared bond between the nitrogen atoms and Pb^{2+}/ Zn^{2+}. Additionally, the oxygen atom could be responsible for heavy metal removal via ionic interaction Pb^{2+}/ Zn^{2+}. As was observed from O 1s peak at 532.29 eV was modeled after curve fitting, which is attributed to the oxygen-rich functional groups of atoms–C=O/–C–O–H groups in –COOH which can interact with heavy metal to form Pb^{2+}•••:O/Zn^{2+}•••:O. Therefore, heavy removal mechanism by cellulose-MT-CBM biosorbent is due to the combined effect of complexation by N atom and ionic exchange by the O atom in the biosorbent (Zhou et al., 2016).

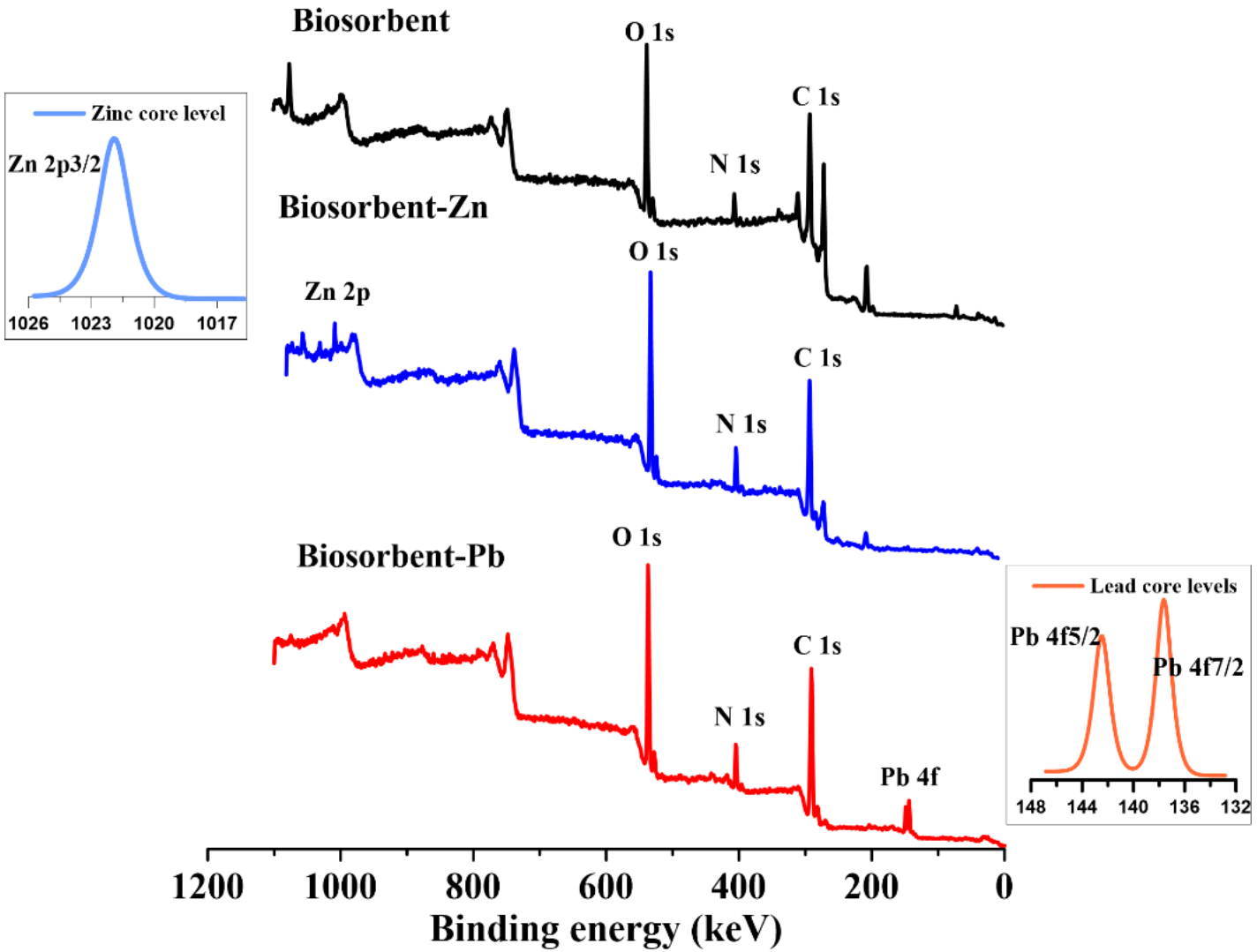

Fig. 5.21: The typical XPS wide scan spectra of cellulose-MT-CBM before and after Pb (II) and Zn (II) adsorption

5.5.5 Wastewater treatment using cellulose-MT-CBM

Table 5.2 shows the results of the treated groundwater collected from Kabwe mine. All the metal ions were below the detection limit of ICP-AES except Zn. The cellulose-MT-CBM would be useful as a final polishing biosorbent.

Table 5.2: Results of groundwater before and after treatment by cellulose-MT-CBM biosorbent

Element	Before (mg/L)	After (mg/L)	WHO Limit (mg/L)
Pb	2.29	BDL	0.01
Zn	1,348	308	2
Ni	0.923	BDL	0.07
Cu	12.27	BDL	2

5.6 Conclusion

In this Chapter, developed and demonstrated for the first time that Pb and Zn can be bioremediated by novel cellulose and metallothionein based biosorbent that was successfully constructed by the fusion protein. The biosorption condition of the cellulose-MT-CBM was favorable at pH 6.5 at room temperature with 20 minutes contact time; the cellulose-MT-CBM biosorbent can be reused and recycled several times.

References

Al-Karaghouli, A., Kazmerski, L.L., 2013. Energy consumption and water production cost of conventional and renewable-energy-powered desalination processes. Renew. Sustain. Energy Rev. 24, 343–356. https://doi.org/10.1016/j.rser.2012.12.064

Al-saad, K. a, Amr, M. a, Hadi, D.T., Arar, R.S., Al-sulaiti, M.M., Abdulmalik, T. a, Alssahamary, N.M., Kwak, J.C., 2012. Iron oxide nanoparticles : applicability for heavy metal removal from contaminated water. Arab J. Nucl. Sci. Appl. 45, 335–346.

Babula, P., Masarik, M., Adam, V., Eckschlager, T., Stiborova, M., Trnkova, L., Skutkova, H., Provaznik, I., Hubalek, J., Kizek, R., 2012. Mammalian metallothioneins: Properties and functions. Metallomics 4, 739–750. https://doi.org/10.1039/c2mt20081c

Banuelos, G.S., Terry., N., 1999. Phytoremediation of contaminated soil and water.

Belgacem, M.N., Gandini, A., 2008. Monomers, polymers and composites from renewable resources. Elsevier.

Boström, M., Tavares, F.W., Finet, S., Skouri-Panet, F., Tardieu, A., Ninham, B.W., 2005. Why forces between proteins follow different Hofmeister series for pH above and below pI. Biophys. Chem. 117, 217–224. https://doi.org/10.1016/j.bpc.2005.05.010

Care, A., Bergquist, P.L., Sunna, A., 2015. Solid-binding peptides: Smart tools for nanobiotechnology. Trends Biotechnol. 33, 259–268. https://doi.org/10.1016/j.tibtech.2015.02.005

Carpenè, E., Andreani, G., Isani, G., 2007. Metallothionein functions and structural characteristics. J. Trace Elem. Med. Biol. 21, 35–39. https://doi.org/10.1016/j.jtemb.2007.09.011

Cui, Y., Ge, Q., Liu, X.Y., Chung, T.S., 2014. Novel forward osmosis process to effectively remove heavy metal ions. J. Memb. Sci. 467, 188–194. https://doi.org/10.1016/j.memsci.2014.05.034

Dąbrowski, A., Hubicki, Z., Podkościelny, P., Robens, E., 2004. Selective removal of the heavy metal ions from waters and industrial wastewaters by ion-exchange method. Chemosphere 56, 91–106. https://doi.org/10.1016/j.chemosphere.2004.03.006

Dziegiel, P., Pula, B., Kobierzycki, C., Stasiolek, M., Podhorska-Okolow, M., 2016.

Metallothioneins in normal and cancer cells. Adv. Anat. Embryol. Cell Biol. 218, 1–117. https://doi.org/10.1007/978-3-319-27472-0_1

El Samrani, A.G., Lartiges, B.S., Villiéras, F., 2008. Chemical coagulation of combined sewer overflow: Heavy metal removal and treatment optimization. Water Res. 42, 951–960. https://doi.org/10.1016/j.watres.2007.09.009

Fakhre, N.A., Ibrahim, B.M., 2018. The use of new chemically modified cellulose for heavy metal ion adsorption. J. Hazard. Mater. 343, 324–331. https://doi.org/10.1016/j.jhazmat.2017.08.043

Freisinger, E., 2011. Structural features specific to plant metallothioneins. J. Biol. Inorg. Chem. 16, 1035–1045. https://doi.org/10.1007/s00775-011-0801-z

Ghoneim, M.M., El-Desoky, H.S., El-Moselhy, K.M., Amer, A., Abou El-Naga, E.H., Mohamedein, L.I., Al-Prol, A.E., 2014. Removal of cadmium from aqueous solution using marine green algae, Ulva lactuca. Egypt. J. Aquat. Res. 40, 235–242. https://doi.org/10.1016/j.ejar.2014.08.005

Hassan, S.H.A., Awad, Y.M., 2010. Bacterial biosorption of heavy metals, in: Biotechnology : Cracking New Pastures.

Hokkanen, S., Bhatnagar, A., Sillanpää, M., 2016. A review on modification methods to cellulose-based adsorbents to improve adsorption capacity. Water Res. 91, 156–173. https://doi.org/10.1016/j.watres.2016.01.008

Hong, J., Ye, X., Zhang, Y.H.P., 2007. Quantitative determination of cellulose accessibility to cellulase based on adsorption of a nonhydrolytic fusion protein containing CBM and GFP with its applications. Langmuir 23, 12535–12540. https://doi.org/10.1021/la7025686

Jafari, N., Senobari, Z., 2012. Removal of Pb (II) ions from aqueous solutions by *Cladophora rivularis* (Linnaeus) hoek. Sci. World J. 2012. https://doi.org/10.1100/2012/793606

Kurniawan, T.A., Chan, G.Y.S., Lo, W.H., Babel, S., 2006. Physico-chemical treatment techniques for wastewater laden with heavy metals. Chem. Eng. J. 118, 83–98. https://doi.org/10.1016/j.cej.2006.01.015

Mahamuni, N.N., Adewuyi, Y.G., 2010. Advanced oxidation processes (AOPs) involving

ultrasound for wastewater treatment: A review with emphasis on cost estimation. Ultrason. Sonochem. 17, 990–1003. https://doi.org/10.1016/j.ultsonch.2009.09.005

Maret, W., 2011. Redox biochemistry of mammalian metallothioneins. J. Biol. Inorg. Chem. 16, 1079–1086. https://doi.org/10.1007/s00775-011-0800-0

Mejáre, M., Bülow, L., 2001. Metal-binding proteins and peptides in bioremediation and phytoremediation of heavy metals. Trends Biotechnol. 19, 67–73. https://doi.org/10.1016/S0167-7799(00)01534-1

Nasiruddin Khan, M., Sarwar, A., 2007. Determination of Points of Zero Charge of Natural and Treated Adsorbents. Surf. Rev. Lett. 14, 461–469. https://doi.org/10.1142/s0218625x07009517

Nguyen, T.T.L., Lee, H.R., Hong, S.H., Jang, J.-R., Choe, W.-S., Yoo, I.-K., 2013. Selective lead adsorption by recombinant Escherichia Coli displaying a lead-binding peptide. Appl. Biochem. Biotechnol. 169, 1188–1196. https://doi.org/10.1007/s12010-012-0073-2

Pehlivan, E., Altun, T., Parlayici, S., 2012. Modified barley straw as a potential biosorbent for removal of copper ions from aqueous solution. Food Chem. 135, 2229–2234. https://doi.org/10.1016/j.foodchem.2012.07.017

Pinto, P.X., Al-Abed, S.R., Reisman, D.J., 2011. Biosorption of heavy metals from mining influenced water onto chitin products. Chem. Eng. J. 166, 1002–1009. https://doi.org/10.1016/j.cej.2010.11.091

Rosca, M., Hlihor, R.M., Cozma, P., Comaniţa, E.D., Simion, I.M., Gavrilescu, M., 2016. Potential of biosorption and bioaccumulation processes for heavy metals removal in bioreactors. 2015 E-Health Bioeng. Conf. EHB 2015 31–34. https://doi.org/10.1109/EHB.2015.7391487

Seker, U.O.S., Demir, H.V., 2011. Material binding peptides for nanotechnology. Molecules 16, 1426–1451. https://doi.org/10.3390/molecules16021426

Shi, J., Lindsay, W.P., Huckle, J.W., Morby, A.P., Robinson, N.J., 1992. Cyanobacterial metallothionein gene expressed in Escherichia coli Metal-binding properties of the expressed protein. FEBS Lett. 303, 159–163. https://doi.org/10.1016/0014-

5793(92)80509-F

Shim, Ho Y, Lee, K.S., Lee, D.S., Jeon, D.S., Park, M.S., Shin, J.S., Lee, Y.K., Goo, J.W., Kim, S.B., Chung, D.Y., Shim, H Y, 2014. Application of electrocoagulation and electrolysis on the precipitation of heavy metals and particulate solids in washwater from the soil washing. J. Agric. Chem. Environ. J. Agric. Chem. Environ. 3, 130–138. https://doi.org/10.4236/jacen.2014.34015

Steffens, J.C., 1990. The heavy metal-binding peptides of plants. Annu. Rev. Plant Physiol. Plant Mol. Biol. 41, 553–575. https://doi.org/10.1146/annurev.pp.41.060190.003005

Tran, H.T., Vu, N.D., Matsukawa, M., Okajima, M., Kaneko, T., Ohki, K., Yoshikawa, S., 2016. Heavy metal biosorption from aqueous solutions by algae inhabiting rice paddies in Vietnam. J. Environ. Chem. Eng. 4, 2529–2535. https://doi.org/10.1016/j.jece.2016.04.038

Vašák, M., Meloni, G., 2011. Chemistry and biology of mammalian metallothioneins. J. Biol. Inorg. Chem. 16, 1067–1078. https://doi.org/10.1007/s00775-011-0799-2

Vymazal, J., 2014. Constructed wetlands for treatment of industrial wastewaters: A review. Ecol. Eng. 73, 724–751. https://doi.org/10.1016/j.ecoleng.2014.09.034

Wojnárovits, L., Földváry, C.M., Takács, E., 2010. Radiation-induced grafting of cellulose for adsorption of hazardous water pollutants: A review. Radiat. Phys. Chem. 79, 848–862. https://doi.org/10.1016/j.radphyschem.2010.02.006

World Health Organization, 2017. Guidelines for drinking-water quality. https://doi.org/10.1016/S1462-0758(00)00006-6

Yang, G., Zhang, G., Wang, H., 2015. Current state of sludge production, management, treatment and disposal in China. Water Res. 78, 60–73. https://doi.org/10.1177/0954406216646137

Yao, Q., Xie, J., Liu, J., Kang, H., Liu, Y., 2014. Adsorption of lead ions using a modified lignin hydrogel. J. Polym. Res. 21. https://doi.org/10.1007/s10965-014-0465-9

Yunus, I.S., Tsai, S.-L., 2015. Designed biomolecule–cellulose complexes for palladium recovery and detoxification. RSC Adv. 5, 20276–20282. https://doi.org/10.1039/C4RA16200E

CHAPTER 6 CONCLUSIONS AND FUTURE WORKS

6.1 Summary of the Thesis and main conclusions

The objectives of this Ph.D. study were to investigate the development of novel bioremediation methods for alleviating heavy metal contamination in soil and water at abandoned Kabwe Mine Zambia as the study area. The following are summaries of each major subsection.

i. In Chapter 1, the research background, literature review, objectives of this study, scope, originality, and usefulness of the thesis were discussed.

ii. Soil bioremediation by MICP is presented in chapter 2 using *Pararhodobacter* sp and indigenous ureolytic bacteria, respectively, with the overall objective of immobilizing the mine waste hence preventing Pb metallic dust dispersion and reduce permeability. The contribution in this part of the thesis was the use of *Pararhodobacter* sp for bioremediation purpose and then evaluate its efficacy, which has never been addressed before. From an experimental point of view, the contribution lies in the comparison of the immersed and flow through methods when stabilizing the mine waste which mimics the possible field application of MICP.

    In chapter 3, another contribution was the isolation of two indigenous ureolytic bacteria from at the abandoned mine site; *O. profundus* KBZ 1-3, and *O. profundus* KBZ 2-5. There are no reports indicating their potential application in biotechnology, bioremediation or biosorption hence *O. profundus* KBZ 1-3 and *O. profundus* KBZ 2-5 isolated from Kabwe represent a novel *Oceanobacillus* species that is being applied for the first time in a bioremediation study. Overall, this contribution allows biocementation of hazardous waste is used in reducing the mobility of contaminant of both fine and coarse materials as an eco-friendly and sustainable method of heavy metal remediation.

iii. Water bioremediation by biosorption and cellulose-based biosorbent is presented in chapter 4 and 5. In Chapter 4, isolated *Oceanobacillus profundus* KBZ 3-2 identified as a novel strain capable of removal of lead and zinc from water. The

results indicate that the biosorption conditions of pH 6.5, the temperature of 30 ºC, and contact time of 120 minutes. The results indicate that accumulation in different cellular parts: the bacteria were able to accumulate mostly in the extracellular polymeric substance (EPS), in the cell protein, and in the cytoplasm and on the cell surface. EPS are responsible for metal sequestration. *O. profundus KBZ 3-2* as a biosorbent is highly efficient and has great potential in upscaling its biosorption purpose for bioremediation at the Kabwe Mine site.

In chapter 5 contributed by developing novel cellulose and metallothionein based biosorbent that was successfully constructed from fusion protein and immobilized on cellulose to form cellulose-MT-CBM. The biosorption condition of the cellulose-MT-CBM was a pH 6.5 at room temperature with 20 minutes contact time. Results show that the approach obtains better results than many cellulose based biosorbents. The cellulose-MT-CBM biosorbent is reusable hence making it sustainable as it is sourced from all bio-based renewable materials. This contribution can certainly be exploited in other biomolecule application for the removal of heavy metals from water hence contributing to safe drinking water.

6.2 Future research works

6.2.1 Suggestions for future works in MICP method for mine waste immobilization using *Pararhodobacter* sp

i. The cost-effectiveness of the developed technology from the laboratory to field scale application depends on the cost of reagents. The biggest cost could be the culturing and the use of cementation solutions used. All chemicals used were analytical grade. The use of cheap and readily available reagents can be explored as well as its application in field investigation that includes beer yeast, corn stupor.

ii. The potential use of *Pararhodobacter* sp for immobilization of mine waste was effective, however, it is needed to explore deeply onsite. Its possible application in the field can bring the environmental safety aspect.

6.2.2 Suggestions for future works in MICP method for mine waste immobilization using locally isolated from Kabwe Mine site

i. Despite its investigation as a promising candidate for MICP, the bacteria isolated need to be investigated further: (a) bioprecipitation using the cheap and locally available replacement of reagent grade chemicals. The use of locally available limestone in Zambia as a calcium source could be investigated.
ii. It is also necessary to investigate the durability of the biocemented sand so as to know the effectiveness of the cover in a field investigation.

6.2.3 Suggestions for future works in metal tolerant indigenous bacteria for biosorption of heavy metals

The study on metal tolerant bacteria for heavy metal removal from water concluded that the use of *Oceanobacillus profundus* KBZ 3-2 as a biosorbent is highly efficient and has great potential in upscaling its biosorption purpose for bioremediation at the Kabwe Mine site. However, the effect of multielement exposure of the bacteria was not investigated despite it being subjected to groundwater from Kabwe mine. Further investigations are required.

6.2.4 Suggestions for future works in cellulose MT-CBM biosorbent

Developed and demonstrated for the first time that heavy metal can be removed from contaminated water by cellulose based biosorbent. However, the use of the way this absorbent can be exploited in the formation of other biomolecule application for the removal of heavy metals from water hence contributing to safe drinking water or restoration of contaminated sites such as the use of tougher immobilization bases such as silica or quartz material where the metallothionein or similar peptides can be applied. The use of Silica or quartz would be novel as it will be easier to separate the liquid and solid phases after biosorption.